Base Metal Catalyzed Dehydrogenation of Formic Acid and Alcohols

Dissertation
zur Erlangung des akademischen Grades
Doctor rerum naturalium (Dr. rer. nat.)
der Mathematisch-Naturwissenschaftlichen Fakultät
der Universität Rostock

vorgelegt von
M. Sc. Wei Zhou
geb. am 29. 01. 1989 in Huanggang, P. R. China

Rostock, 25. 04. 2019

https://doi.org/10.18453/rosdok_id00002525

This work was conducted at the Leibniz-Institute for Catalysis e.V. at the University of Rostock under the supervision of Professor Dr. Matthias Beller during the period from July 2016 to February 2019.

Reviewer 1:
Prof. Dr. Matthias Beller
Leibniz-Institut für Katalyse an der Universität Rostock

Reviewer 2:
Prof. Dr. Gabor Laurenczy
Ecole polytechnique fédérale de Lausanne Institut des sciences et ingénierie chimiques

Date of submission: 26.04.2019
Date of defense: 16.07.2019

Acknowledgement

When reflecting on three years of doctoral study, I realize that it would be impossible for me to get where I am now without the help from so many kind people along the way. I would like to take this chance to express my deepest gratitude to those who have provided exceptional support, guidance, and motivation through this experience.

First, and foremost, I would like to thank my advisor Prof. Dr. Matthias Beller for offering me the invaluable opportunity to study in his world-class research laboratory and leading me through the trials of my research. His unique perspective in chemistry and remarkable enthusiasm as well as his kind and patient personality has motivated me a lot.

I'm also grateful to my group leader Dr. Henrik Junge for accepting me in his group as a member of the NoNoMeCat project, and for all his support during my PhD studies.

I want to thank all the past and present members of the "Catalysis for Energy" group, I am so lucky to work with you. I appreciate the discussions with you, from which I benefit so much, both on a professional and on a personal level. Special thanks to María Andérez Fernández, who taught me about the burette setup at the starting of my project; Dr. Elisabetta Alberico and Maximilian Marx for careful correction of this thesis.

My appreciation also goes to Dr. Haijun Jiao and Zhihong Wei for their help with the DFT calculations and for fruitful discussions. Many thanks to Dr. Anke Spannenberg for her skilled resolution of my crystal samples.

I would like to thank our Chinese community at LIKAT, we had so much unforgettable moments in Rostock. With your company I never felt I'm far away from my homeland.

I also thank the European Union for the financial support during my PhD study.

Last but not least, I want to thank my family for all the sacrifice they have made in allowing me to follow my dreams. This work would not have been possible without the support of my wife Ms. Dan Wang, her patience and encouragement always helped me to overcome any difficulties. Words are powerless to express my gratitude.

Abstract

The content of this thesis is about base metal catalyzed dehydrogenation reactions and it contains two parts. In the first part, a cobalt catalyzed formic acid dehydrogenation in aqueous media is disclosed. Comparisons of catalytic performance among different cobalt PNP pincer complexes show that both the oxidation state of the metal and the substituents on the phosphorus donors of the pincer ligands are crucial to success. Mechanistic studies indicate that CO coordination to cobalt poisons the catalyst thus leading to its deactivation. DFT calculations support a non-classical innocent bifunctional outer-sphere mechanism where the N-H group of the pincer ligand allows for stabilization of the active Co-formate intermediate.

The second part deals with a manganese catalyzed dehydrogenation of alcohols which was developed by *in-situ* combination of manganese pentacarbonyl bromide with phosphine free oxamide ligands. Even though this system is inactive in methanol dehydrogenation, our preliminary results show that it is suitable for acceptorless dehydrogenation of isopropanol and ethanol. Further endeavors towards the preparation of well-defined Mn complexes allow us to isolate and characterize an unique anionic Mn complex ligated by deprotonated *N,N′*-dimethyloxamide which is proposed as an active intermediate during the dehydrogenation process.

List of abbreviations

DBU	1,8-Diazabicyclo[5.4.0]undec-7-ene
DMOA	*N,N*-Dimethyloctylamine
dmpe	1,2-Bis(dimethylphosphino)ethane
FA	formic acid
KIE	Kinetic isotope effects
MIL	Materials Institute Lavoisier
Mtoe	one million tonne of oil equivalent
MOFs	metal–organic frameworks
NMR	Nuclear Magnetic Resonance
NP	Nano particle
PC	Propylene carbonate
PEM fuel cells	Proton-exchange membrane fuel cells
ppm	parts per million
TEA	Triethylamine
TEM	Transmission electron microscope
THF	Tetrahydrofuran
TMEDA	Tetramethylethylenediamine
TOF	Turnover frequency
TON	Turnover number
tpy	2,2′:6′,2″-Terpyridine

Table of Contents

Acknowledgement I

Abstract III

List of abbreviations IV

1 Introduction 1

1.1 Hydrogen as energy vector 1

1.2 Dehydrogenation of formic acid and alcohols 3

1.3 Noble metal catalyzed dehydrogenation reactions 4

1.3.1 Dehydrogenation of formic acid 4

1.3.2 Dehydrogenation of alcohols 14

1.4 Non-noble metal catalyzed dehydrogenation reactions 20

1.4.1 Non-noble metal catalyzed dehydrogenation of fromic acid 21

1.4.2 Non-noble metal catalyzed dehydrogenation of alcohols 25

1.5 Objective of this research 26

2 Cobalt catalyzed dehydrogenation of formic acid 28

2.1 Background 28

2.2 Results and discussion 31

2.2.1 Initial investigation of Co(II) pincer complexes 32

2.2.2 Development of a catalytic active Co(I) system for formic acid dehydrogenation 33

2.2.3 Mechanistic studies 36

2.3 Summary 46

3 Manganese catalyzed dehydrogenation of alcohols 47

3.1 Background 47

3.2 Results and discussion 51

3.2.1 Reaction optimization 52

3.2.2 The synthesis of well-defined Mn complexes 57

3.2.3 Proposed mechanism 60

3.3 Summary 60

4 Conclusion and outlook 61

5 Experiments and data analysis 63

5.1 General information 63

5.2 Cobalt catalyzed dehydrogenation of formic acid 66
5.2.1 Preparation of coblat complexes 66
5.2.2 General procedure for cobalt catalyzed dehydrogenation of formic acid 70
5.3 Manganese catalyzed dehydrogenation of alcohols 71
5.3.1 Synthesis of ligands 71
5.3.2 General procedure for manganese catalyzed dehydrogenation of isopropanol 72
Reference 73
Appendix ..... A
I. Spectra of synthesized compounds ..... A
II. Representative GC spectra of gas samples ..... K

1 Introduction

Due to an explosion of global population and the development of human society, nowadays, we have much higher energy demand than ever. Currently, our energy supply is heavily dependent on fossil fuels such as oil, coal and natural gas,[1] however, the reserve of fossil resources is limited[2] and they cannot be regenerated. In addition to this, a lot of environmental problems were caused by the consumption of fossil fuels, for example, the production of tremendous amounts of carbon dioxide which contributes to global warming.[3] Thus, it is imperative to develop renewable and environmental friendly energy sources.[4]

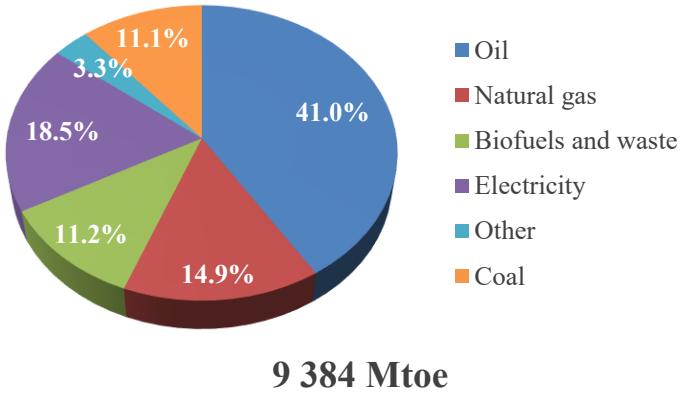

Figure 1.1: World total final consumption by fuel in 2015[1]

Renewable energy sources such as solar, wind and geothermal are promising choices,[5] but these resources are discontinuous and strongly affected by climate and geography. Thus, they need to be converted into a secondary energy resource to enable a stable and safe energy supply. There are several ways to store energy, and the factors time scale of availability, e.g. discharge time, storage capacity and energy density are important criteria to evaluate their utility and versatility. For example, the flywheel technology offers a very rapid provision of energy, while its storage capacity is limited to max. 100 kWh. Batteries are more adaptable and can provide electric energy in the range of 5 kWh to 10 MWh, nevertheless, they still suffer from low energy density and limited lifetime.

In this respect, hydrogen (H_2) is a potential secondary energy carrier through the power-to-gas process, since its high gravimetric energy density and the added advantage of releasing water as the sole product after its combustion with oxygen.[6]

1.1 Hydrogen as energy vector

Hydrogen is a non-toxic, environmentally benign gas, it can serve as a promising secondary energy carrier for an energy economy based on renewable resources.[7] The combustion of H_2 in

internal combustion engines has a higher efficiency (η = 38.2%) compared to diesel (η = 35.1%) or gasoline (η = 30.1%).[8] Remarkably, the efficiency of polymer electrolyte membrane (PEM) fuel cells is much higher with a theoretical value up to 85% for the conversion to electricity.[9] The gravimetric energy density of H_2 (33.33 kWh kg^{-1}) is more than two times higher than that of gasoline (12.4 kWh kg^{-1}). However, as a gaseous compound under standard conditions, the corresponding volumetric energy density of H_2 (2.5 Wh L^{-1})) is far less than that of gasoline (8.07 kWh L^{-1}).[6] For this reason, H_2 needs to be stored in a way which entails higher volumetric energy density.

To date, there are several methods to store H_2 chemically or physically.[10] For physical storage, pressured tanks (up to 700 bar) and cryo tanks (-253 ℃) are the most direct and popular ways. However, the procedure of compression or liquefaction will consume a lot of energy. In addition to that, extra weight caused by the containers will also undermine the overall energy capacity. Additional physical storage solutions through adsorption on high-surface materials such as zeolites and MOFs are currently under investigation, but problems such as low hydrogen adsorbing capacity as well as material degradation caused by hydrogen remain unsolved.[11]

On the other hand, H_2 storage via chemical bonds offers a promising choice, since it allows hydrogen to be stored at ambient conditions, exhibiting high gravimetric and volumetric energy densities. It also benefits from safer and easier handling and transportation without significant loss of energy. Several classes of chemical compounds including hydrides (saline, covalent or metal hydrides),[12] ammonia borane [13] and liquid organic compounds[14] are potential candidates for the storage of H_2. However, hydrides are often very highly reactive compounds which poses safety issues regarding storage and transportation, except for that, their low hydrogen content also makes them less favorable for H_2 storage. Ammonia borane, though with a high hydrogen content up to nearly 20 wt%, faces drawbacks such as reversibility difficulty and possible risk of releasing hazardous ammonia. In comparison, liquid organic compounds especially alcohols and formic acid (FA) are very attractive molecules because of their high hydrogen content, low toxicity and easy availability,[14] which would enable the realization of a hydrogen economy (Figure 1.2). This thesis mainly focused on the dehydrogenation of liquid organic compounds (alcohols and FA), with a concentration on homogeneous non-noble metal catalysts.

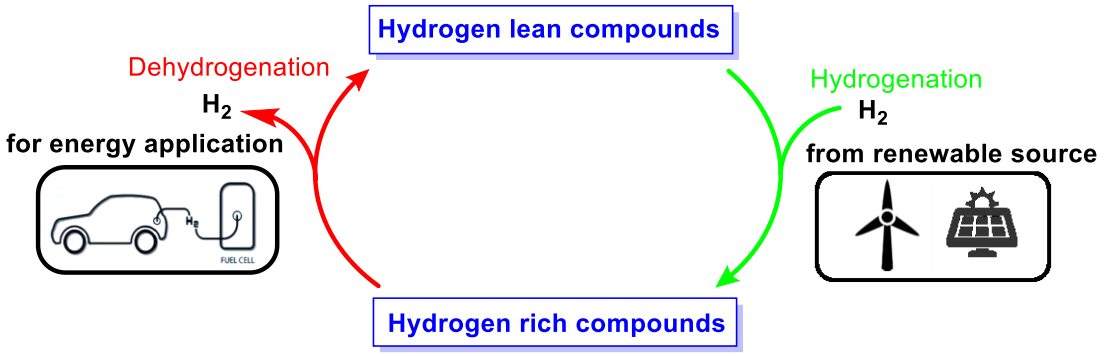

Figure 1.2: Hydrogen economy based on liquid organic compounds

1.2 Dehydrogenation of formic acid and alcohols

FA, as the simplest carboxylic acid, is a kinetically stable liquid at room temperature and has a hydrogen content of 4.4 wt%, being only slightly lower than the desired target of the U.S. Department of Energy (DOE).[15] It is produced on an industrial scale through the carbonylation of methanol. Besides, it can also be generated by catalytic hydrogenation of CO_2 or biomass fermentation.[16] The decomposition of FA proceeds via two pathways: decarboxylation toward CO_2 and H_2, and decarbonylation to CO and H_2O (Scheme 1.1).[17] For the storage of H_2, the decarbonylation pathway should be avoided, since it not only decreases the dehydrogenation efficiency but also contaminates H_2 generated from FA, making it unsuitable for following applications (e.g. PEM fuel cells).[18] In general, the decomposition can be affected by parameters such as temperature, concentration, solvent etc. By applying a suitable catalyst, the dehydrogenation process can proceed with very high selectivity, thereby meeting the standards required for hydrogen storage technology.

$$HCO_2H\ (l) \longrightarrow H_2\ (g) + CO_2\ (g) \qquad \Delta G^\circ = -32.9\ kJ\ mol^{-1}$$

$$HCO_2H\ (l) \longrightarrow H_2O\ (l) + CO\ (g) \qquad \Delta G^\circ = -12.4\ kJ\ mol^{-1}$$

Scheme 1.1: Decomposition pathway of FA

In addition to FA, alcohols also represent promising substances for H_2 storage. Traditionally, alcohols were oxidized in the presence of a sacrificial oxidant to give the corresponding carbonyl products. In recent years, the notion of acceptorless dehydrogenation has evolved rapidly.[19] This method features alcohols oxidized to carbonyl compounds, concomitant release of molecular

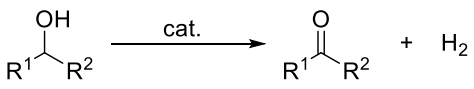

Scheme 1.2: Acceptorless dehydrogenation of alcohols

hydrogen as a valuable product. Small alcohol molecules such as methanol, ethanol and *iso*-propanol are of interest due to their high hydrogen content and as high boiling point liquid under

ambient conditions. Especially in the case of methanol, it can be fully dehydrogenated together with water to give three equivalents of H_2. This process incorporates three consecutive dehydrogenation steps (Scheme 1.3): the first step is general acceptorless alcohol dehydrogenation to liberate one equivalent of H_2 and formaldehyde, formaldehyde then reacts with water to give methanediol which in the second step is dehydrogenated to give a second equivalent of H_2 and FA. Finally, FA is converted into H_2 and CO_2.

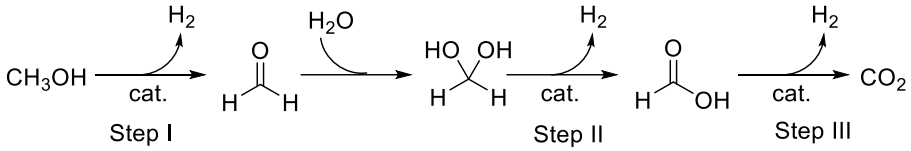

Scheme 1.3: Aqueous dehydrogenation of methanol

1.3 Noble metal catalyzed dehydrogenation reactions

1.3.1 Dehydrogenation of formic acid

The first report about the dehydrogenation of FA dates back to the early 1910s, when Sabatier and Mailhe studied the behaviour of FA towards different oxide catalysts.[20] Following this seminal work, Adkins and Nissen investigated the decomposition of FA at the surface of alumina.[21] Early experiments of heterogeneous FA decomposition typically conducted at high temperature (>100 ℃), thus in gas phase.[22] Research afterwards mainly focused on highly active Pd and Au catalysts in order to run the reaction under milder conditions and obtain higher selectivity. Notably, in the late 1970s, Williams and co-workers reported dehydrogenation of FA at room temperature by applying Pd on carbon particles as catalyst, around 60 mL of H_2 was obtained after 10 min reaction time with 1% Pd loading.[23] In recent years, significant achievements have been made in the design and application of heterogeneous catalysts for FA dehydrogenation, some selected examples are introduced below, detailed discussion about heterogeneous catalysts on FA dehydrogenation can be found in recent reviews.[24]

In 2008, Xing and co-workers reported H_2 production from Pd-Au/C and Pd-Ag/C catalyzed decomposition of FA.[25] Compared to Pd/C catalyst, the stability of Pd-Au/C and Pd-Ag/C alloy catalysts was dramatically improved. However, at maximum gas evolution rate, a concentration of 80 ppm CO was detected. The authors further improved the activity through addition of $Ce(NO_3)_3$•H_2O during the preparation of the catalysts, 1250 mL of gas was obtained through the dehydrogenation of FA/sodium formate by applying 60 mg of Pd-Au/C-CeO_2 (10 wt%) catalyst at 92 ℃ in 2 hours (TOF = 227 h^{-1}), besides CO contamination was also avoided possibly due to oxidation of CO by cationic palladium species in the presence of CeO_2 from the catalyst (Figure 1.3).

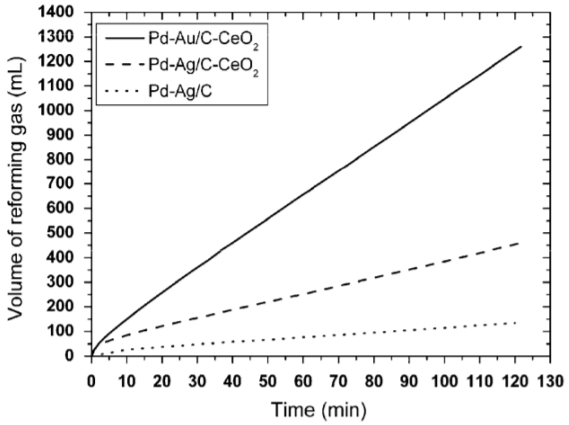

Figure 1.3: Gas evolution at 92 ℃ with 5 mL FA/HCOONa[24]

Later, Iglesia and Ojeda found well-dispersed Au species on Al_2O_3 catalyze FA dehydrogenation at higher rates than Pt, which was previously considered as the most active metal. They were able to obtain high quality H_2 (CO content < 10 ppm) through the dehydrogenation of FA using the Au/Al_2O_3 catalyst.[26] Tsang and co-workers showed that core–shell nanoparticles consisting of an ultrathin Pd shell on a Ag core can be engineered by wet chemical synthesis to produce a dramatic enhancement in hydrogen production, but with no CO contamination from formic acid in an aqueous phase at comparably low temperature. This nanocatalyst exhibited an outstanding TOF of 252 h^{-1} at 50 ℃ and remained active even at ambient temperature (TOF = 125 h^{-1} at 20 ℃).[27]

Sun and co-workers demonstrated a facile approach to a composition-controlled synthesis of monodisperse 2.2 nm AgPd nanoparticles (NPs). These NPs are highly active and stable for the dehydrogenation of FA. At 50 ℃ the $Ag_{42}Pd_{58}$ NPs have the highest activity with an initial TOF of 382 h^{-1} and an apparent activation energy of 22±1 $kJ \cdot mol^{-1}$ (Figure 1.4).[28] These results showed through alloying, the performance of NP catalysis can be enhanced.

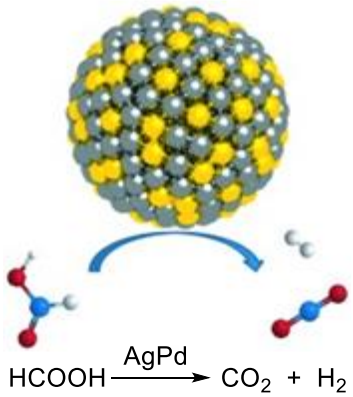

Figure 1.4: Monodisperse AgPd alloy nanoparticles catalyzed dehydrogenation of FA[28]

Even though, ultrasmall metal NPs showed high performance for the dehydrogenation of FA, these particles inevitably undergo aggregation during synthesis and catalysis because of their

high surface energy. The immobilization of highly dispersed metal NPs to well-designed supports is a promising approach to produce stable ultrasmall NPs with clean surfaces (uncapped) and ensure optimum catalyst utilization. In 2011, Xu and co-workers reported the use of bimetallic Au−Pd NPs immobilized into a mesoporous MOF as efficient catalysts for the generation of H_2 from FA.[29a] Through the immobilization into MIL-101(Cr) materials, they obtained bimetallic Au−Pd NPs within 2-8 nm size ranges. The catalyst (Au−Pd loading: 20.4 wt %; Au:Pd = 2.46) exhibited high catalytic performance, 3 mmol of FA was completely converted to H_2 and CO_2 in 65 min (n_{AuPd}/n_{FA} = 0.0085) at 90 °C. Later on, the same group developed a sodium hydroxide-assisted reduction approach for the synthesis of highly dispersed Pd NPs deposited on nanoporous carbon MSC-30. The catalyst reached a TOF of 2623 h^{-1} at 50 °C with 100% H_2 selectivity and a TOF as high as 750 h^{-1} could be achieved even at room temperature.[29b]

In 2012, Cao and co-workers applyed an ultradispersed gold catalyst comprising TEM-invisible gold subnanoclusters deposited on zirconia for the dehydrogenation of FA-amine adducts, TOF up to 1590 h^{-1} and a TON of more than 118 400 at 50 °C were obtained.[30a] The authors suggested a unique amine-assisted formate decomposition mechanism on Au−ZrO_2 interface (Scheme 1.4). In 2016, they reported Pd NPs catalyzed room temperature dehydrogenation of FA under base free conditions.[30b] They found pyridinic-*N*-doped carbon hybrids as support materials can significantly boost the efficiency of Pd NPs for H_2 generation. Under mild conditions, their optimized Pd/$CN_{0.25}$ catalyst exhibited high performance in FA dehydrogenation, achieving almost full conversion, and a TOF of 5530 h^{-1} at 25 °C. Besides, the catalyst also showed high activity for CO_2 hydrogenation into FA, thus lead to a full carbon-neutral energy cycle.

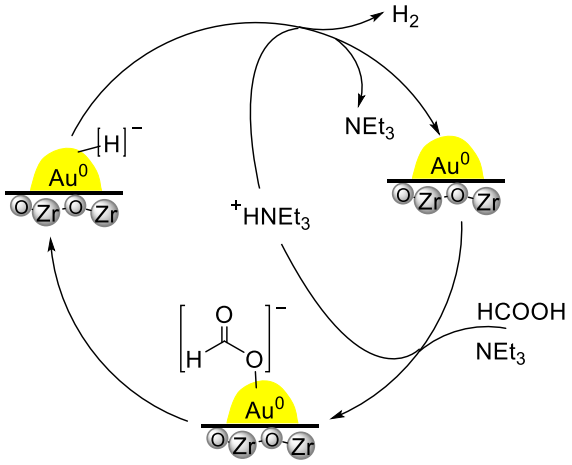

Scheme 1.4: Proposed pathway for hydrogen evolution over the Au/ZrO_2 nanoclusters catalyst[30a]

Except for conventional methods such as alloying and dispersion to improve the catalytic activity of heterogeneous catalyst, visible light can also be used if a photo active catalyst is applied. Recently, Chen and co-workers introduced a Pd nanoparticle-based Mott–Schottky photocatalyst

for highly efficient dehydrogenation of FA.[31a] The catalyst exhibited much higher activity under photoirradiation than without, nanostructured carbon nitride was found to be of vital importance in this system for not only acted as the stabilizer for Pd NPs, but also as semiconductive support for the coupling of metal NPs to form the required rectifying Mott–Schottky nanoheterojunctions. While in another report, Majima and co-workers showed plasmon-enhanced catalytic FA dehydrogenation by using anisotropic Pd-Au nanorods, the bimetallic nanorods act both as light absorber and catalytically active site.[31b]

Although a lot of progress has been made in the field of heterogeneous catalysis for the dehydrogenation of FA, homogeneous catalysts provide generally higher selectivity and activity at much lower temperatures.[32] The first study of homogeneously catalyzed dehydrogenation of FA dates back to 1967 when Coffey described the use of soluble metal complexes for FA decomposition in acetic acid under reflux conditions.[33] A series of Pt, Ru and Ir phosphine complexes were tested, among which $IrH_2Cl(PPh_3)_3$ gave the highest rate of decomposition. H_2 was obtained with very high selectivity without CO contamination. Later on, Foster and Beck reported the decomposition of FA by Rhodium and Iridium iodocarbonyls with hydroiodic acid.[34] The Rh catalyst can promote the decomposition at a rate of 0.31 mol L^{-1} h^{-1} at 100 °C with H_2 as the main product, however, large quantities of CO was observed in the system. In 1979, the group of Strauss used a Rh complex containing Rh–C σ-bond as precatalyst for the dehydrogenation of FA.[35] The Rh precatalyst was converted into a formate complex during the reaction that subsequently catalyzed the formation of H_2 from FA. In 1982, Paonessa and Trogler found that a platinum dihydride complex catalyzed the reversible formation of carbon dioxide and hydrogen from FA,[36] the system showed an obvious dependence on the choice of solvent. They also investigated the influence of pressure: the activity was suppressed when internal pressure builds up and restored again after the release of gas.

A major breakthrough in the field of dehydrogenation of FA by homogeneous catalysts was made by Puddephatt's group in 1998. They reported extensive studies on the usage of a binuclear, diphosphine-bridged diruthenium catalyst $[Ru_2(\mu\text{-}CO)(CO)_4(\mu\text{-}dppm)_2]$ for the conversion of FA to H_2 and CO_2, an average TOF value of 70 h^{-1} was obtained in a sealed NMR tube.[37a] The mechanism of this system was studied in detail and several intermediates were isolated and characterized. The catalytic circle involves the initial formation of hydride dimer from precatalyst, it then reacts with FA to liberate H_2 and forms Ru-formate species, which next transfers a hydride from formate ligand to ruthenium to give coordinatively saturated complex. Afterwards, CO_2 is dissociated to regenerate the hydride dimer and complete the catalytic cycle (Scheme 1.5). The reversibility of the reaction was studied, and the same catalyst was found to be capable of hydrogenating CO_2 to FA.[37b]

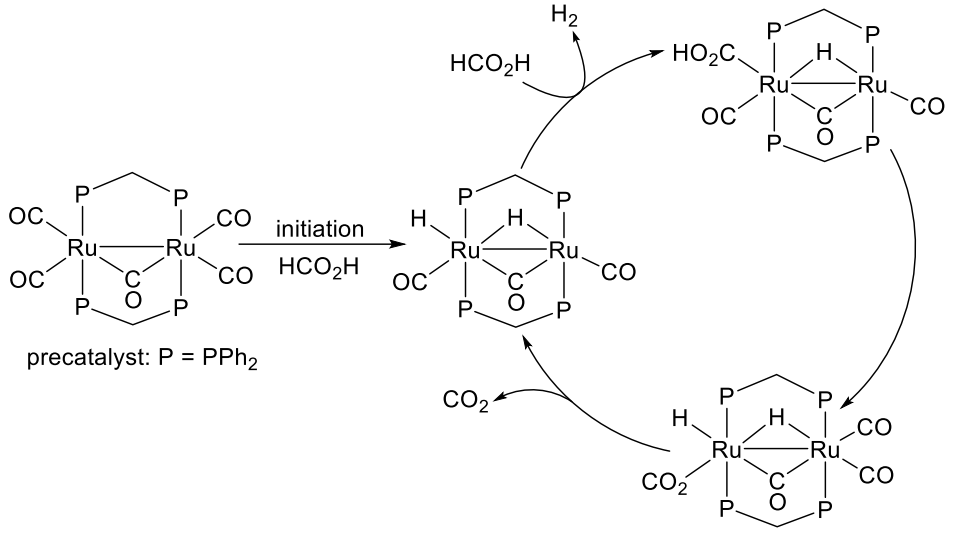

Scheme 1.5: Proposed mechanism for H_2 generation from FA by a dimeric diruthenium complex.[37a]

Over the last two decades, many interesting results of H_2 generation from FA were disclosed, most of which were based on the application of homogeneous Rh, Ru and Ir catalysts. In 2005, Ogo, Fukuzumi and co-workers initiated the study of stoichiometric H_2 generation from a rhodium diformate complex $[Rh^{III}(tacn)(HCO_2)_2]OTf$ (tacn = 1,4,7-triazacyclononane). Through X-Ray analysis, ESI-MS and ^1H NMR experiments, they found that the rhodium hydride formate complex which formed via β-H elimination from the diformate species to be a key intermediate for the H_2 formation (Scheme 1.6). Furthermore, a dihydride carbonyl complex was formed after H_2 evolution, this implied dehydration of FA also occurred during this process.[38]

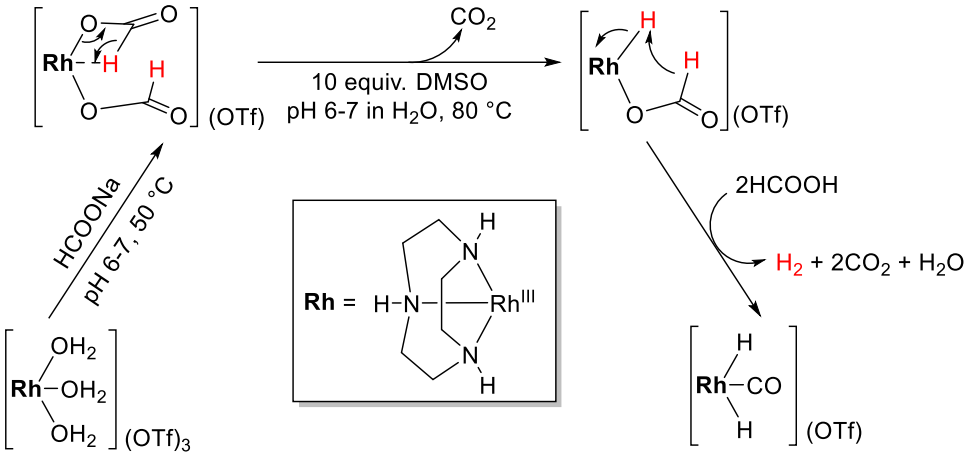

Scheme 1.6: H_2 evolution from a rhodium diformate complex[38]

Shortly after, the same group reported a catalytic version for the decomposition of FA/formate mixtures by applying a water soluble rhodium complex $[Rh^{III}(Cp^*)(bpy)(H_2O)]^{2+}$ (Cp^* = pentamethylcyclopentadienyl, bpy = 2,2'-bipyridine).[39] H_2 generated smoothly under room

temperature at optimal pH value (pH = 3.8), a maximum TON of 80 was obtained after around 6 h. In comparison, Wills and co-workers applied a "tethered" Rh complex, previously designed for asymmetric hydrogenation of acetones, for H_2 generation from FA/TEA under mild conditions.[40] A maximum TOF of 490 h^{-1} and a total gas evolution of 350 mL were obtained.

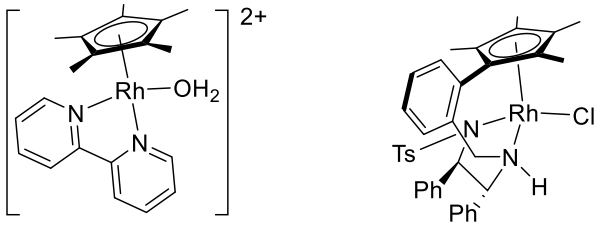

Fukuzumi Wills

Scheme 1.7: Rh complexes for catalytic dehydrogenation of FA

As inspired by Puddephatt's work on Ru catalyzed dehydrogenation of FA,[37] different types of Ru precursors and Ru complexes were intensively investigated for H_2 generation from FA. In 2008, the Beller group investigated the performance of different Ru precursors for H_2 generation from FA/amine adducts under ambient conditions.[41a] The Ru dimer $[RuCl_2(cymene)]_2$ was found to be active even in the absence of phosphine ligands, and a TON of 30 was obtained at 40 °C. Phosphine containing ruthenium complexes, on the other hand, showed much higher activity, an initial TOF of more than 2688 h^{-1} at 40 °C was found when applying $[RuCl_2(PPh_3)_3]$ in a DMF solution of FA/TEA (5:2 molar ratio) mixture[41a]. An *in-situ* generated catalyst from $RuBr_3/PPh_3$ exhibited higher activity with a TOF up to 3630 h^{-1}, while the combination of $[RuCl_2(benzene)]_2$ and 1,2-bis(diphenylphosphino)ethane (dppe) resulted a more stable system and a TON of 1376 was obtained after 3h.[41b] The system showed very high selectivity of dehydrogenation with no CO being detected in the gas product (CO detection limit below 10 ppm). The application of this system was highlighted by direct combination of the dehydrogenation system with a polymer electrolyte fuel cell (PEMFC) without prior high temperature purification and a power of 26 mW at 370 mV was obtained for more than 42 hours (Figure 1.5).

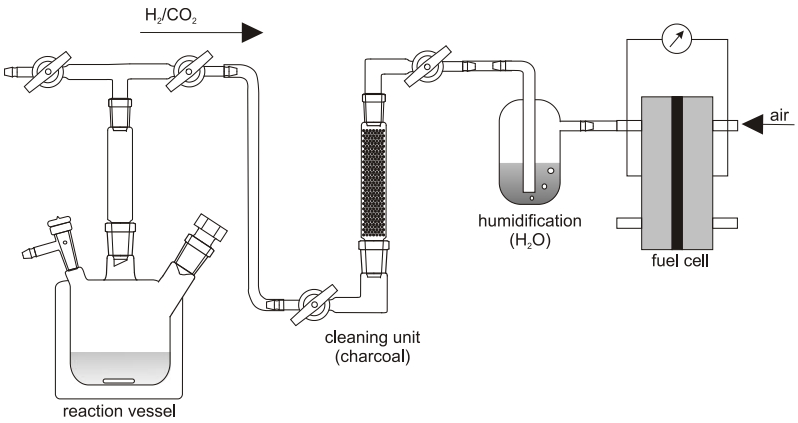

Figure 1.5: Setup for direct usage of H_2 from formic acid in a fuel cell[41b]

Further studies by Beller and co-workers revealed that more than 2.4 L of gas could be obtained from a batch reaction applying an active catalyst system containing 19.1 µmol of $[RuCl_2(benzene)]_2$ and dppe (Ru/dppe molar ratio 1:6) in the presence of N,N-dimethyl-n-hexylamine resulting in a TON of 2616.[41c] Remarkably, this catalyst system could be reused after full conversion of initial FA by simply adding fresh FA, no significant decrease of activity was observed even after the 10 runs during a period of two months. Thus, a total TON of approximately 60000 at 40 ℃ in 30 h was obtained. A continuously driven reaction system was also built to evaluate the performance of the Ru system under continuous conditions. An unprecedented TON of approximately 260000 with an average TOF over 900 h^{-1} at room temperature was achieved, which represented the highest activity for the low temperature H_2 generation from FA at that time. Later on, the effect of photo irradiation on this system was studied in detail.[42] It was found that the light triggered H_2 production increases by more than one order of magnitude compared with the non-irradiated one. Photo irradiation was proved to exhibit twofold effect: firstly, it activates the precatalyst to generate the active species; secondly, it prevents the active species from deactivation. In addition, a $[RuCl_2(benzene)]_2$/dppe system capable of generating H_2 from a formate water solution as well as hydrogenating bicarbonate was developed,[43] which enables a CO_2 neutral hydrogen storage (Scheme 1.8).

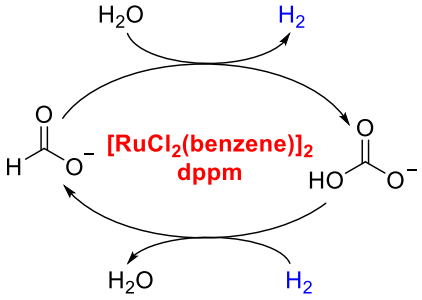

Scheme 1.8: CO_2-neutral hydrogen storage based on bicarbonate/formate system[43]

Concurrent with Beller's work, Laurenczy and co-workers developed a water soluble phosphine ligand TPPTS (tris-m-sulfonated triphenylphosphine trisodium salt), which allowed dehydrogenation of FA in water by employing $[Ru(H_2O)_6](tos)_2$ (tos = toluene-4-sulfonate) as precursor. A continuous set-up was developed under which conditions the catalyst showed to be stable for up to 90 hours, a TOF of 460 h^{-1} and TON of 40000 were obtained at 120 ℃ from an aqueous solution of FA/HCOONa (9:1 mole ratio).[44a] Interestingly, no inhibition of catalytic activity was observed up to a pressure of 750 bar, which is different from the observation previously made by Paonessa and Trogler.[36] Based on kinetic data and NMR experiments, two competing catalytic cycles were proposed for the reaction mechanism: the first pathway involves a cationic monohydride species, while the second pathway involves a neutral dihydride species.[44b] The authors suggested that the dihydride mechanism is predominant in the system as a result of its lower activation energy barrier (Scheme 1.9). Follow up work from the same group indicated TPPDS has comparable activity to TPPTS.[44c]

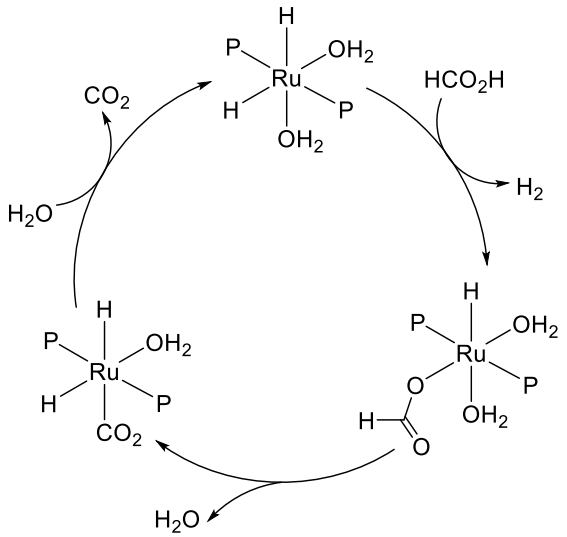

Scheme 1.9: Proposed dihydride pathway for FA dehydrogenation by a Ru^{II}/TPPTS catalyst, P = TPPTS[44b]

During a mechanistic study of various Ru precursors catalyzed dehydrogenation of FA, Wills and co-workers were able to identify a Ru formate dimer from the system, a related study showed addition of PPh_3 resulted catalyst deactivation due to the formation of a much less active Ru-phosphine dimer.[39] In 2011, Prakash and Olah reviewed the development of H_2 generation from FA by ruthenium carbonyl complexes. They also reported the isolation of a tetraruthenium hydride complex, which was indicated as an active catalyst or catalyst intermediate for FA decomposition.[45a] Later on, they reported the use of emulsions as reaction media, it was found that both the activity and the selectivity of reported catalysts were enhanced by adding surfactants.[45b] Very recently, Huang and co-workers reported dehydrogenation of FA catalyzed by a phosphine free Ru complex with N,N'-diimine ligand, a TOF of 12000 h^{-1} and a TON of 350000 at 90 °C were achieved yielding a high pressure (24 MPa) H_2 and CO_2 mixture.[46]

Apart from mono- and bidentate phosphine ligands, polydentate ligands were also employed for Ru catalyzed dehydrogenation of FA. In 2012, the Gonsalvi group showed that homogeneous Ru catalysts bearing the polydentate tripodal ligands 1,1,1-tris-(diphenylphosphinomethyl)ethane (triphos) and tris-[2-(diphenylphosphino)ethyl]-amine (NP_3) can selectively dehydrogenate FA.[47a] The results showed superior performance of complex [Ru(κ^3-triphos)(MeCN)$_3$](OTf)$_2$ with a TON of 10000 after 6 h, and recycling up to eight times giving a total TON of 8000 after *ca.* 14 h at 80 ℃ . Pidko and co-workers developed a Ru PNP-pincer catalyst for FA dehydrogenation, the catalyst also capable of hydrogenating CO_2 to formate.[47b] A ligand innocent mechanism was proposed by the authors for this reversible process.

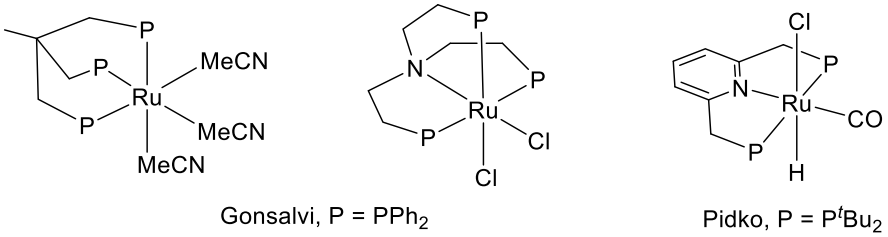

Scheme 1.10: Polydentate Ru complexes for FA dehydrogenation

In addition to Ru, another noble metal catalyst Ir was also extensively investigated for FA dehydrogenation reaction. Pioneer work of water soluble Ir complex catalyzed H_2 generation from FA was made by Himeda in 2009. Based on their previous report about a recyclable catalyst for the conversion of CO_2 into formate,[48a] a new Ir complex bearing proton-responsive ligand was developed for H_2 generation from FA. A remarkable TOF of 14000 h^{-1} at 90 °C (TOF = 450 h^{-1} at 40 °C) from a 2 M formic acid solution was obtained.[48b] Notably, the activity was strongly dependent on the pH as well as the electronic effect of the substituent in the bipyridine ligand, an increase of the pH caused a decrease of TOF and conversion. Subsequent research by Fujita led to the development of a more active Ir catalyst which enabled the reversible H_2 storage in FA,[48c] a TOF up to 228000 h^{-1} at 90 °C and a TON of 308000 at 80 ℃ was achieved for dehydrogenation of FA. Moreover, an Ir complex with a non-functionalized pyridyl imidazoline ligand turned out to be active in pure FA solution without any base additives.[48d] FA was dehydrogenated completely in low pH solution, as a consequence, 1020 L of gas was produced and a TON of 2000000 was achieved using 20 mol of FA and 10 μmol of Ir complex in 363 h. Very recently, Li and Beller developed an efficient route for H_2 production by employing similar bifunctional Ir complexes. H_2 generation from non-food-related biomass was realized in a one-pot, two-step fashion with up to 95% yield, CO and CH_4 content was below 22 and 2 ppm, respectively.[49] This system allows streamlined conversion of biomass to electricity via H_2, which is of interest to promote the hydrogen economy.

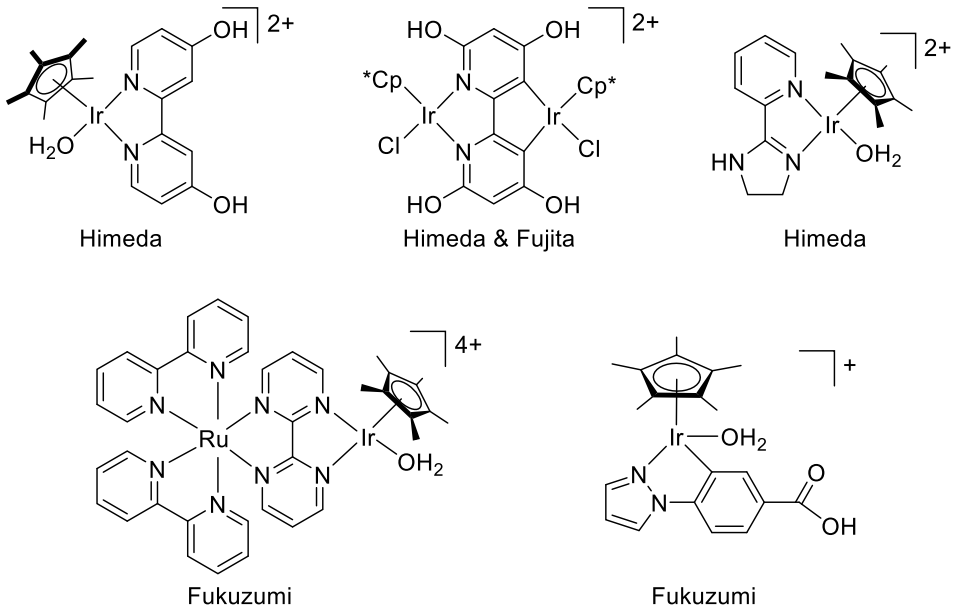

Scheme 1.11: pH-tunable Ir-complexes for catalytic FA dehydrogenation

Fukuzumi and co-workers reported a heterodinuclear iridium−ruthenium complex catalyzed dehydrogenation of FA, where they found that the highest TOF (426 h^{-1}) could be obtained at pH 3.8 which agrees with the pKa value of FA, such a saturation dependence of TOF on [$HCOO^-$] indicates that H_2 is produced via the formate complex.[50a] For the first time, an unusually large tunneling effect was observed in H_2O vs D_2O. The selective formation of HD was also achieved by adjusting pH, providing a convenient way to produce HD. Later on, a monometallic phenylpyrazolyl organoiridium catalyst was prepared for room temperature H_2 generation from FA, a maximum TOF value of 1880 h^{-1} was obtained at pH 2.8,[50b] which is remarkably higher than the one achieved with the heterodinuclear catalyst.

Results from Nozaki's group showed that an Ir pincer catalyst is able to decompose FA in the absence of base, however with much lower activity than in the presence of amines.[51] In 2013, Reek and co-workers designed an iridium–bisMETAMORPhos complex featuring an internal base functionality based on $^-O-S=N/O=S-NH$ interconversion[52] (Scheme 1.12). Initial experiments with the pure catalyst at 65 °C afforded TOF of 929 h^{-1} and 652 h^{-1} with and without triethylamine, respectively. In the presence of acacH (originated from Ir precursor, acac = acetylacetonate), the catalyst existed as a mixture of several isomeric forms in solution. Interestingly, the isomeric mixture led to an improved activity with a TOF up to 1050 h^{-1} under base free conditions. Besides, the Ir complex is tolerant toward air and stable in pure FA, which makes the Ir catalyst attractive for the development of a practical hydrogen generation device.

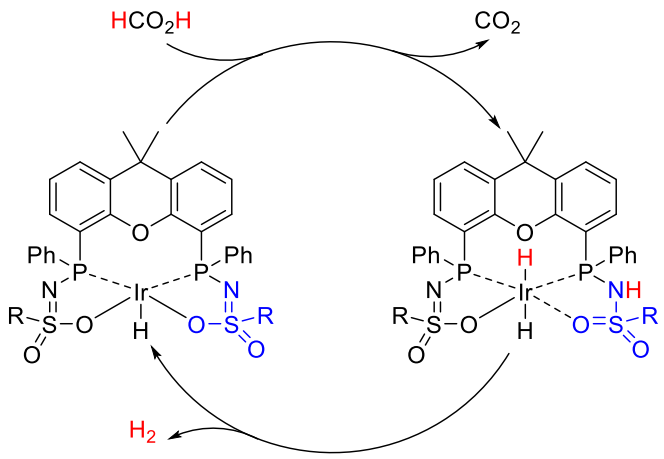

Scheme 1.12: Ir complex bearing internal base functional ligand catalyzed dehydrogenation of FA[52]

Recently, Williams and co-workers reported a novel Ir complex with a pyridylphosphine ligand for FA dehydrogenation.[53] The catalyst precipitated as a pale orange solid from the solution at the end of the reaction, this heterogeneous character allows straightforward recovery of the catalyst. The catalyst could be recycled up to 50 times under aerobic conditions, yielding over 66000 turnovers and 89% FA conversion at 90 °C without loss of activity. The first homogeneous system that operated in neat FA was also developed based on this catalyst. However, CO contamination was observed in this case due to thermal decomposition of FA, which was suppressed in the presence of 10 vol % water or at a high sodium formate concentration (50 mol % with respect to FA). Mechanistic studies revealed that the generation of a formate-bridged dimer from the precatalyst with treatment of FA is of critical importance for the observed activity (Scheme 1.13).

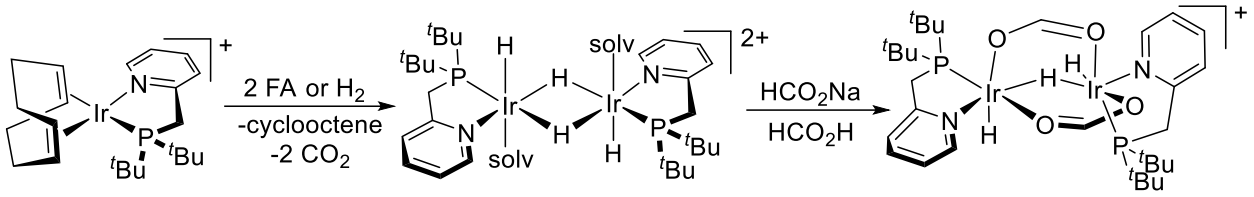

Scheme 1.13: Formation of a formate-bridged Ir dimer[53]

1.3.2 Dehydrogenation of alcohols

Compared with FA, the dehydrogenation of alcohols to obtain H_2 is less investigated. Traditionally, alcohols were dehydrogenated to obtain the desired oxidized carbonyl products for the purpose of organic synthesis. This process can be carried out in the presence of a sacrificial reagent, which is concurrently hydrogenated, known as transfer hydrogenation process. The Meerwein–Ponndorf–Verley[54] reduction and its reverse reaction the Oppenauer oxidation[55] are

among the most well-known examples, involving the transfer hydrogenation between alcohols and ketones, both of which were discovered almost a hundred years ago.

Acceptorless alcohol dehydrogenation has received much attention nowadays because of its atom-economical and environmentally friendly merits.[19] Early research on acceptorless alcohol dehydrogenation was already started in the 1960s when Charman reported dehydrogenation of isopropanol catalyzed by $RhCl_3$, while decreased activity was observed as Rh metal precipitated from solution.[56a] Later, improved stability was obtained by using rhodium-tin complexes.[56b] In the 1970s, Robinson and co-workers employed ruthenium and osmium complexes of the general formula $[M(OCOR_F)_2(CO)(PPh_3)_2]$ (RF = CF_3, C_2F_5, or C_6F_5) as catalysts for the dehydrogenation of primary and secondary alcohols in the presence of small amounts of R_FCOOH.[57] One decade later, the group of Cole-Hamilton shifted the attention of this process to the production H_2 from alcohols, $[Rh(bipy)_2]Cl$ and $[RuH_2(N_2)(PPh_3)_3]$ were employed as catalysts, TOF >100 h^{-1} was obtained, and the activity could be further enhanced under light irradiation.[58]

On the basis of these pioneering works, several novel systems were developed for acceptorless alcohol dehydrogenation. In 2004, Beller and co-workers described a Ru catalyzed dehydrogenation of *iso*-propanol, a Ru precursor $RuCl_3 \bullet xH_2O$ in the presence of a phosphine ligand 2-di-*tert*-butyl-phosphinyl-1-phenyl-1*H*-pyrrole showed to be active catalyst. TOF up to 155 h^{-1} was obtained after 2 h at 90 ℃ , a temperature lower than those previously reported.[59a] Subsequently, an improved Ru catalyst was reported with a combination of $[RuCl_2(p\text{-cymene})]_2$ and TMEDA, a TOF of 519 h^{-1} and catalyst stability over 250 h were achieved.[59b] Aside from *iso*-propanol, 1-phenylethanol and ethanol were also tested, however, almost one order of magnitude lower in activity was found for these substrates.

In 2011, the Beller group developed an efficient H_2 evolution from alcohols. A range of ruthenium precursors and PNP pincer ligands were evaluated for the dehydrogenation of *iso*-propanol.[60a] The *in-situ* system consisting PNP^{iPr} ligand and $[RuH_2(PPh_3)CO]$ precursors gave remarkable TOF of 2048 h^{-1} in 2 h and 1109 h^{-1} in 6 h respectively under base-free conditions under refluxing, a higher TOF of 8382 h^{-1} in 2 h was obtained when reducing the catalyst loading by a factor of ten. Ethanol dehydrogenation was also performed with this *in-situ* system giving a TOF of 1483 h^{-1}. An outer-sphere mechanism concerning metal-ligand cooperation process was proposed for this system: upon heating, the *in-situ* formed Ru-dihydrido complex lose one molecule of hydrogen, giving the active Ru-amido intermediate, the latter then interacts with alcohols through an outer-sphere mechanism[61] to give the dehydrogenative products and regenerate the Ru-dihydrido. (Scheme 1.14) During the following research, they employed a defined ruthenium PNP pincer complex for the dehydrogenative condensation of ethanol towards

ethyl acetate. An impressive TOF exceed 1000 h^{-1} was obtained in 2 h under refluxing, and the TON reached 15400 after 46 h.[60b]

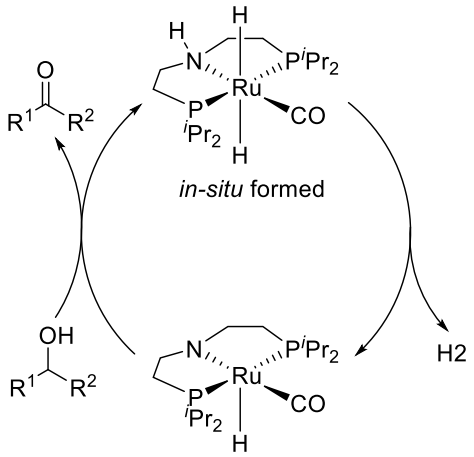

Scheme 1.14: Ru PNP pincer complex catalyzed dehydrogenation of alcohols[60a]

Even though the ruthenium pincer catalyst showed very high activity in alcohol dehydrogenations, the application of the system is still limited for H_2 storage since only one molecule of H_2 per molecule of substrate can be obtained in these reactions, leading to a relative low hydrogen content. In 2013, an aqueous phase reforming of methanol was reported by Beller and co-workers, this system allows for completely decomposition of methanol to yield three equivalents of H_2 along with one equivalent of CO_2. Molecularly defined ruthenium pincer catalysts were employed as catalysts for dehydrogenation of a 9:1 mixture of methanol and water under highly basic conditions. A TOF over 2000 h^{-1} was obtained at 91 ℃ , with a catalyst amount of less than 1 ppm, a long-term experiment of more than 23 days resulted in a TON greater than 350000.[62a] Subsequent mechanistic studies showed the C-H cleavage steps occur through the inner-sphere coordination of the methanolate, gem-diolate, and formate, which is contrary to previously postulated outer-sphere mechanism.[62b] (Scheme 1.15) It was demonstrated that the base enables this energetically favorable anionic, inner-sphere pathway, furthermore, it makes the key step (**II** to **III**) thermodynamically more feasible by absorbing the dehydrogenation byproducts, namely, CO_2.

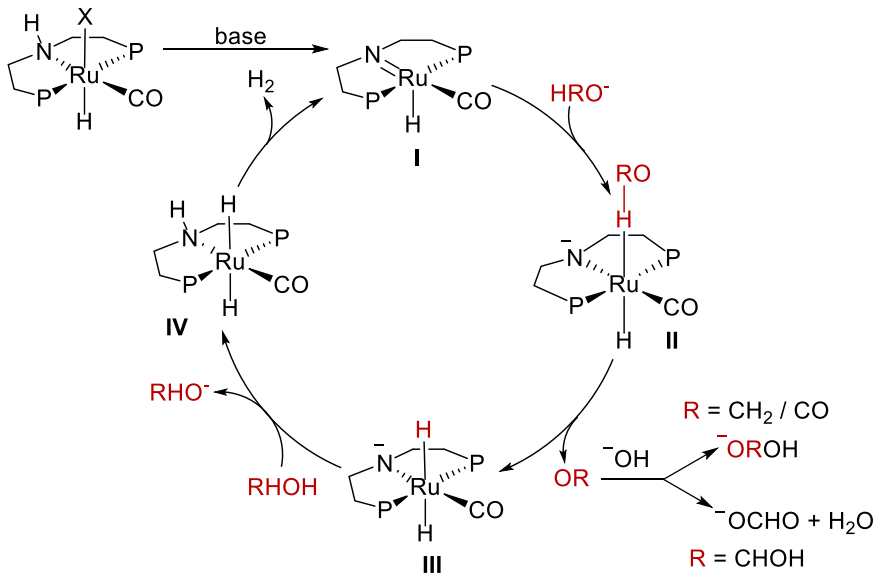

Scheme 1.15: Proposed mechanism for aqueous methanol reforming[62b]

In parallel with Beller's work, the groups of Trincado and Grützmacher reported the usage of a homogeneous ruthenium complex based on the chelating bis(olefin) diazadiene ligand for H_2 production from methanol-water mixture. At 0.5 mol % catalyst loading, 80% conversion of MeOH was achieved after a reaction time of 10 h at 90 ℃ with tetrahydrofuran as cosolvent (H_2 storage capacity of 42 g of H_2 per liter of solution). FA also turned out to be dehydrogenated smoothly by this catalyst and a TOF of 24000 h^{-1} was observed at the initial stage of the reaction.[63] Mechanistic studies indicated that the trop2dad ligand behaves as a chemically non-innocent ligand through the diazadiene backbone (Scheme 1.16).

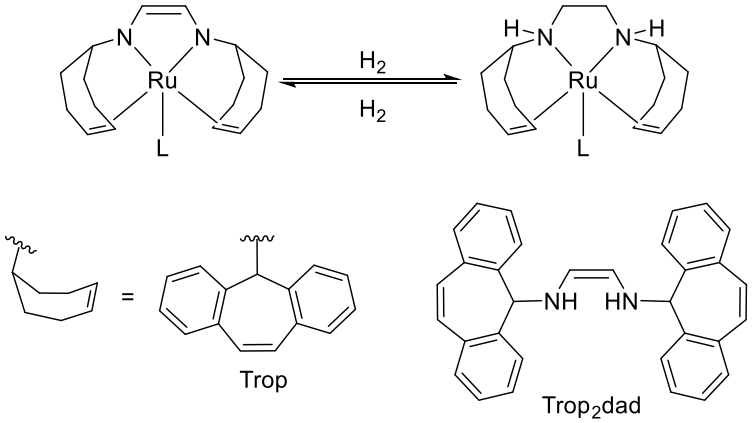

Scheme 1.16: Non-innocent cooperative effect of Ru-diazadiene–olefin complex[63]

Pincer complexes with aromatic nitrogen-containing heterocyclic backbones represent another well-known type of catalysts featuring metal-ligand cooperation. At the beginning of this century, Milstein's group introduced a new mode of metal-ligand cooperation, involving

aromatization−dearomatization of ligands. Pincer-type ligands based on pyridine or acridine exhibit such cooperation, leading to unusual bond activation processes and novel, environmentally benign catalysis.[64] In 2004, they reported an example of Ru pincer complexes catalyzed dehydrogenation of secondary alcohols. However metal-ligand cooperation was not mentioned in that publication.[65] Subsequently, new Ru PNN pincer complexes were developed by the same group for facile conversion of alcohols into esters and H_2, where the aromatization−dearomatization transformation was observed. The dearomatized Ru pincer complex allowed the reaction take place under neutral conditions.[66a] Later, the same catalyst was employed for dehydrogenative condensation of alcohols and amines to amides, along with release of H_2.[66b] A mechanism involving labile nitrogen coordination from the PNN pincer ligand was proposed by the authors (Scheme 1.17). Firstly, the alcohol is dehydrogenated to the corresponding aldehyde via β-H elimination, subsequent reaction of aldehyde with amine forms the hemiaminal intermediate, which can be further dehydrogenated to yield amide and a second equivalent of H_2.

Afterwards, a series of different type PNN/PNP pincer complexes were prepared by Milstein and co-workers, which showed promising activities in dehydrogenative reactions including direct conversion of alcohols to acetals, esters and carboxylic acids (Scheme 1.18).[67] Recently, they reported an efficient system for methanol dehydrogenation catalyzed by complex **D**, a conversion of methanol up to 82% was obtained and the catalyst could be reused over a period of about one month without detectable decrease in catalytic activity.[68]

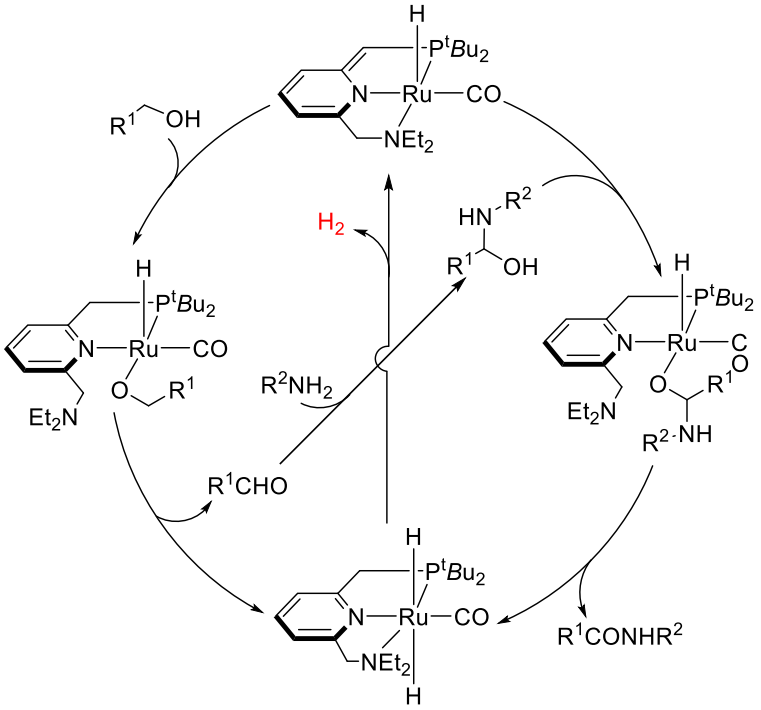

Scheme 1.17: Proposed mechanism for the direct acylation of amines by alcohols[66b]

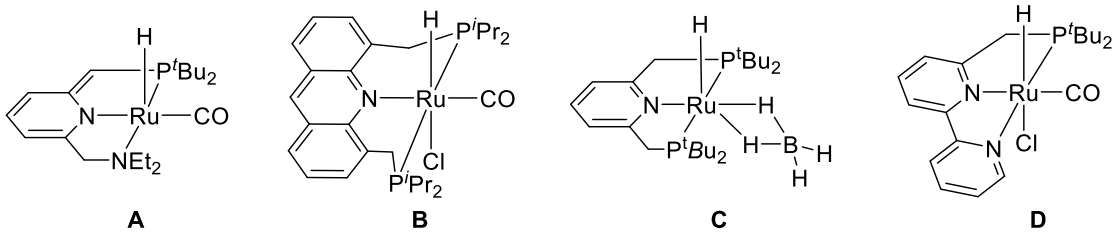

Scheme 1.18: Ru pincer complexes developed by Milstein and co-worker

Ir represents another intensively studied noble metal system aside from Ru. One of the most well-known Ir system is the half sandwich Ir complexes developed by Yamaguchi, Fujita and Fukuzumi. In 2007, Yamaguchi and co-workers reported a Cp*Ir complex having 2-hydroxypyridine as a functional ligand for the dehydrogenation of alcohols. TONs up to 2000 were obtained for secondary alcohols, while the activity for primary alcohols turned out to be much lower.[69a] Later, a functional C,N-chelate ligand was developed for Ir with improved activity for both primary and secondary alcohols dehydrogenation, mechanistic investigations revealed that a hydrido iridium complex is the catalytically active species.[69b] In 2012, together with Fujita, they established a water-soluble Ir system bearing a functional bipyridine ligand for dehydrogenation of alcohols in aqueous media, it is noteworthy to mention that the catalyst could be recycled after reaction since it separated readily from organic phase.[69c] Follow-up work showed this system was also suitable for H_2 production from methanol water mixtures, continuous H_2 production was accomplished over150 h giving 210 mmol of H_2, with a TON 10510. It was found to be crucial to keep pH value between 8 to 12 in order to maintain the active anionic catalyst species, since at lower pH, the formation of neutral and cationic species was observed which resulted in reduced activity.[69d] At the same time, Fukuzumi and co-workers described an interesting C,N cyclometalated Ir complex which allows dehydrogenation of alcohols in water at room temperature, the performance of this system also has a dependence on the pH value.[69e]

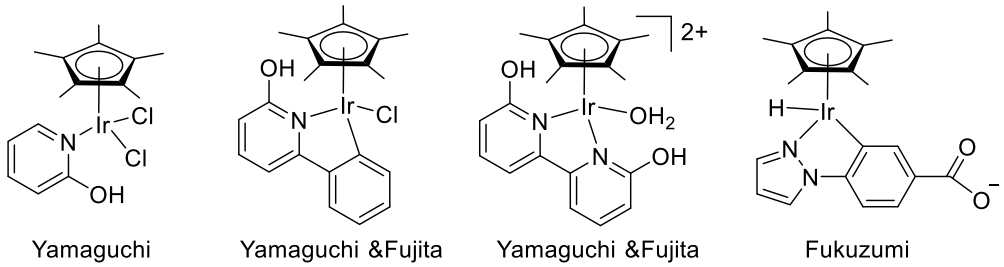

Scheme 1.19: Half sandwich Ir complexes for alcohols dehydrogenation

In 2015, a family of iridium bis(N-heterocyclic carbene) catalysts were presented by Crabtree and co-workers for methanol dehydrogenation.[70a] The activity of the catalysts can be varied by altering the substituents on the N-heterocyclic ligands, with reactivity decreased in the order of

^{n}Bu < Et < Me, a similar observation for the dehydrogenation of sugar alcohols noted earlier by the same group.[70b] TONs of up to 8000 were achieved with 6.7 M aqueous KOH solution, and 3 mL of MeOH as both a reagent and a solvent after 40 h at 91 °C.

In addition to these results, Gelman and co-workers designed a new iridium PCP pincer catalyst based on dibenzobarrelene as a ligand scaffold.[71] This unique scaffold facilitates intramolecular cooperation between the structurally remote functionality and the metal center (Scheme 1.20). A series of alcohols were dehydrogenated in high yield to give ketones and carboxylates under basic conditions.

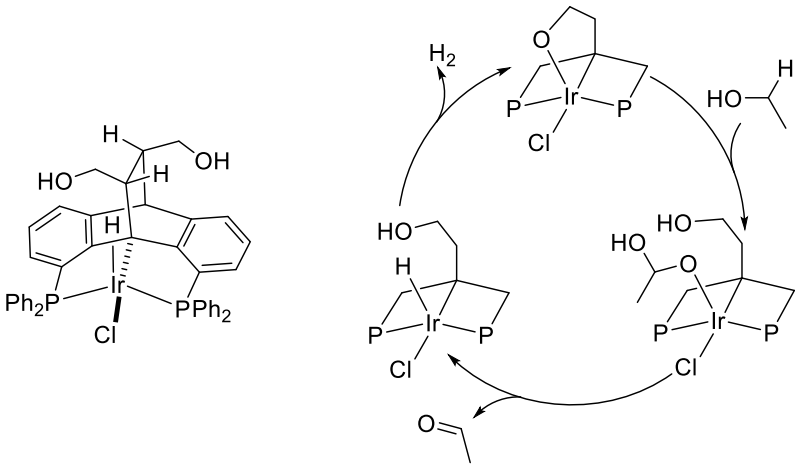

Scheme 1.20: Ir PCP pincer complex and its catalytic dehydrogenation of alcohols[71]

1.4 Non-noble metal catalyzed dehydrogenation reactions

Even though a lot of noble metal catalysts showed high activity and stability in FA and alcohols dehydrogenations, their applications are still limited by the fact of high cost as well as high toxicity of these metals which causes environmental concerns. Nowadays, first-row metals or non-noble metals (Mn, Fe, Co, Ni, Cu) are emerging as promising alternatives, because they are more abundant, less toxic compare with their 4d/5d homologues. During the past ten years, a lot of non-noble catalysts especially those based on Fe and Mn have been reported for dehydrogenations, some of which even showed higher activities than the system based on noble ones.[72] In the following part, examples of non-noble metal Fe, Ni and Cu catalyzed dehydrogenation reactions will be introduced, while dehydrogenation reactions catalyzed by Co and Mn will be discussed in chapters 2 and 3 respectively.

1.4.1 Non-noble metal catalyzed dehydrogenation of fromic acid

The first attempt to generate H_2 from FA/amine mixture using non-noble metals was made by Wills and co-workers. In 2009, during their investigation of Ru catalyzed H_2 production from

FA/amine, they also tested a series of different non-precious metals including Co, Fe and Ni, however, the catalytic performance of these metals was very limited (TONs less than 5).[39]

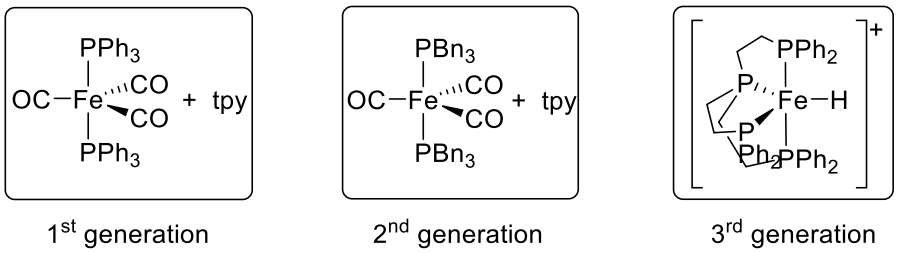

Scheme 1.21: Iron catalysts for the dehydrogenation of FA developed by Beller and co-workers

During the last decade, novel homogeneous non-precious metal based catalysts were explored for FA dehydrogenation. One of the major breakthrough was made by the Beller group in 2010 when they explored the versatility of several non-noble metals, especially Fe, in combination with various ligands. Iron carbonyl [$Fe_3(CO)_{12}$] was applied *in-situ* together with different phosphines and terpyridines for FA/amine dehydrogenation under visible light irradiation.[73a] After extensive examination, a system formed from [$Fe_3(CO)_{12}$]/PPh_3/2,2′:6′,2″-terpyridine turned out to be an active catalyst. H_2 was generated with an initial TOF of 200 h^{-1}, however the catalyst deactivated quickly due to CO dissociation. By changing the N-ligands, the stability of this system could be slightly improved and a TON over 100 was observed. Spectroscopic and computational investigations revealed PPh_3 is necessary to generate the active species while *N*-ligands can enhance the stability of the resulting system. A mechanism involves iron hydride species which are generated exclusively under visible light irradiation was proposed.

Interestingly, when the phenyl groups on the phosphine are replaced by benzyl substituents, a 2-fold-enhancement of catalytic activity and stability (TON 1266) was observed. It was suggested that cyclometallation of the benzyl moiety in PBn_3 to the Fe centre is possible and [$Fe(CO)_3(PBn_3)_2$] is proposed to be an active species.[73b] However, a high content of CO in the gas product was detected, which limits the application of this system.

On the basis of this pivotal work, a third generation of Fe catalyst was developed by the group of Beller and Laurenczy. In 2011, they reported a highly active system formed *in situ* from $Fe(BF_4)_2 \cdot 6H_2O$ and tetradentate tris[*2*-(diphenylphosphino)ethyl]phosphine (tetraphos, PP_3).[74a] Notably, a biodegradable solvent propylene carbonate (PC) was employed in this system, FA was fully converted within 24 h at 40 °C without light irradiation and under basic free conditions. The *in-situ* system generated from Fe/PP_3 showed similar activity (TON_{3h} = 1942) as the preformed cationic iron complex [$FeH(PP_3)$]BF_4 in combination with another equivalent of PP_3 ligand. The extra ligand was suggested to be necessary for the formation of the formate intermediate, which substantially enhances the reaction rate. In the absence of second equivalent of ligand, a significant lower productivity was observed (TON_{3h} = 825). Surprisingly, the application of the

iron chloride analogue $[FeCl(PP_3)]BF_4$ under the same condition was entirely inactive, this poisoning effect was further confirmed by adding chloride to the active system of $Fe/2PP_3$. Besides, the performance of the catalyst decreases significantly if the water content in the system is too high. In a continuous set up, FA was added at 0.27±0.04 mL min^{-1} via pump to a solution of $Fe/4PP_3$ in propylene carbonate, the system was stable for 16 h generating an average gas flow (H_2/CO_2) of 325.6 mL min^{-1} with less than 20 ppm of CO. Remarkably, a TON of 92000 and TOF of 5390 h^{-1} was observed at 80 °C.

Kinetic studies, NMR experiments as well as DFT calculations were performed in order to get a better understanding of the system, two possible catalytic circle starting from the same active species $[FeH(PP_3)]^+$ were proposed (Scheme 1.22). In the left cycle, the hydride of the Fe-H species is protonated by FA, releasing H_2 and a formate complex $[Fe(HCO_2)(PP_3)]^+$. In the next step, β-H elimination occurs and after dissociation of CO_2, the active species Fe-H is regenerated. While in the right catalytic cycle, formate coordination to the Fe-H complex happens prior to β-H elimination, generating a neutral hydrido formato species. In this case, the hydride in Fe-H species acts as a spectator ligand which is not involved in the catalysis.[74a] Later, Laurenczy and co-workers extended this system for dehydrogenation of FA in aqueous media by changing the PP_3 ligand to a water soluble ligand, *m*-trisulfonated-tris[2-(diphenylphosphino)ethyl]phosphine sodium salt (PP_3TS),[74b] a TOF of 240 h^{-1} was obtained at 80 °C with full conversion of FA.

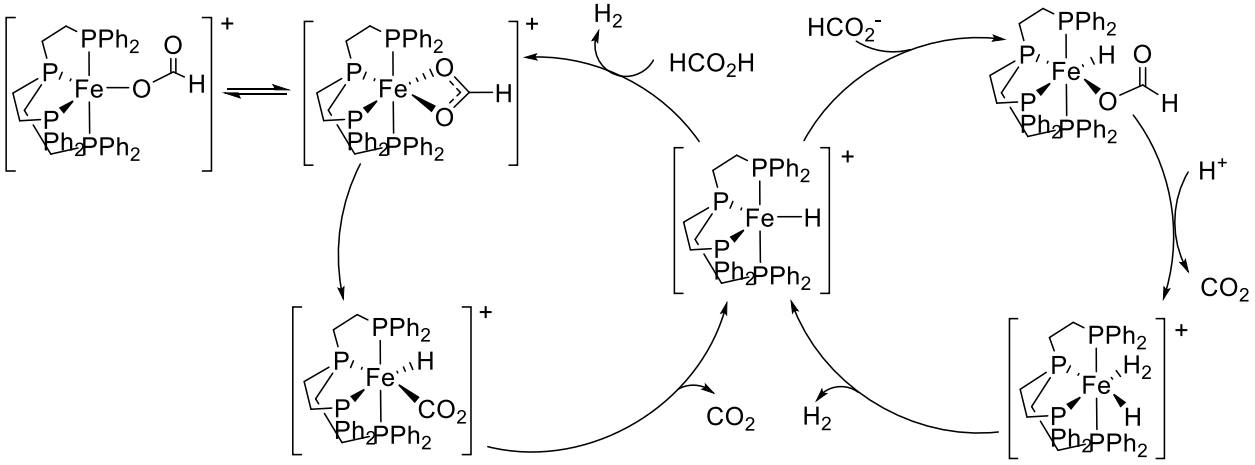

Scheme 1.22: Proposed mechanism for H_2 evolution from FA catalyzed by $[FeH(PP_3)]^+$[74a]

In 2015, the group of Gonsalvi also disclosed base-free H_2 production from FA utilizing $Fe(BF_4)_2 \cdot 6H_2O$ in combination with a tetraphosphine ligand 1,1,4,7,10,10-hexaphenyl-1,4,7,10-tetraphosphadecane (P_4).[75] Surprisingly, initial tests showed that the well-defined Fe complex was inactive in the dehydrogenation of FA in PC at 40 °C, whereas the in situ formed $Fe(BF_4)_2 \bullet 6H_2O/P_4$ (meso/rac = 3) yielded 4% FA conversion after 6 h. When rac-P_4 was used at

a Fe/ligand ratio of 1:2, complete FA conversion was accomplished with a TOF of 139 h^{-1}. However, recycling tests at 40 °C showed a 70% decrease in catalytic activity during the third cycle, with higher Fe/ligand ratio (1:4), improved activity was obtained (TON = 6061, initial TOF = 1737 h^{-1}), while the pure *meso*-P_4 ligand was significantly less active regardless of the Fe/P_4 ratio employed. In addition, this system is also capable of bicarbonate hydrogenation.

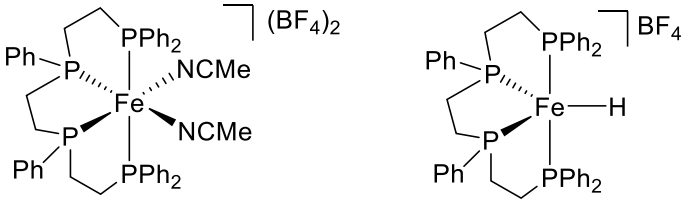

Scheme 1.23: Fe/P_4 system developed by Gonsalvi and co-workers for FA dehydrogenation[75]

Milstein and co-workers reported the first example of selective FA dehydrogenation with an iron PNP pincer complex at 40 °C in the presence of trialkylamines. When FA was decomposed in a 1:1 mixture with trimethylamine in THF a TOF of 836 h^{-1} was achieved in the first hour, long term experiments resulted in full conversion of 1 mol of FA in the presence of 50% mol NEt_3 in dioxane at 40 °C after 10 days with a catalyst loading of 0.001 mol %, reaching a TON of 100000.[76a] The authors investigated the mechanism of this system experimentally and computationally. Reaction of the Fe dihydride complex with a stoichiometric amount or a slight excess of FA leads rapidly to the formation of the hydride η^1-formate complex, and concomitant liberation of H_2, CO_2 liberation from the hydride formate complex to regenerate the dihydride complex was observed upon exposure of the formate complex to vacuum, or upon prolonged stirring of its solution under a nitrogen atmosphere. DFT calculations suggest that the conversion of formate complex to dihydride complex involves a reversible, nontraditional β-hydride elimination process. This step is strictly intramolecular and does not involve the dissociation of the formate anion followed by recoordination through the hydrogen atom.[76a] Recently, a new family of Fe PNP pincer complexes based on the 2,6-diaminopyridine scaffold were described by Kirchner and Gonsalvi for H_2 generation from FA under basic conditions. [76b] It was shown that the methylated diaminopyridine complex (R' = Me) exhibits much higher activity than the non-methylated on (R' = H), with a concentration of FA of 10 M in PC solution, the highest TOF of 2635 h^{-1} and full conversion after 6 h at 80 °C was achieved.

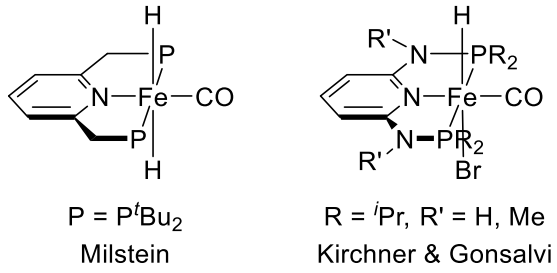

Scheme 1.24: Fe-PNP pincer complexes for FA dehydrogenation under basic conditions

In 2014, the groups of Hazari and Schneider prepared a pincer-ligated five-coordinate iron amido species, upon addition of FA, it formed a six coordinate formate complex, both Fe complexes showed activity in FA dehydrogenation from FA/TEA. Interestingly, when these catalysts were used in the presence of a Lewis acid (LA) cocatalyst such as $LiBF_4$ or NaCl, neither base nor additional ancillary ligand was required. Outstanding TONs of 983600 and a TOF of 197000 h^{-1} were obtained in the presence of 10 mol % $LiBF_4$ from a dioxane solvent of FA at 80 °C.[77] The dramatically enhancement effect of the LA was investigated, in agreement with Milstein's speculation,[76a] a rearrangement of an O-bound formate to an H-bound formate prior to the turnover limiting decarboxylation was proposed by the authors. Stoichiometric experiments suggest that the LA is crucial for facilitating decarboxylation, as it is able to stabilize the negative charge that develops on the formate ligand in the transition state (Scheme 1.25).

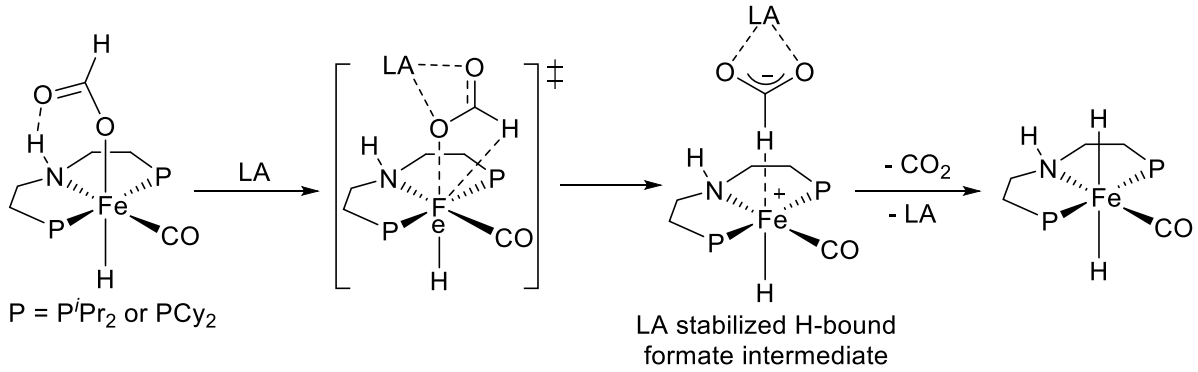

Scheme 1.25: Proposed pathway for LA assisted decarboxylation of iron formate

Even though less explored than Fe, catalysts based on Ni and Cu have also been reported for FA dehydrogenation. In 2015, Enthaler and Junge reported the application of Ni PCP pincer complexes for H_2 generation from FA/amine as well as for hydrogenation of bicarbonate, a TON of 626 was obtained for dehydrogenation.[78a] Ravasio and co-workers investigated decomposition of different FA/amine adducts by various simple Cu precursors, unfortunately, only limited activity (TONs less than 30) was observed.[78b]

1.4.2 Non-noble metal catalyzed dehydrogenation of alcohols

The first example of structurally defined iron pincer complexes able to catalyze the dehydrogenation of methanol was described by Beller and co-workers in 2013.[79a] Based on their expertise on H_2 generation from alcohols, new iron pincer compounds were synthesized and tested under similar conditions previously employed in Ru catalyzed methanol dehydrogenation.[62] With 1 μmol catalyst loading, the highest productivity (TON = 9834) was obtained using 9:1 MeOH/H_2O mixture at 91 °C before the system deactivates. Improved stability was observed with addition of an excess of the PNP ligand. Later, this complex was tested for intramolecular dehydrogenative coupling of diols and amino alcohols to lactones and lactams respectively, good to excellent yields were obtained with H_2 as the sole by-product.[79b] Concurrently, the groups of Jones and Schneider investigated the performance of the same complex in acceptorless reversible dehydrogenation-hydrogenation of alcohols and ketones.[80] Secondary alcohols were dehydrogenated to the corresponding ketones, while primary alcohols were dehydrogenated to esters and lactones. Mechanistic studies showed that metal−ligand cooperativity plays a crucial role in the reaction and a five coordinate iron amido hydrido species is proposed to be the active intermediate in the dehydrogenation reaction.

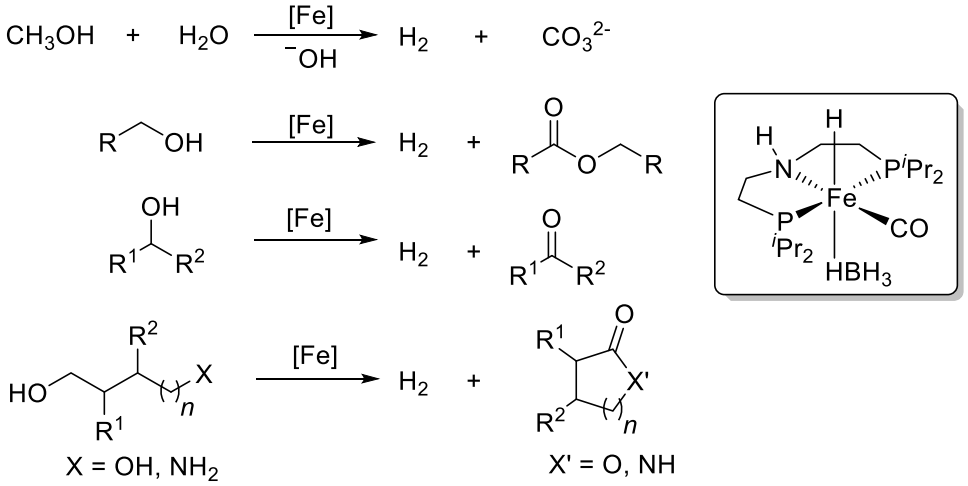

Scheme 1.26: Iron pincer complex catalyzed dehydrogenative reactions

In accordance to their observation of Lewis acid enhanced Fe pincer catalyzed H_2 evolution from FA, the groups of Hazari, Bernskoetter and Holthausen recently investigated the effect of Lewis acid in methanol dehydrogenation. It was shown that the use of 10 mol % of the Lewis acid $LiBF_4$ as a cocatalyst significantly increased the catalytic activity, with 0.006 mol% Fe pincer catalyst and 10 mol% $LiBF_4$ under reflux, TON up to 51000 after 94 h was reported from a 4:1 MeOH/H_2O mixture,[81] which represents the highest productivity for first-row transition-metal-catalyzed methanol reforming so far. Mechanistic experiments suggest a stepwise process based

on metal−ligand cooperativity, while the role of the Lewis acid cocatalyst was explained by DFT calculations.

In 2016, Chang and co-workers reported o-aminophenol (apH_2) based iron photocatalysts *trans*-[$Fe^{II}(apH)_2(MeOH)_2$] promoted dehydrogenation of anhydrous methanol at room temperature.[82] Under excitation at 289±10nm and in the absence of additional photosensitizers, these photocatalysts generate hydrogen and formaldehyde from anhydrous methanol with external quantum yields of 2.9±0.15%, 3.7±0.19% and 4.8±0.24%, respectively. Mechanistic studies suggested that hydrogen radicals induced by photocatalysis trigger the reaction.

Except for Fe, Ni complexes have also been explored for dehydrogenation reactions. As inspired by the work from the groups of Fujita and Yamaguchi,[69] Jones and co-workers investigated a Ni complex supported by tris(3,5-dimethylpyrazolyl)borate (Tp') ligand and 2-hydroxyquinoline ancillary ligand for alcohols dehydrogenation, carbonyl compounds were obtained in good yields concomitant with H_2 production.[83a] Mechanistic investigations highlighted the critical role of the 2-hydroxyquinoline ligand in the catalysis and a concerted dehydrogenation pathway was proposed. In 2016 Datta and Goswasmi reported an interesting Ni system for the dehydrogenation of alcohols.[83b] In contrast to previous reported systems, which were either based on metal centered catalysis or based on metal-ligand cooperative catalysis, this system is exclusively ligand-mediated dehydrogenation. A hydrogenated intermediate, [$Ni^{II}Cl_2(H_2L)$], was isolated and characterized, suggesting azo−hydrazo couples in the system. In addition, Zhang and Peng recently reported Ni complexes bearing pyridine-based NNN type pincer ligands catalyzed dehydrogenation of primary alcohols to carboxylic acids.[83c] Etherification of the alcohols was observed in the system which provides the oxygen needed for the second dehydrogenation step.

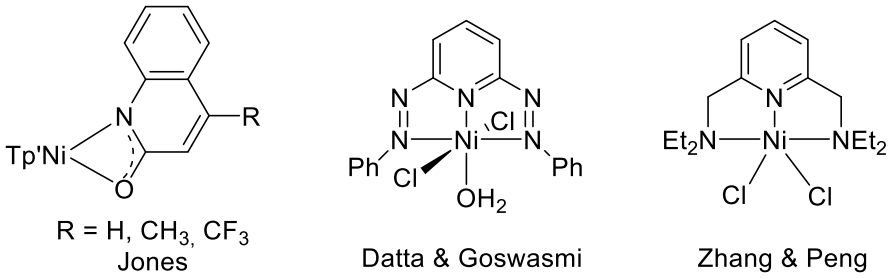

Scheme 1.27: Ni complexes reported for the dehydrogenation of alcohols

1.5 Objective of this research

As described above, a variety of noble and non-noble metal based systems were developed for dehydrogenation reactions. In general, those catalysts based on non-noble metals are less developed and their activity/stability still needs to be improved. This work mainly focus on the

development of more efficient catalysts based on non-noble metals for dehydrogenation reactions, thus contributing to the H_2 storage technology using organic liquid compounds.

Co and Mn are the metals of choice for the development of new catalysis system in combination with different types of bidentate tripodal and even multidentate ligands. The influence of the metal center and the coordinating ligand will be investigated, catalyst development will be accompanied by kinetic and mechanistic studies to gain further insight on how the catalysts act, while this understanding help to increase the activity and stability of the catalyst, therefore the catalyst performance can be improved in an iterative way. Besides, the obtained knowledge will also help to understand other related process such as hydrogenation and dehydrogenative coupling reactions.

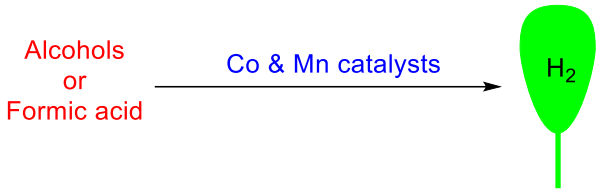

Scheme 1.28: Objective of this research: non-noble metal catalyzed dehydrogenation reactions

2 Cobalt catalyzed dehydrogenation of formic acid

2.1 Background

Cobalt is one of the most abundant transition metals in earth crust, it has been used to color glass since the bronze age. Nowadays, it is usually produced as a by-product of copper and nickel mining. Cobalt is is the active center of a group of coenzymes called cobalamins, vitamin B_{12}, the best-known example of this type, is an essential vitamin for all animals.

Cobalt has been used as catalysts ever since the discovery of hydroformylation reactions,[84] although it was later often replaced by more efficient iridium- and rhodium-based catalysts. During the last decade, there was a renaissance of cobalt catalyzed reactions mainly due to the high demand of green chemistry and the diverse reactivities of cobalt. A variety of cobalt complexes have been explored for polymerization, cross coupling C-H bond functionalization, (transfer)hydrogenation, hydrofunctionalization and dehydrogenative reactions.[85]

For example, in 2012 Hanson an co-workers reported a novel aliphatic PNP pincer Co(II) complex for the hydrogenation of unsaturated double bonds under mild conditions. Substrates including olefins, ketones, aldehydes, and imines are hydrogenated smoothly to the corresponding saturated compounds (Scheme 2.1).[86a] Later, they realized the synthesis of imines from alcohols and amines based on a strategy of cobalt catalyzed acceptorless alcohols dehydrogenation by the same complex.[86b] In addition, examples for transfer hydrogenation of carbonyl and imine groups were also shown by the group.[86c]

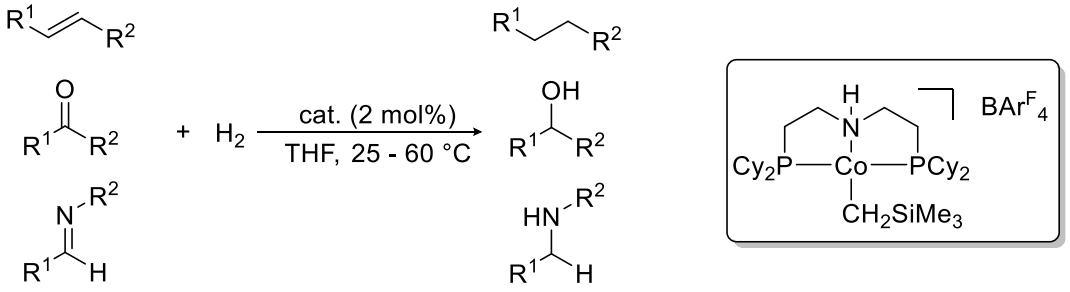

Scheme 2.1: Co catalyzed hydrogenation reported by Hanson and co-workers

Subsequent mechanistic studies by the same group revealed that the hydrogenation of olefins and the dehydrogenation of ketones follow different pathways.[87] In the olefin reduction cationic Co(II) species were proposed as active intermediates, while the reduction of ketones involves a Co(III) resting state which was characterized experimentally (Scheme 2.2).

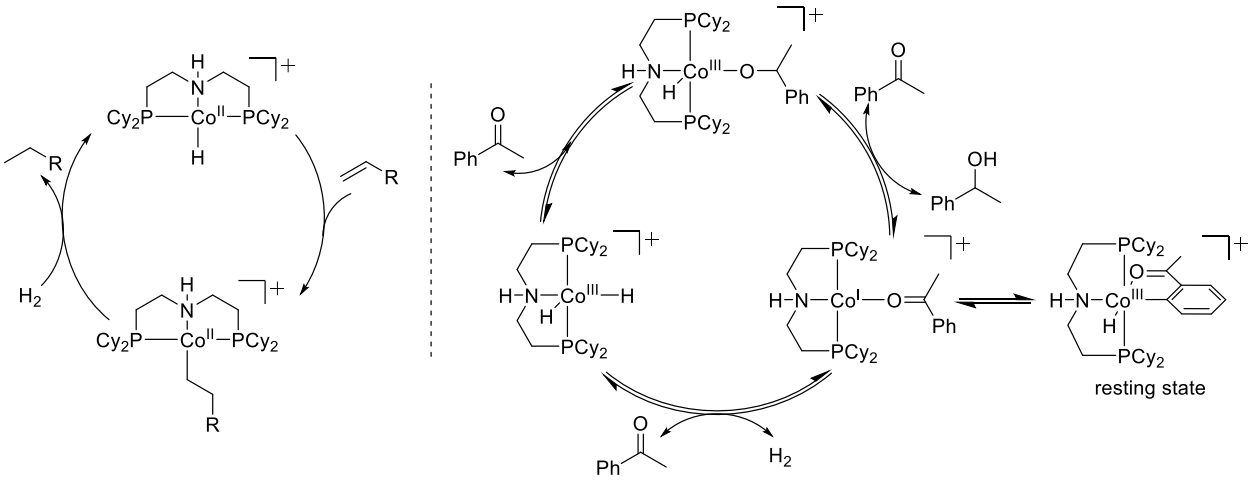

Scheme 2.2: Proposed mechanism for Co catalyzed hydrogenation of olefins and acetophenone[87]

At the same time, the group of Chirik described examples of C_1-symmetric bis(imino)pyridine cobalt methyl complexes which catalyze the asymmetric hydrogenation of alkenes.[88] On the other hand, Fout and co-workers developed a series of Co pincer complexes featuring a *meta*-phenylene-bridged bis-*N*-heterocyclic carbene (^{Ar}CCC, Ar = 2,6-diispropylphenyl or mesityl) ligands with different cobalt(I–III) oxidation states.[89a] One of these Co complexes ^{Mes}CCC-Co(PPh$_3$)N$_2$ was tested for alkene hydrogenation. NMR experiments demonstrated a dihydrogen species is generated under H_2 atmosphere by displacing the N_2 ligand from the complex, subsequent oxidative addition of H_2 to the metal center generates a Co^{III}-dihydride intermediate, which is responsible for the formation of the reduced products after migratory insertion and reductive elimination.[89b]

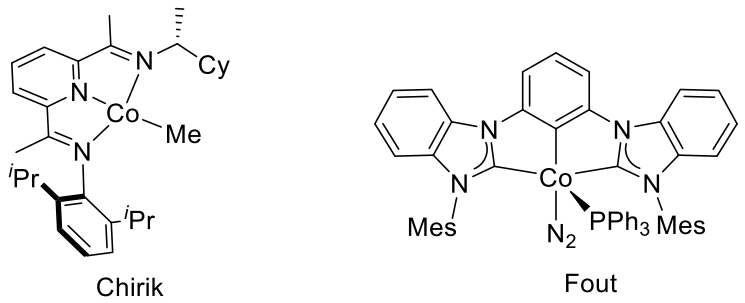

Scheme 2.3: Co pincer complexes for (asymmetric) hydrogenation of olefins

In 2015, Milstein and co-workers reported Co PNN pincer complex catalyzed hydrogenation of esters to alcohols. Co(II) complexes were activated by NaHBEt$_3$ and subsequently used for hydrogenation in the presence of KO^{t}Bu as base.[90a] Under optimized conditions, aliphatic esters were reduced smoothly with good yields, while surprisingly, aromatic esters were totally unreactive. This unexpected inverse reactivity led the authors to conclude an ester enolate intermediate was generated during the reduction. Even though efforts to isolate active species

failed, a cobalt hydride complex was believed to be formed in-situ from Co(II) precursor and $NaHBEt_3$ under H_2 pressure. Following work from their group showed this complex is also suitable for hydrogenation of nitriles to primary amines.[90b]

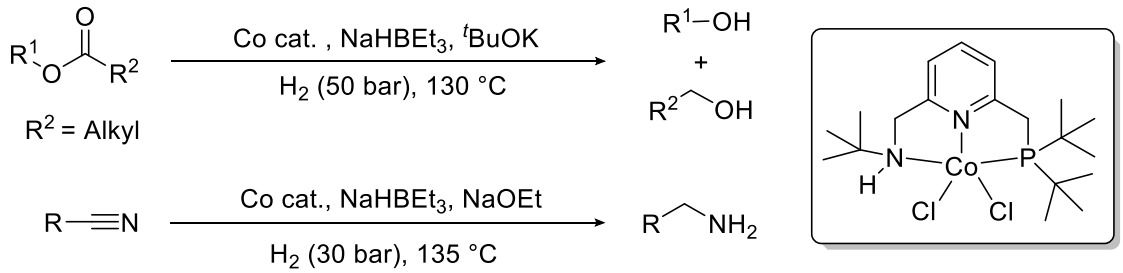

Scheme 2.4: PNN-Co pincer catalyzed hydrogenation of esters and nitriles

Lately, this system was applied in dehydrogenative coupling of alcohols and amines for the synthesis of different *N*-heterocyclic compounds by Milstein's group. In 2016, they reported the synthesis of pyrroles from diols and amines with water and H_2 as byproducts.[91a] It was noticed that base is required for this system, thus in the absence of base, only 16% of product was obtained. Interestingly, for the synthesis of benzimidazoles from aromatic diamines and alcohols, high yields of products were obtained even in the absence of base.[91b]

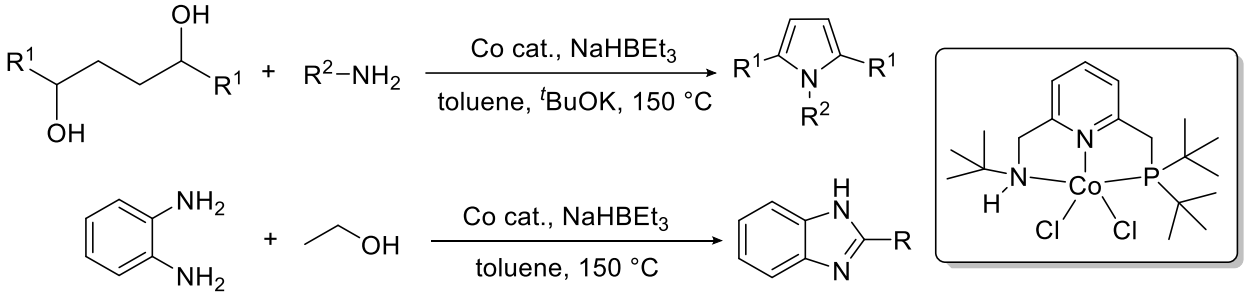

Scheme 2.5: Co catalyzed dehydrogenative coupling of alcohols and amines to *N*-heterocyclic products.

Last year, Beller and co-workers reported hydrogenation of esters catalyzed by Co complexes coordinated by aliphatic pincer ligands. Compared with Milstein's system, both aliphatic and aromatic esters were reduced, and no activating agent, i.e. $NaBHEt_3$ was used in this system.[92]

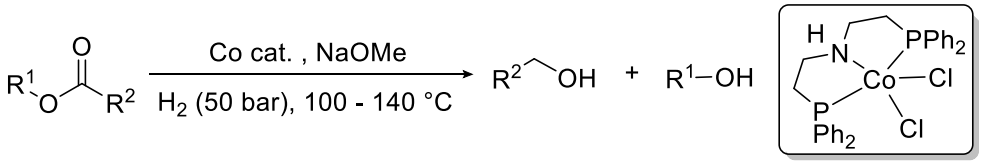

Scheme 2.6: Co catalyzed hydrogenation of esters reported by Beller and co-workers

In addition to Co catalyzed hydrogenation of unsaturated organic compounds, reductions of CO_2 by Co complexes were also reported. For instance, the Beller group described the catalytic

hydrogenation of CO_2 and bicarbonates with an *in-situ* generated catalyst prepared from a Co(II) precursor and a tetraphos ligand. NMR experiments revealed the existence of a Co dihydrogen species which rapidly converts into dihydride as an active intermediate, without the formation of monohydride complex.[93a] Linehan and co-workers reported $Co(dmpe)_2H$ catalyzed hydrogenation of CO_2, remarkable activity was observed with a TOF of 3400 h^{-1} at room temperature and 1 atm of 1:1 CO_2:H_2 (74 000 h^{-1} at 20 atm) in THF.[93b] In 2013 Cp*Co(III) catalysts with proton-responsive ligands for CO_2 hydrogenation in aqueous media were developed by the groups of Muckerman, Himeda and Fujita, which is the first example of Co(III) catalyzed reduction of CO_2 in water.[93c] In addition to these reports, Bernskoetter reported effective Co precatalysts for CO_2 hydrogenation bearing methylated aliphatic PNP pincer ligand. With Lewis acid as additive, a notable increase in activity was observed, affording turnover numbers close to 30000 (at 1000 psi, 45 °C) for CO_2-to-formate.[93d] A mechanism involving labile N coordination from the pincer ligand was proposed by the authors. Besides, Milstein and wo-workers also reported reduction of CO_2 in the presence of amines to make substituted formamide, a Co(I) hydride species was proposed as the active intermediate.[93e]

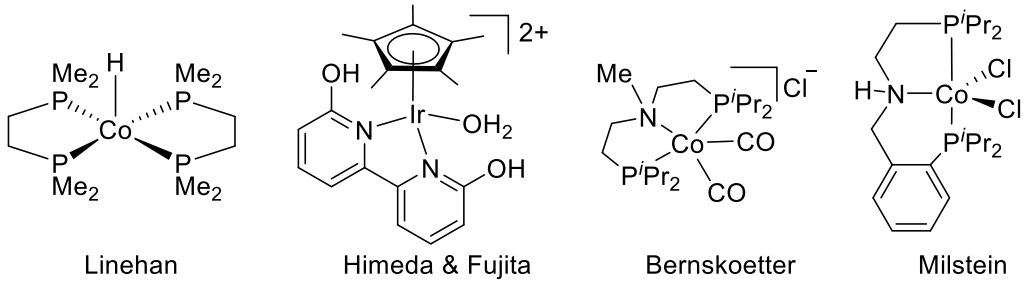

Scheme 2.7: Co complexes applied for CO_2 hydrogenation

Although extensive research has been done in the field of Co catalyzed hydrogenation of organic compounds and CO_2, the reverse process, especially dehydrogenation of FA catalyzed by Co is relatively unexplored.[94] One prominent example was reported by Beller and co-workers, in 2016 they developed a novel nanocobalt catalyst for the selective dehydrogenation of FA.[95] Long-term experiments and recycle investigation demonstrated excellent stability and recyclability of this catalyst. However, the relatively harsh reaction conditions and low activity hamper the application of this system. Based on our long interest in non-noble metal catalyzed dehydrogenation reactions, we started our investigation of homogeneous cobalt complexes catalyzed dehydrogenation reactions.

2.2 Results and discussion

Part of this work was published in *Chemistry – A European Journal*,[96] I would like to thank Dr. Haijun Jiao and Zhihong Wei for their contributions to the proposed mechanism.

2.2.1 Initial investigation of Co(II) pincer complexes

At the beginning of our work, we tested a series of Co(II) complexes which have been reported to be active in the hydrogenation of esters[92], we anticipated that under suitable conditions these Co(II) complexes might also be active in the dehydrogenation reaction, as these two processes are obviously related. A mixture of FA/DMOA (11:10 molar ratio) was chosen as our model substrate since this mixture gave rapid H_2 evolution in the Ru catalyzed dehydrogenation of FA.[41] Besides, the higher boiling point of DMOA compared to that of TEA prevents organic vapours from contaminating the evolved gases. Five different Co(II) complexes were tested at 65 °C in propylene carbonate (Scheme 2.8). However, none of these complexes showed activity for FA dehydrogenation. Variation of reaction conditions including solvents (toluene, triglyme, water, solvent free), bases (fromate, KOH, amines), reaction temperature (65-90 °C) and complex loading (10-50 μmol) resulted no success.

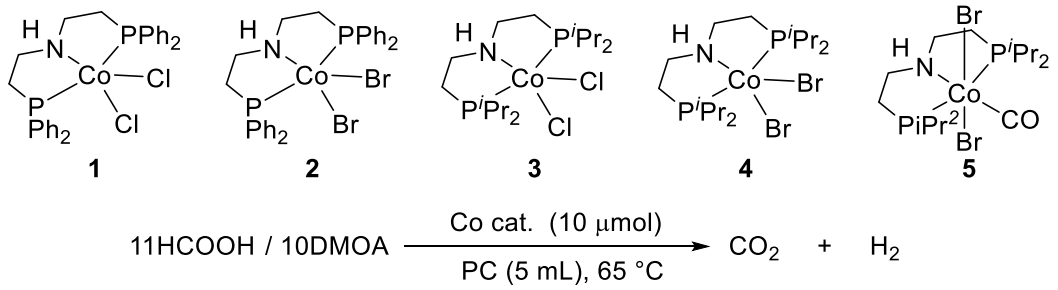

Scheme 2.8: Test of Co(II) complex for FA dehydrogenation

Since all our attempts to dehydrogenate FA with the Co(II) complexes failed, we investigated the dehydrogenation system in depth. By comparing the difference between the hydrogenation system and dehydrogenation one, we realized that during the hydrogenation of esters the starting Co(II) complexes are likely being reduced to Co(I) species under pressured H_2 atmosphere (Scheme 2.9),[92] and the *in-situ* formed Co(I) species are indeed the active compound that initiate the catalytic cycle. However, the reduction of the Co(II) catalytic precursor cannot take place under dehydrogenative conditions, and this might explain why no activity was observed. Therefore we considered if preformed Co(I) complexes were employed as catalysts in the dehydrogenation system, there might be some activity observed. Based on this assumption, we turned our attention towards the exploration of Co(I) complexes in dehydrogenation reactions.

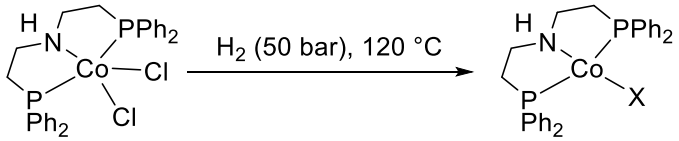

Scheme 2.9: Hypothetic formation of Co(I) species under reductive conditions

2.2.2 Development of a catalytic active Co(I) system for formic acid dehydrogenation

Being aware that Co(I) species might be the active one to initiate dehydrogenation of FA, we synthesized several Co(I) PNP pincer complexes through direct reduction of the corresponding Co(II) precursors with one equivalent of $NaHBEt_3$ (Scheme 2.10). While complex **6** is a known compound which was first reported by Arnold and co-workers[97] **7** and **8** are new compounds which were characterized by NMR, combustion analysis and X-Ray crystallography. All three complexes are paramagnetic species resulting from a high spin ground state in solution and share a tetrahedral geometry in the solid state.

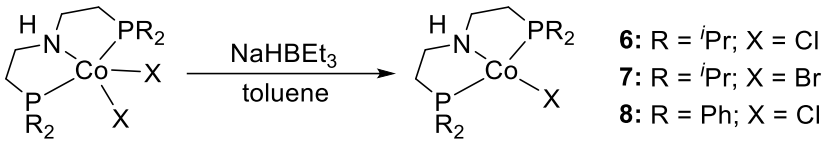

Scheme 2.10: Synthesis of Co(I) pincer complexes

With these Co(I) complexes in hand, we tested their performance in the dehydrogenation of FA. To our delight, when Co complexes bearing *iso*-propyl substituted PNP pincer ligand were employed, hydrogen evolution was detected from FA/DMOA mixture at 80 °C, albeit with very low efficiency (Figure 2.1). Surprisingly, when the analogous phenyl substituted complex **8** was used, a dramatic improvement of activity was observed with FA being fully decomposed into H_2 and CO_2 in 90 minutes.

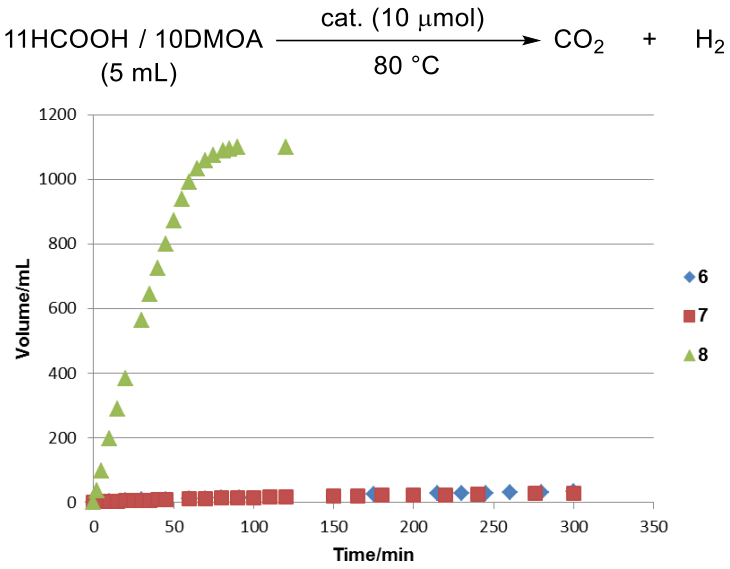

Figure 2.1: H_2 evolution form FA/DMOA mixture catalyzed by Co(I) complexes[96]

Encouraged by the high activity of complex **8** in FA/DMOA, we tested its performance under aqueous conditions. With HCOOK as the base, the system was still relatively active, and 376 mL of gas was generated in one hour at 80 ℃ , which corresponds to a TON of 770. Since water is the

ultimate green solvent and thus favoured over any other solvents, we continued all further optimization by using water as the solvent.

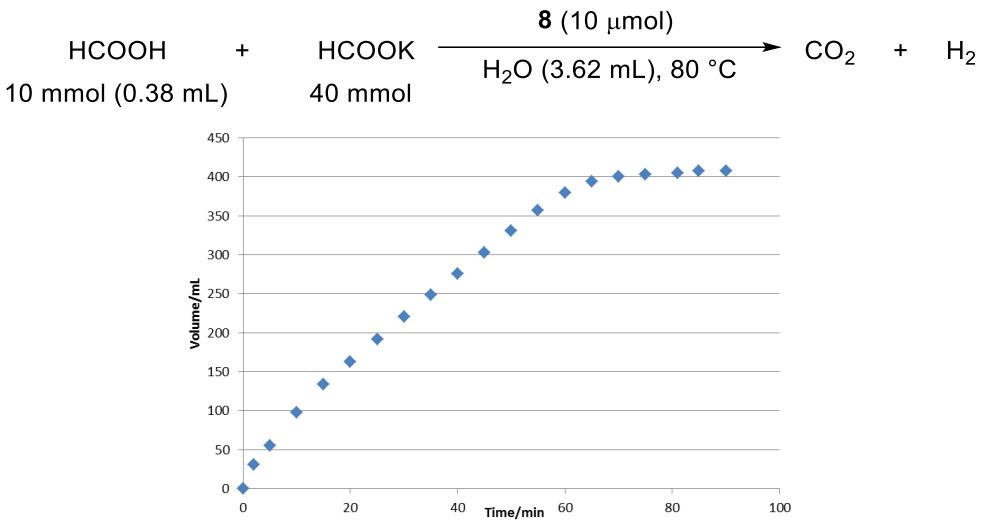

Figure 2.2: Co catalyzed dehydrogenation of FA under aqueous conditions

At 60 ℃ , the rate of gas evolution slowed down significantly, but still satisfactory results were obtained (Table 2.1, entry 1). Due to the high air sensitivity of complex **8**, which makes its handling inconvenient, we also tried the reaction with its precursor complex **1** under *in-situ* activation by sodium triethylborohydride ($NaBEt_3H$). When one equivalent of $NaBEt_3H$ was used as activator (entry 2), the resulting activity was lower than that observed with the preformed

Table 2.1: Optimization of Co(I) catalyzed dehydrogenation of FA in aqueous system

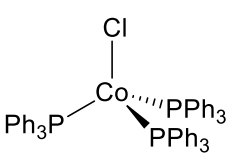

9

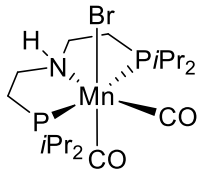

10

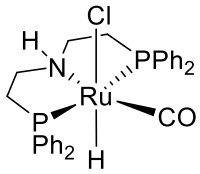

11

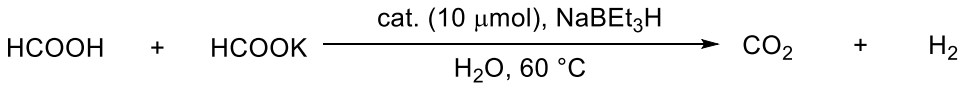

Entry	Complex	$NaBEt_3H$ (μmol)	HCOOH (mmol)	HCOOK (mmol)	V_{1h} (mL)	V_{3h} (mL)
1	**8**	0	10	40	131	396
2	**1**	10	10	40	64	220
3	**1**	20	10	40	134	426
4	**1**	20	10	20	133	448
5	**1**	20	10	10	125	436
6	**1**	20	10	5	71	200
7	**1**	20	20	10	70	170
8	**1**	20	20	20	102	292
9	**1**	20	40	40	69	171
10	**1**	20	10	0	14	26
11	**1**	20	0	10	12	22
12	**8**	10	10	10	118	432
13	**2**	20	10	10	100	300
14	**9**	0	10	10	0	0
15	**10**	0	10	10	0	0
16	**11**	0	10	10	6	18

In all cases, the total volume of formic acid and water is 4 mL, gas evolution was measured by using a manual burette with correction by blank value.

Co(I) complex. This can be attributed to uncomplete reduction of the Co(II) precursor, since we observed a pale pink solution in the aqueous phase, indicating the presence of residual Co(II) species. Indeed, with two equivalents of $NaBEt_3H$, the *in-situ* system showed a slightly higher activity compared to the preformed catalyst (entry 3). We next examined influence of the formate amount on the performance of the *in-situ* system. From the results, we can conclude the ratio of formate salt to FA can be reduced from 4/1 to 1/1 without a significant loss of activity (entries 3, 4, 5). However, if this ratio is lowered to 0.5, with an initial excess of FA, the reaction rate was

much affected to almost halved (entry 6). Besides, reaction slowed down obviously when substrates concentration is increased (entries 5, 8 and 9). In the absence of base, only a very slow gas evolution was observed (entry 10). H_2 generation still proceeded when an aqueous solution of potassium formate was used as substrate (entry 11), this may due to the equilibrium established in solution between formate and FA, which is subsequently dehydrogenated. To understand the difference between preformed Co(I) complex **8** and the *in-situ* formed system from complex **1** with two equivalents of $NaBEt_3H$, we also performed an experiment using **8** in the presence of one equivalent of $NaBEt_3H$. The result showed this system exhibited the same activity as complex **1** with two equivalents of reductant, which suggests the same active species is generated in both systems (entries 5, 12). In addition, the bromide analogue of complex **1**, complex **2,** showed a slightly lower activity under the *in-situ* conditions (entry 13). One commercially available Co(I) complex **9** was also tested, however, no gas evolution was observed which highlights the importance of the pincer ligand in the system (entry 14). Finally, we compared the activity of these novel complexes with other well-known pincer complexes, which are active in methanol and/or FA dehydrogenation.[62, 98] Surprisingly, the manganese complex **10** was completely inactive under these aqueous conditions (entry 15), and even the ruthenium benchmark complex **11** gave only marginal hydrogen production (entry 16). Obviously, Co(I) complex **8** is a superior catalyst for the dehydrogenation of FA under aqueous conditions compared with other metal catalysts.

With the optimized conditions in hand, we investigated the stability of the system. As shown in Figure 2.3, gas evolution ceased after 70 hours, and a maximum TON of 7166 was obtained.

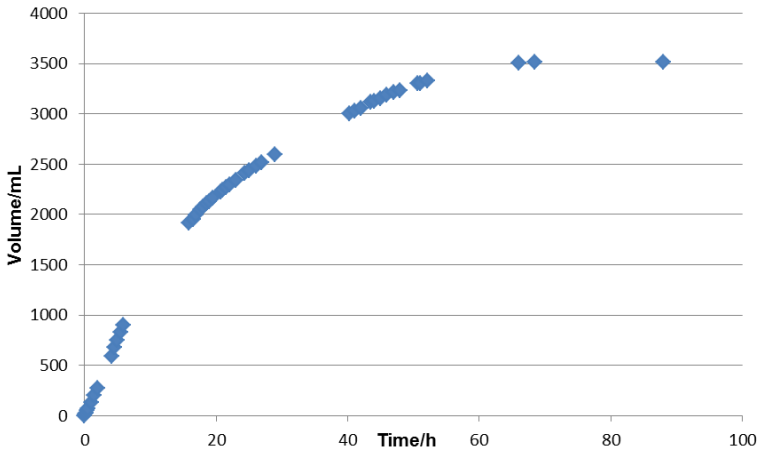

Figure 2.3: Long term experiment of Co catalyzed aqueous dehydrogenation of FA

2.2.3 Mechanistic studies

After established the active system for Co catalyzed dehydrogenation of FA, we performed several experiments in order to disclose the reaction mechanism and to identify the active species,

especially in the *in-situ* system. It is showed by Chirik and co-workers that a Co hydrido species coordinated by similar PNP pincer ligand could be obtained either by treatment of the parent Co(II)Cl_2 complex with two equivalents of $NaBEt_3H$ or the Co(I)Cl one with one equivalent of $NaBEt_3H$ (Scheme 2.11).[99] Accordingly, we examined the possible existence of Co(I) hydride species in our system: complex **1** was treated with two equivalents of $NaBEt_3H$, then the crude product mixture was submitted to NMR analysis. The ^{31}P NMR turned out to be quite complicated with several peaks with chemical shifts ranging from 20 to 150 ppm which were hard to assign, while no hydride peak was observed in the proton NMR even up fielded to – 50 ppm.

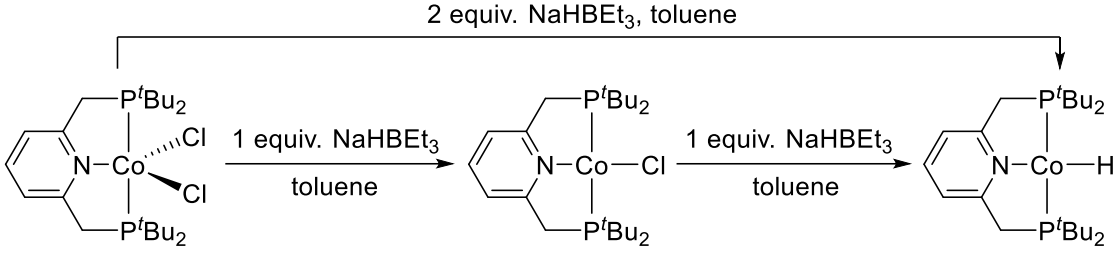

Scheme 2.11: Synthesis of a Co(I)-H complex reported by Chirik and co-workers[99]

Through a perusal of the literature, we noted there two reported examples in which the authors also tried to isolate Co(I) hydride species bearing aliphatic PNP pincer ligand. One example was described by Chirik and co-workers, during their investigation of Co complexes bearing tridentate pincer ligands for catalytic C−H borylation, when complex **6** was reacted with $NaBEt_3H$, instead of the desired Co hydride, a bimetallic cobalt cation [**6**-Co]$_2^+$ species was isolated from the reaction mixture following recrystallization.[100a] In another case, Bernskoetter and co-workers tried to substitute chloride of the methylated analogue of complex **6**. By treating Me-6 with different borohydride reagents, they can only obtain intractable mixtures of product along with metallic precipitate, which indicates reduction and/or disproportionation side reactions occurred in the system.[100b]

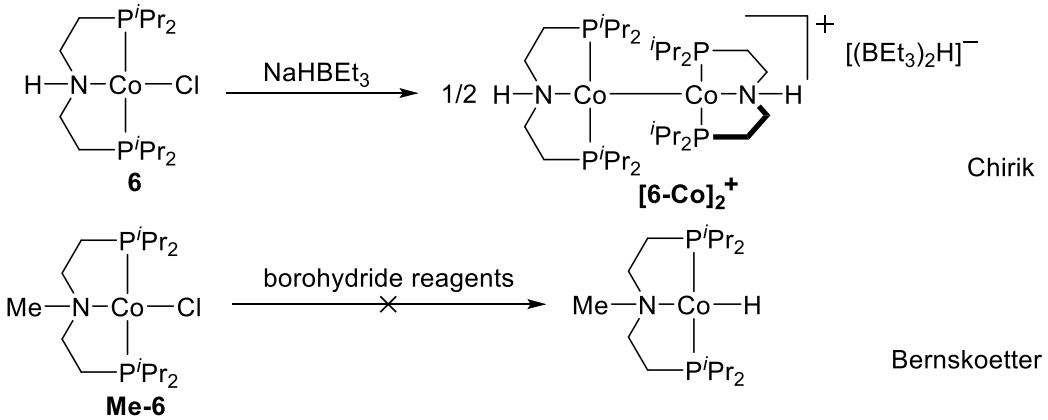

Scheme 2.12: Reported attempts for the synthesis of Co(I)-H complexes bearing aliphatic PNP pincer ligands

After realizing that the direct synthesis of Co(I) hydride species may not be successful, we opted for another route inspired from the work by Chirik and co-workers, in which they were able to prepare the hydride product $(Ph_3P)_3Co(N_2)H$ with dinitrogen as co-ligand through reduction of $(Ph_3P)_2CoCl_2$ with $NaBEt_3H$ under a nitrogen. Therefore we also The synthesis of the PNP-Co(I) hydride under a nitrogen atmosphere, hoping that the additional dinitrogen ligand may stabilize the hydrido complex. The ^{31}P NMR spectrum showed a much cleaner this time with one main peak at $\delta = 27.7$ ppm (Scheme 2.13), while still no hydride peaks observed from proton NMR.

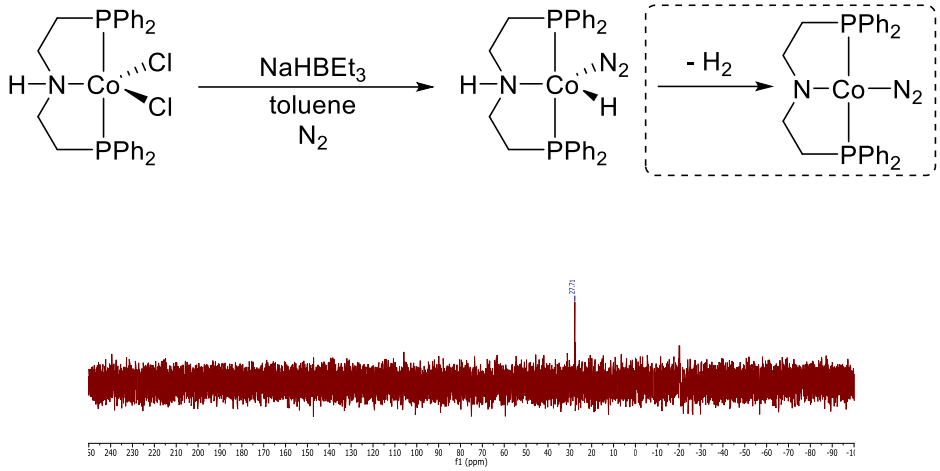

Scheme 2.13: Synthesis of Co hydride species under N_2 atmosphere and the ^{31}P NMR of crude product

In a paper published by Arnold and co-workers, they showed a pincer Co(I) imido complex was obtained through the reduction of the corresponding Co(II) imido complex with potassium graphite (KC_8) under nitrogen atmosphere.[97] We also tried to synthesize a similar Co(I) imido complex in our system in order to verify whether it might be a possible intermediate in the dehydrogenation reaction (Scheme 2.14). Reacting complex **8** with one equivalent of K^{t}OBu under N_2, we obtained a new species. The ^{31}P NMR exhibits one main peak at $\delta = 27.7$ ppm, which is almost identical to the ^{31}P chemical shift of the product obtained from the synthesis of the Co hydride species as mentioned above. This observation might be explained by fast loss of H_2 from the presumable hydride product (dashed box in Scheme 2.13), resulting in the formation of the Co(I) imido complex which is the product proposed in Scheme 2.14.

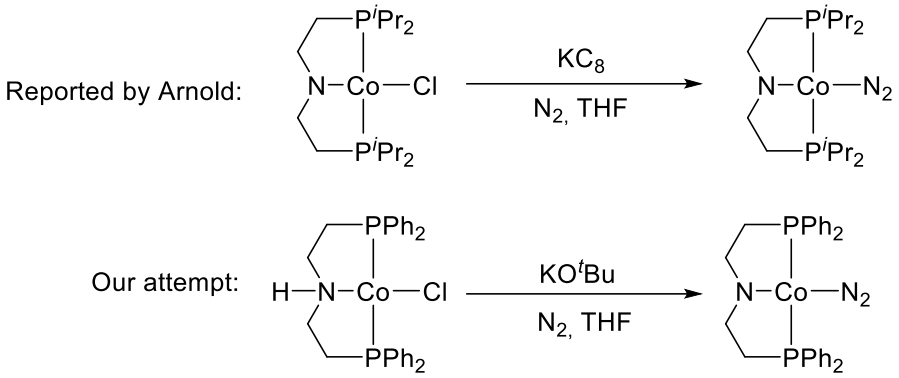

Scheme 2.14: Synthesis of Co(I) imido dinitrogen complex

Catalytic testing of the product from the reaction of Scheme 2.14 showed that the imido complex affords similar activity as the precatalyst complex **8**, which indicates it might be an active intermediate. However, attempts to fully characterize this product via NMR, elemental analysis and x-ray crystallography failed, possibly due to instability of this complex.

Regarding the slight difference in activity observed between the preformed Co(I) complex and the *in-situ* activated Co(II), one possible factor might be triethylborane (BEt_3) remained in the *in-situ* system, which can act as a Lewis acid to promote dehydrogenation process. A related enhancing effect of BEt_3 on activity has been reported by Fout and co-workers in the Co catalyzed hydrogenation of nitriles.[102] Two comparison experiments were performed under optimized conditions to investigate the effect of BEt_3 in our system: in one case, two equivalents of BEt_3 were added to a solution of complex **8**; in another one, BEt_3 was removed from the *in-situ* system, no influence on activity was observed in either case (Figure 2.4), which excludes the beneficial effect of BEt_3 in our system.

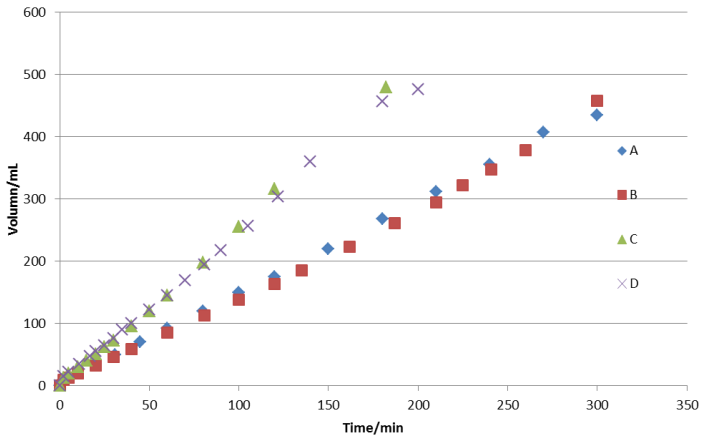

Figure 2.4: Effect of BEt_3 on Co catalyzed dehydrogenation of FA. Conditions: FA (10 mmol), HCOOK (10 mmol), H_2O (3.62 mL). cat.(10 μmol in 0.4 mL toluene). A:complex **8**; B: complex **8** + 2 eq. BEt_3; C: complex **1** + 2 eq. $NaBEt_3H$; D: complex **1** + 2 eq. $NaBEt_3H$, solvent removed and residue dried *in vacuo* for 30 min before being redissolved in toluene

In order to understand the deactivation of the system two Co(I) carbonyl complexes **12** and **13** were synthesized. The dicarbonyl complex **12** was prepared through bubbling CO into a toluene solution of complex **8**, treatment of **12** with base afforded the monocarbonyl species **13** (Scheme 2.15). Interestingly, neither **12** nor **13** was active in FA dehydrogenation under optimized conditions. These results indicate that CO coordination to Co may contribute to the deactivation of the catalyst, since FA decomposed into CO and H_2O was frequently observed in previous dehydrogenation systems (see examples from section 1.3.1 and 1.4.1).

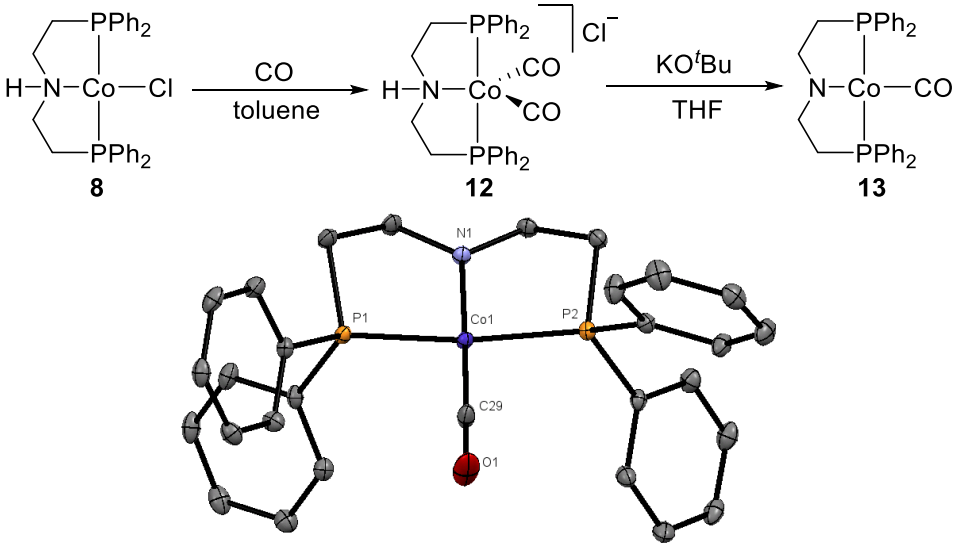

Scheme 2.15: Synthesis of carbonyl complexes **12**, **13** and X-Ray structure of **13**: thermal ellipsoids at 50% probability, hydrogens were eliminated for clarity

Indeed, when 10 mL of CO was bubbled through the active system, gas evolution stopped almost immediately (Figure 2.5), which further confirms the poisoning effect of CO.

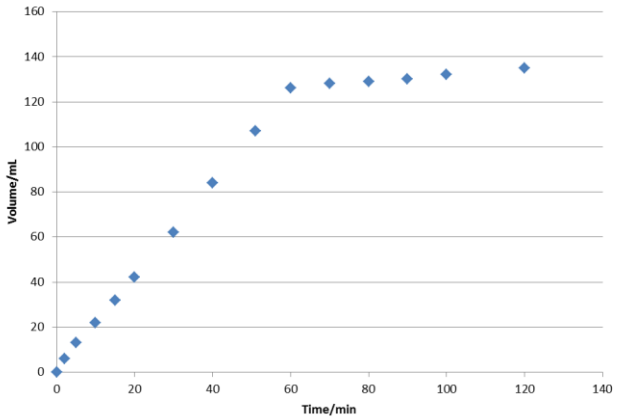

Figure 2.5: Gas evolution curve for CO poisoning experiment under optimized conditions. At 60 min of reaction time, 10 mL of CO was bubbled through the system *via* an air tight syringe within one minute

Besides, we also investigated the influence of different carboxylates. When potassium acetate was employed instead of potassium formate, the rate of gas evolution decreased significantly, while in the presence of potassium benzoate no H_2 was detected (Figure 2.6). To further confirm the effect of different carboxylates, their potassium salts were used as an additive in the optimized system based on FA and potassium formate, the results clearly indicated a strong inhibition effect on activity by benzoate (Figure 2.7).

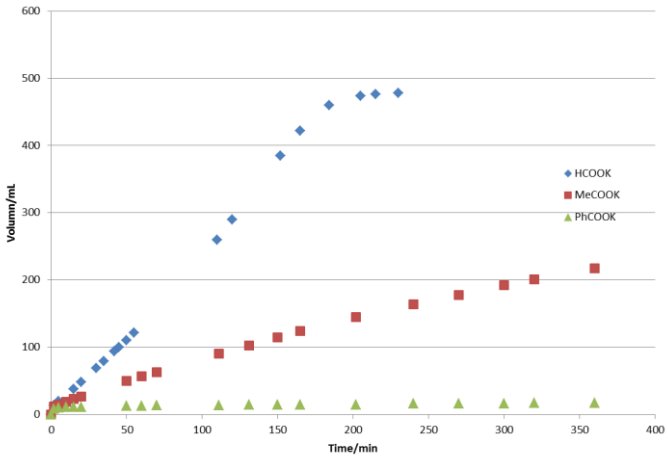

Figure 2.6: Effect of different carboxylates on the rate of dehydrogenation reaction. Conditions: FA (10 mmol), RCOOK (10 mmol), H_2O (3.62 mL), 60 °C. cat. (*in-situ* prepared from 10 μmol complex **1** and 20 μmol $NaBEt_3H$)

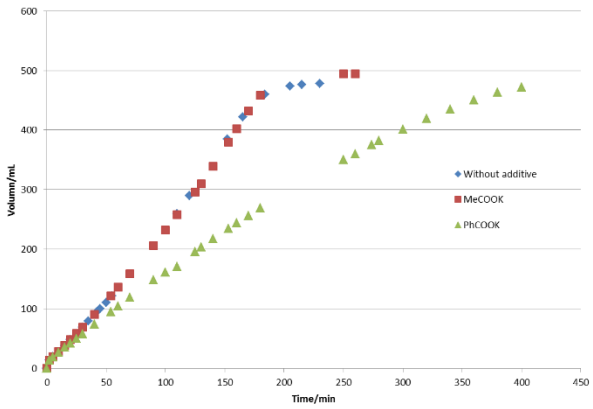

Figure 2.7: Effect of carboxylates as additive under optimized conditions. FA (10 mmol), HCOOK (10 mmol), H_2O (3.62 mL), 60 °C, cat. *in-situ* prepared from 10 μmol complex **1** and 20 μmol $NaBEt_3H$), additive (20 μmol)

Based on these observations, we propose that a Co(I) carboxylate intermediate is generated during the reaction.[103] If a carboxylate other than formate is present in the system, a Co(I) carboxylate resting species which is not involved in the catalytic cycle is formed and slows down the overall rate of the reaction by sequestering part of the Co (Scheme 2.16). In the case of potassium benzoate used as base or additive, the resulting Co(I) benzoate is so stable that it will never go back to the active formate intermediate, thus even a very low loading of potassium

benzoate compared to potassium formate would be enough to deactivate the system. The high affinity between the Co(I) metal center and benzoate can be partly explained through hard and soft acids and bases theory[104], since Co(I) is a relatively soft Lewis acid and might therefore binds stronger to benzoate, which is a softer base than formate and acetate.

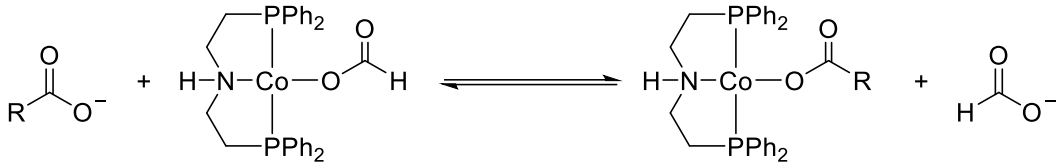

Scheme 2.16: Interconversion between Co(I) formate and other Co(I) carboxylate species

However, except for this reasoning based on our knowledge, there is no other information from which we can put forward a convincing explanation. The best proof would be the independent synthesis of these proposed Co(I) carboxylates, which might allow to draw more solid conclusion from their structure. Accordingly, we first tried the synthesis of Co(I) acetate by stirring AgOAc and complex **8** in a THF solution. After workup, one product from the reaction was characterized as a Co(II) dimmer by X-ray crystallographic analysis (Scheme 2.17), which clearly showed the initial Co(I) was oxidized by Ag(I). Indeed, similar observation of oxidation of Co(I) by Ag(I) was also noticed by Arnold and co-workers in their paper.[97]

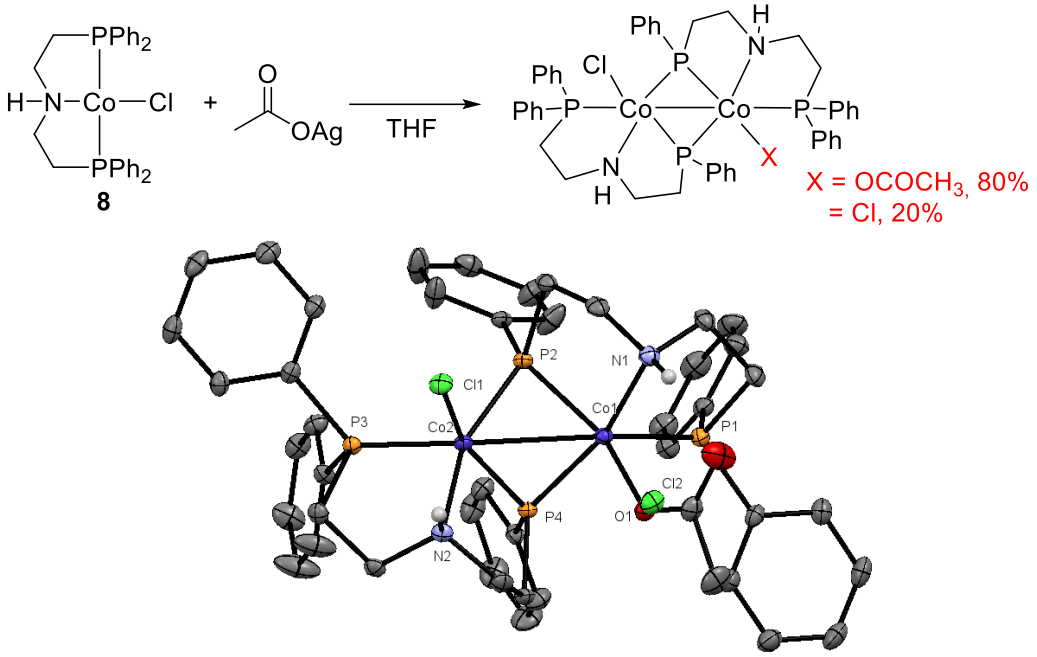

Scheme 2.17: Reaction of complex **8** with AgOAc and X-ray structure of the resulting Co(II) dimmer: thermal ellipsoids at 50% probability. All hydrogens except that attached to nitrogen were eliminated for clarity

Although we failed to obtain the desired Co(I) carboxylate complex, this unexpected result gave us some hints about the mechanism. Therefore we turned our attention to the reaction of the much

less active Co(I) complex **6**. By adding FA to a blue solution of complex **6** in toluene, the system turned to red immediately with precipitates and H_2 evolution was confirmed by GC measurement. One complex from the reaction mixture was characterized as the Co(II) complex **3** (Scheme 2.18). Our speculation is that complex **6** is tend to be oxidized by FA, forming a Co(III) compound[89] which then reacts with the starting complex **6** to give inactive Co(II) species. According to the values of standard electrode potential, the reduction potential of Co(III)/Co(II) is much higher than that of Ag(I)/Ag[105], this indicates that the comproportionation of Co(I) and Co(III) to give Co(II) is feasible.

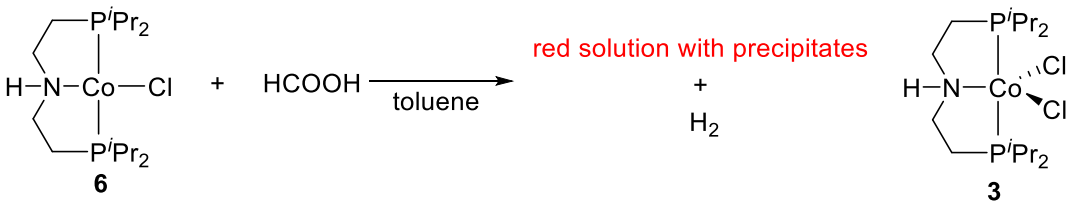

Scheme 2.18: Reaction of complex **6** and FA

To gain more mechanistic insight into the catalytic system, kinetic isotope effect (KIE) studies were performed. In the formic acid/amine system as well as under aqueous conditions primary KIE values of 2.91 and 2.05 for HCOOH/DCOOH, respectively, were obtained, while the KIE value of HCOOH/HCOOD in FA/amine system is only 1.34. These results indicate that the decarboxylation step may be the rate determining step.

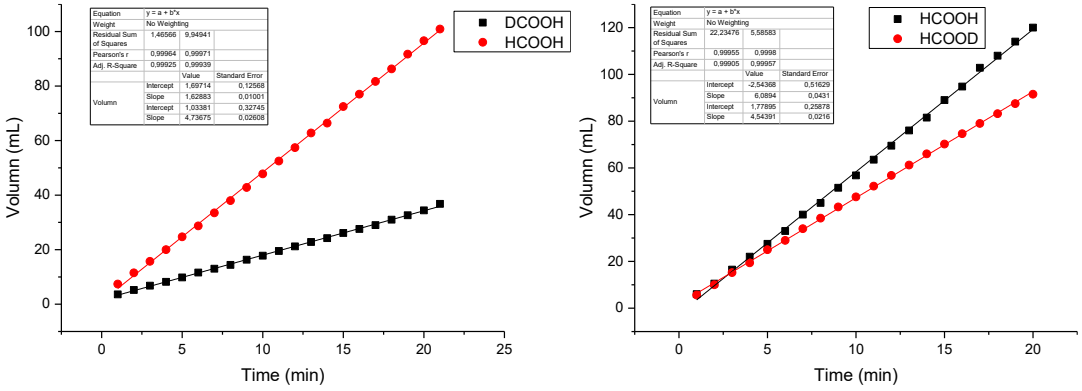

Figure 2.8: KIE curves for HCOOH/DCOOH and HCOOH/HCOOD in FA/DMOA mixture

Along with our experimental work, we further performed DFT calculations to elucidate the reaction mechanism. The calculations were performed by Dr. Haijun Jiao and Zhihong Wei at the B3PW91 level of theory and the results are summarized in Figure 2.9. The first step of the reaction is the substitution of the chloride in complex **8** by formate resulting in the formation of complex **8A1**. It is found that in **8A1** additional H-bonding between the second O atom and the H atom of the N-H group could stabilize the complex. Next, complex **8A1** transferred from O-

bounded formate to H-bounded formate intermediate, subsequent decarboxylation leads to the Co(I) hydride species **8B**. A similar decarboxylation mechanism, made by a possible switch in formate coordination mode was also proposed by Milstein, Hazari, Gonsalvi and Schneider for Fe catalyzed dehydrogenation of FA.[76, 77]

Starting from the Co(I) hydrido complex **8B**, there are three possible routes for H_2 release. The first one (red line) involves protonation of the Co-H group by formic acid and this step is very endergonic with a barrier of 102.80 kcal/mol and thus can be discarded. The second one (green line) is direct release of molecular H_2 from intermediate **8B** *via* a non-innocent metal-ligand cooperation mechanism with the formation of the imido complex **8C**. In the transition state (**TS-8B/8C**), the forming H-H distance is 0.974 Å; and the distance of dissociating N-H and Co-H bonds is 1.451 and 1.757 Å, respectively. This step has free energy barrier of 17.64 kcal/mol and is exergonic by 3.97 kcal/mol.

The last route (blue line) involves a formic acid assisted innocent mechanism, where H_2 is formed from the Co-H group of complex **8B** and proton from FA. In the transition state the structure is stabilized by H-bonding between the N-H group and the carbonyl oxygen. The forming H-H distance is 0.934 Å; and the dissociating Co-H and H-O distances are 1.699 and 1.360 Å, meanwhile the distance of the O-H H-bonding is 1.753 Å. This step has negative Gibbs free energy barrier (–3.00 kcal/mol) and is highly exergonic (–31.42 kcal/mol). Release of H_2 regenerate the formate intermediate **8A1**. On the basis of the computed potential energy surface, all species have formal Co(I) oxidation states and triplet states; and the rate-determining step is the C-H activation accompanied with CO_2 release, which is in good agreement with the observed KIE for HCOOH/DCOOH.

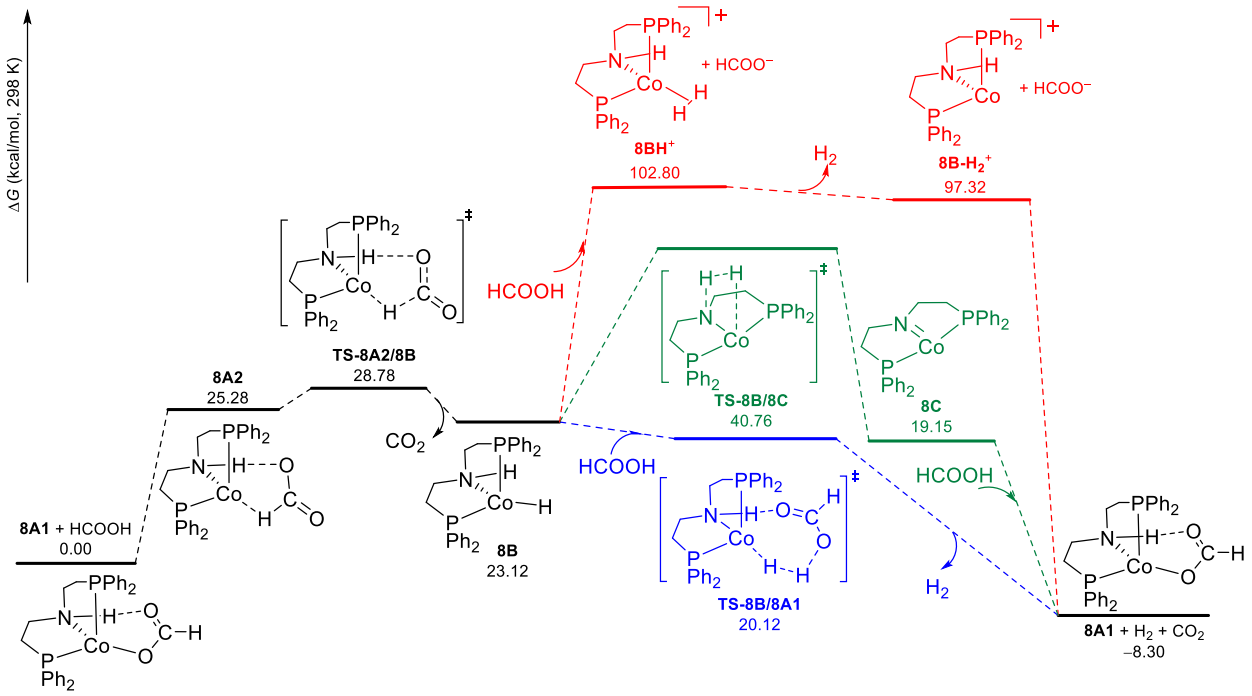

Figure 2.9: Gibbs free energy profile for formic acid dehydrogenation at B3PW91/TZVP level[96]

Based on our experimental data and DFT results, we conclude the mechanism of Co catalyzed dehydrogenation of FA as following (Scheme 2.19): when phenyl substituted pincer complex **8** is employed, ligand exchange between chloride of **8** and formate would be preferred, resulting in the formation of the Co-formate intermediate **8A1**, it then isomerize to **8A2**. From this species, CO_2 is released, giving the Co hydride species **8B**. Reaction of the latter with FA liberates H_2 and regenerates the formate intermediate **8A1**. While in the case of *iso*-propyl substituted complexes, oxidative addition of FA to Co(I) is preferred because of higher electron density on phosphorus, which renders the metal center more electronic rich due to the stronger σ-donation. The resulting Co(III) product together with the starting Co(I) complex yield inactive Co(II) species, which accounts for the low activity observed for complexes **6** and **7**.

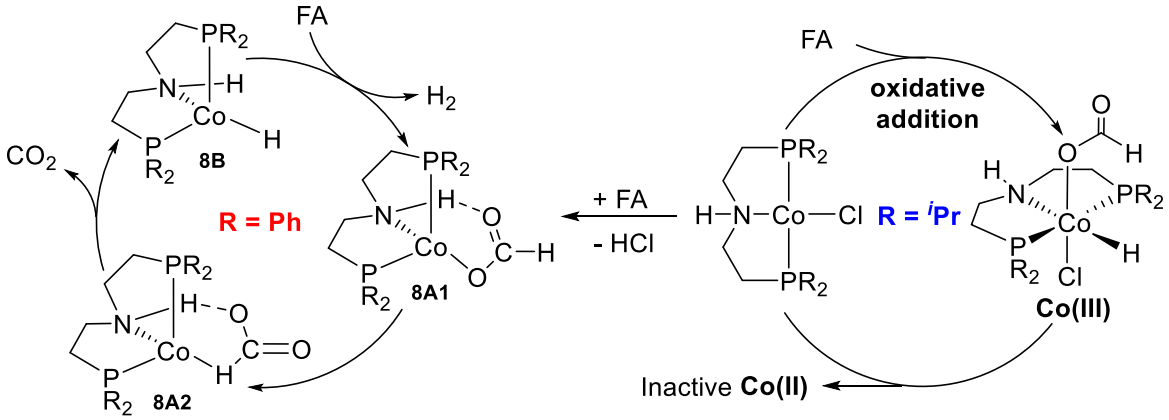

Scheme 2.19: Proposed mechanism for the Co catalyzed dehydrogenation of FA

2.3 Summary

In this work, highly active Co(I) complexes bearing aliphatic PNP pincer ligand were developed for the dehydrogenation of FA in aqueous system under mild conditions. Comparison experiments showed that the coordination of CO to the metal results in poisoning of the catalyst, which explains the deactivation of the system in long term experiments. This behaviour is quite different from what observed in other dehydrogenation systems based on Ru, Mn and Fe where CO acts as a co-ligand (see examples in chapter 1).

Mechanistic studies combined with DFT calculations suggest a Co(I) formate intermediate as the active species and decarboxylation of this intermediate to give a Co(I) hydride is the rate determine step during the catalytic cycle. Two different reaction pathways are put forward to explain the dramatic difference in activity showed by the Co(I) complexes with different substituents on phosphine of pincer ligand.

These results will be helpful for the understanding of Co(I) catalyzed (de)hydrogenation, transfer hydrogenation as well as dehydrogenative coupling reactions. Besides, these results will be of interest for the further development of non-noble metal catalyzed (de)hydrogenation reactions.

3 Manganese catalyzed dehydrogenation of alcohols

3.1 Background

Being the third most abundant transition metal in the Earth's crust after iron and titanium, manganese (Mn) is an attractive choice to catalyze chemical reactions. However, until now, there are only a few examples where Mn complexes have been utilized as catalysts, most of these reports are mainly focused on oxidative transformations using high-valent Mn complexes.[106] In contrast, the development of well-defined, low-valent Mn complexes in catalytic hydrogenation and dehydrogenation reactions were virtually unexplored until quite recently.

In 2016, Milstein and co-workers reported their pioneering work on Mn catalyzed imine synthesis *via* acceptorless dehydrogenative condensation of alcohols and amines.[107] A Mn complex bearing a dearomatized pyridyl pincer ligand was employed as catalyst under base free conditions, a variety of alcohols and amines were employed to furnish imines in good to excellent yields. Mechanistic studies involving NMR spectroscopy, intermediate isolation, and X-ray crystallography suggest a catalytic pathway similar to that of the analogous Ru-PNP catalyzed reactions. Firstly, the alcohols were dehydrogenated through a concerted bifunctional proton and hydride transfer to yield aldehyde which was then condensed with amines to give the final products. After H_2 is released from the Mn hydride intermediate, catalyst is regenerated and start the next catalytic cycle (Scheme 3.1).

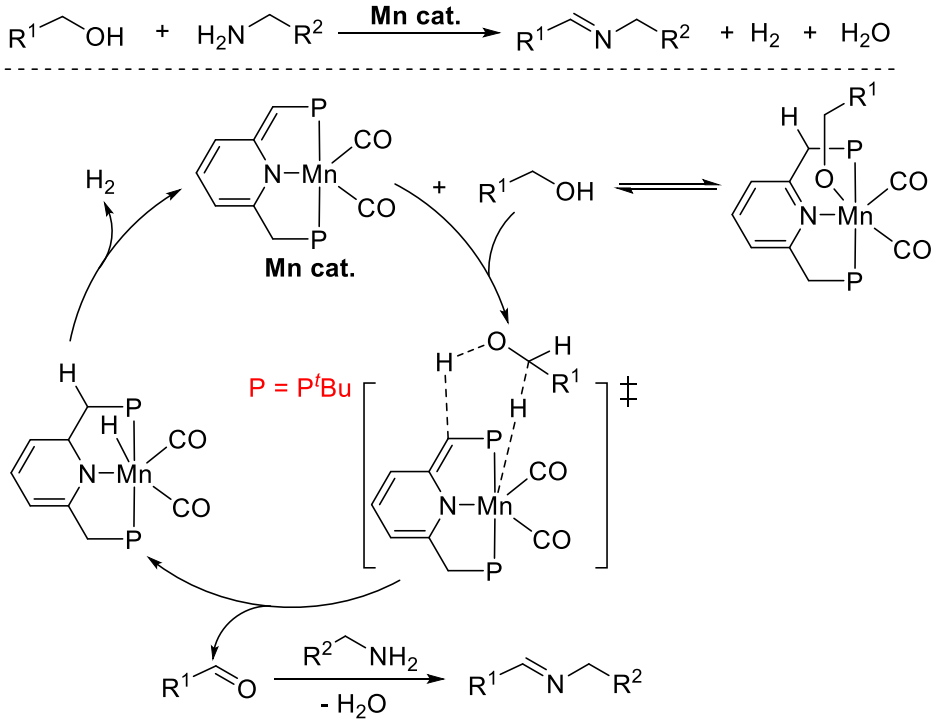

Scheme 3.1: Mn catalyzed dehydrogenative condensation to imines and the proposed reaction mechanism[107]

Later on, other related Mn pincer complexes were developed and have been extensively investigated in Milstein's group as the catalysts in dehydrogenative coupling reactions for the synthesis of amides, esters, imines, hydrazones and α-olefinated nitirles (Scheme 3.2).[108] Except for dehydrogenative couplings, these Mn complexes have also been employed for the hydrogenation of ester to alcohols and organic carbonates to methanol.[109]

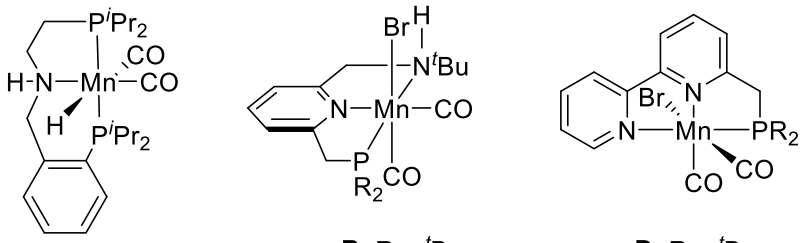

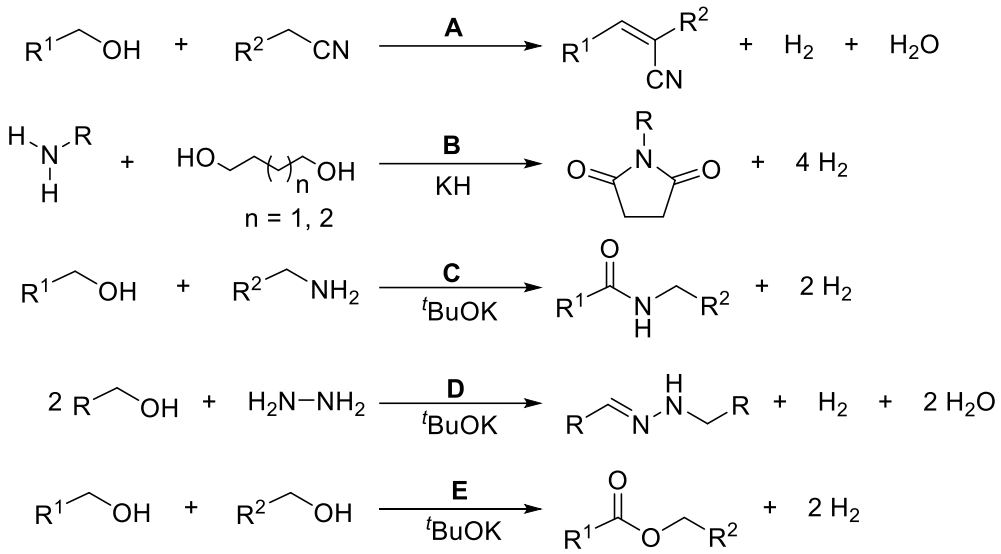

Scheme 3.2: Mn catalyzed dehydrogeantive reactions reported by Milstein and co-workers

Concurrent with Milstein's work, the Beller group described the utilization of Mn pincer complexes for hydrogenation reactions. Mn complexes coordinated with aliphatic PNP pincer ligands were employed for selective hydrogenations of nitriles, ketones, aldehydes and esters.[110] A cationic Mn compound was also prepared for amides hydrogenation. Based on the concept of borrowing hydrogenation, two examples of alkylation of organic molecules using alcohols as reagent were disclosed by the same group,[111] it is worth to mention that water is the only by-product in these systems. Besides, a Mn *N,N,N*-pincer complex was also reported which is competent for transfer hydrogenation of ketones with isopropanol as hydrogen source.[112]

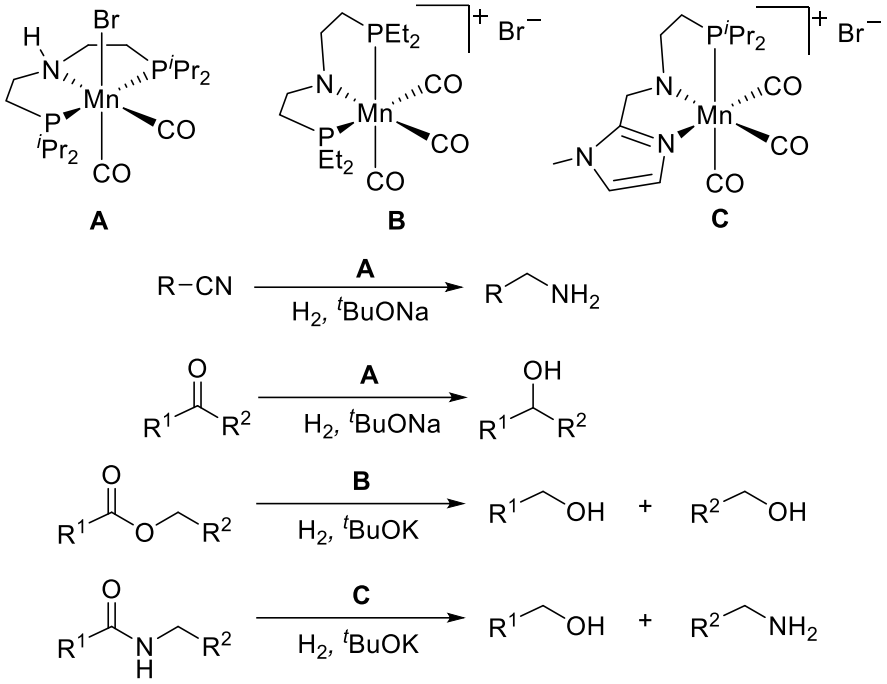

Scheme 3.3: Mn catalyzed hydrogenation developed by Beller and co-workers

Subsequent contributions from the group of Kirchner and Kempe further expand the range of Mn pincer complexes, the application of these novel Mn complexes in catalytic organic synthesis was explored accordingly.[113]

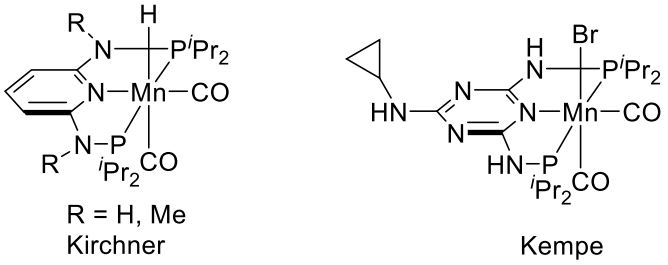

Scheme 3.4: Mn pincer complexes reported by Kirchner and Kempe

Besides, the application of Mn complexes in the field of H_2 storage was also investigated. In 2016, Boncella and co-workers pioneered the area of Mn catalyzed dehydrogenation of FA.[114] A novel Mn-formate complex was prepared from the same Mn complex (Scheme 3.3, complex **A**) reported by the Beller group as mentioned above (Scheme 3.5). The Mn-formate complex was showed to be active for the decomposition of FA in 1,4-dioxane under base free conditions, TON up to 190 was obtained after 14 hours. Later on, the Beller group investigated the catalytic activity of these Mn complexes in the dehydrogenation of methanol, excellent long-term stability was demonstrated for the Mn-PNP^{i}Pr catalyst, an impressive TON over 20000 was attained after one month without deactivation of the system.[98]

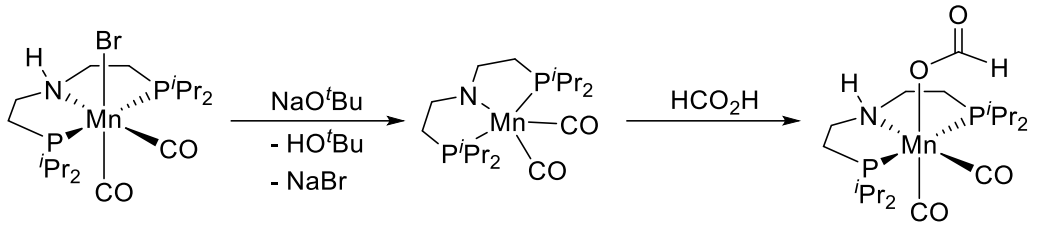

Scheme 3.5: The synthesis of a Mn-formate complex[114]

In 2017, Kirchner and Gonsalvi reported the first example of Mn catalyzed hydrogenation of CO_2 to FA. Higher stability and activity was observed for the Mn system compared to its Fe(II) analogue, TONs up to 10000 and quantitative yields were obtained after 24 h using DBU as the base at 80 °C and 80 bar total pressure. At catalyst loadings as low as 0.002 mol%, TONs larger than 30000 could be achieved in the presence of LiOTf as a co-catalyst, which are among the highest activities reported for base-metal catalysed CO_2 hydrogenations to date.[115a] Later, a Mn catalyzed sequential one-pot homogeneous CO_2 hydrogenation to methanol was demonstrated by Prakash and co-workers,[115b] CO_2 was reduced to formamide in the presence of amine then further to methanol and regenerate amine by using the same Mn pincer complex under different conditions.

Lately, a bio-inspired Mn complex with a simple N-donor ligand, 6,6'-dihydroxy-2,2'-bipyridine was developed by the groups of Nervi and Khusnutdinova. The complex acts as an efficient catalyst for CO_2 hydrogenation, TON of 6250 for hydrogenation of CO_2 to formate in the presence of DBU were achieved.[116a] Another example of Mn complex bearing a phosphine free bidentate ligand was described by Sortais and co-workers for the transfer hydrogenation of carbonyl compounds, 2-(aminomethyl)pyridine was employed as the ligand, TON up to 2000 and TOF of 3600 h^{-1} were obtained.[116b]

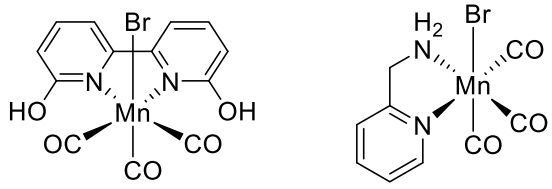

Nervi & Khusnutdinova Sortais

Scheme 3.6: Mn complexes bearing P-free bidentate ligands

In addition to Mn(I) complexes, Mn(III) compounds were also explored for dehydrogenative reactions. Last year, Madsen and co-workers reported a Mn(III) catalyst for the acceptorless dehydrogenation of alcohols. N,N'-Bis(salicylidene)-1,2-cyclohexanediamino (salen) Mn(III) chloride was shown to catalyze the direct synthesis of imines from a variety of alcohols and amines with the liberation of hydrogen gas.[117] Mechanistic studies indicate a metal–ligand

bifunctional pathway in which both imine groups in the salen ligand are first reduced to form a Mn(III) amido complex as the catalytically active species. Dehydrogenation of alcohol then takes place by a stepwise outer-sphere hydrogen transfer generating a Mn(III) salan hydride from which H_2 is released (Scheme 3.7).

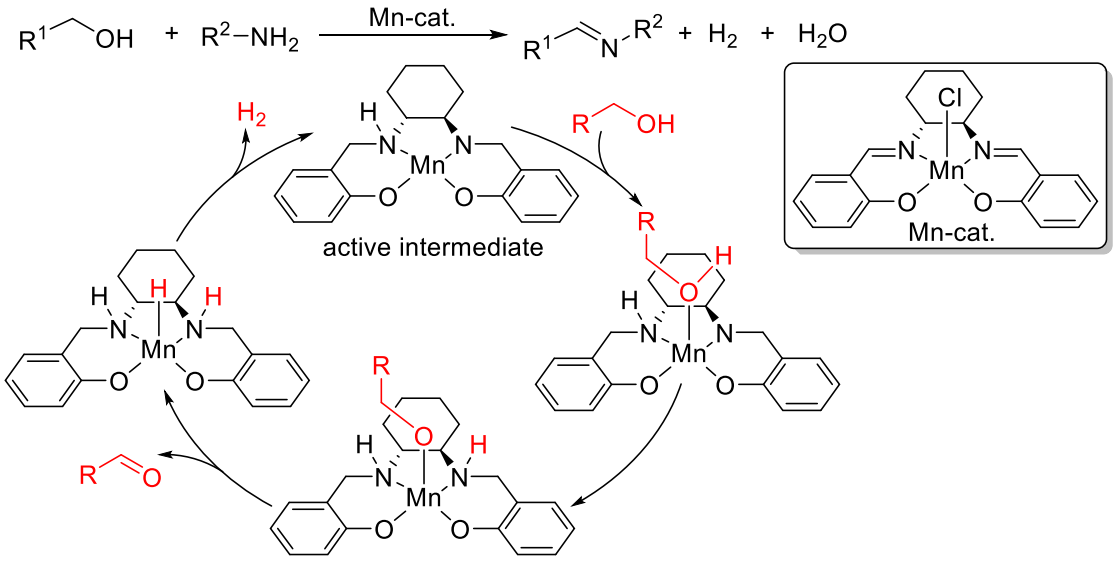

Scheme 3.7: Mn(III) salen-catalyzed dehydrogenation of alcohols[117]

3.2 Results and discussion

Based on reported systems of Mn catalyzed (de)hydrogenations and our previous results on Mn catalyzed dehydrogenation of methanol,[98] we were interested to know if Mn complexes with phosphine free ligands could promote dehydrogenation of alcohols. The initial inspiration of this work came from the results obtained by Jacob Schneekönig where chiral oxamides were employed for asymmetric transfer hydrogenation of acetophenone (Scheme 3.8),[118] so we chose two of these oxamide ligands which exhibited the highest activity in the transfer hydrogenation reaction for the dehydrogenation of alcohols.

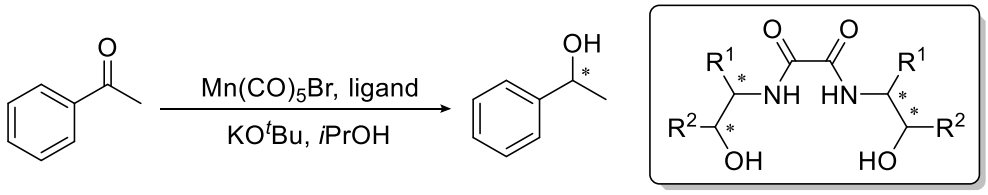

Scheme 3.8: Mn catalyzed asymmetric transfer hydrogenation of acetophenone with chiral oxamide ligands[118]

3.2.1 Reaction optimization

Isopropanol was chosen as model substrate to examine different oxamide ligands and Mn precursor, when chiral oxamides **L1** and **L2** were employed together with $Mn(CO)_5Br$, H_2 evolution was detected in both cases, albeit at very low amount (Scheme 3.9).

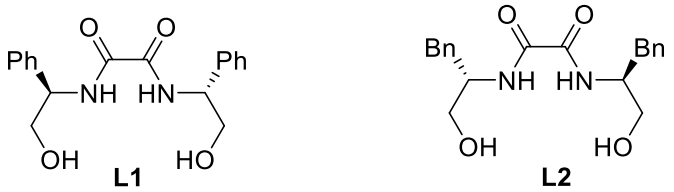

Ligand	V_{5h}(mL)	GC Result (H_2)
L1	23.2	2.0%
L2	44.0	8.2%

Conditions: ^{i}PrOH (8 mL), NaO^{i}Pr (1 mmol), $Mn(CO)_5Br$ (40 µmol), Ligand (80 µmol)

Scheme 3.9: Initial test of oxamides in Mn catalyzed dehydrogenation of isopropanol

With these initial results, a series of differently substituted oxamide compounds were prepared. Since a chiral center on the ligand is not necessarily needed for the dehydrogenation reaction, and the hydroxyl group in **L1** and **L2** might not coordinate to the metal center and thus can be removed, we focused on structurally simpler oxamides substituted by alkyl and aryl groups. When methyl substituted oxamide **L3** was used as ligand, slightly higher activity was observed than with **L1** and **L2** (Table 3.1, entry 1). Similar activities were observed for oxamide ligands bearing long alkyl chains (entries 2 and 4), while **L5** was much less active (entry 3), probably due to the steric hindrance of the isopropyl group. Unsubstituted oxamide **L7** also showed limited activity (entry 5), while nitrogen fully substituted oxamide **L8** was entirely inactive (entry 6), which indicates the importance of having a hydrogen atom on nitrogen. Interestingly, aryl substituted ligand **L9** was also inactive in this reaction (entry 7). Other nitrogen containing molecules were tested, no activity was observed for 1,3-diethylurea (entry 8), *N,N'*-dimethylglycinamide was less active than oxamide ligand **L3** (entry 9). No H_2 was detected when ethylenediamine and its analogue **L13** were utilized as ligands (entry 10). Polydentate ligands were investigated as well, unfortunately, none of these compounds could promote this Mn catalyzed dehydrogenation reaction (entry 10). The presence of an additional ligand is indeed necessary as no H_2 was detected when only $Mn(CO)_5Br$ precursor was used (entry 11).

Table 3.1: Screening of different phosphine free ligands for Mn catalyzed dehydrogenation of ^{i}PrOH

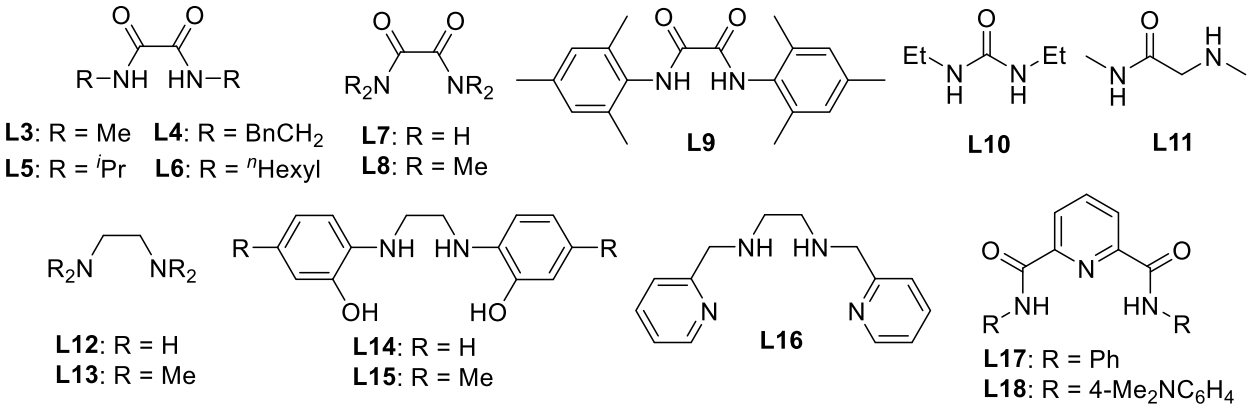

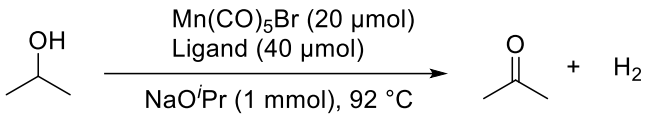

Entry	Ligand	V_{5h}(mL)	TON_{5h}
1	**L3**	35	78
2	**L4**	14	31
3	**L5**	7.5	17
4	**L6**	16	35
5	**L7**	4.6	10
6	**L8**	0	0
7	**L9**	0	0
8	**L10**	0	0
9	**L11**	17	38
10	**L12 - L18**	0	0
11	**none**	0	0

It is noted in our previous work on Mn pincer complex catalyzed dehydrogenation of methanol, excess pincer ligand in the system improves activity as well as stability.[98] Therefore we examined the effect of ligand loading in the present system. The results showed similar decayed H_2 evolution curve at different ligand loading, gas evolution slowed down after one hour (Figure 3.1). Hence, we can conclude, that the ligand concentrations is not the limiting factor causing deactivation of the system.

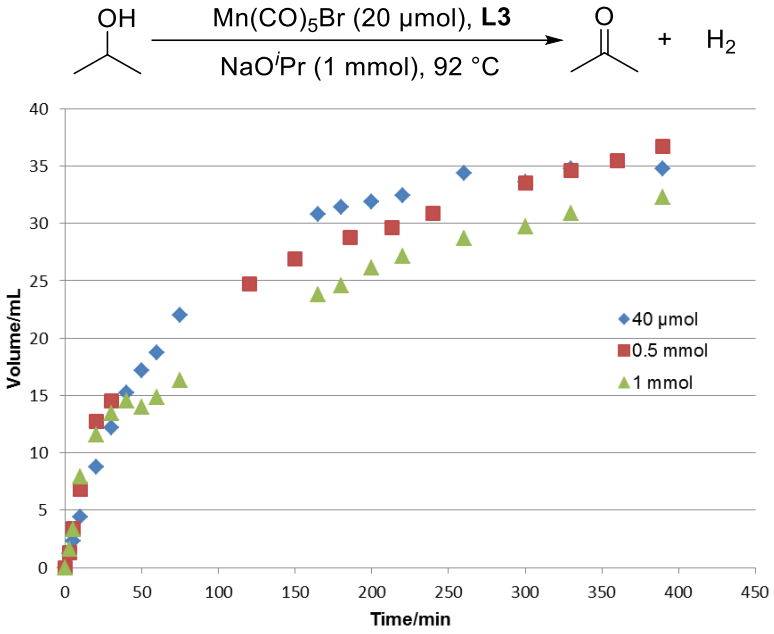

Figure 3.1: Gas evolution curve with different ligand loadings

Next, we evaluated the influence of different bases on the performance of this system with **L3** as optimal ligand (Table 3.2). Aside from Na^{i}OPr, other alkali metal alkoxides including NaO^{t}Bu, NaOEt and KOMe are also suitable for this reaction, albeit slightly less active than Na^{i}OPr. However, inorganic base such as NaOH and KOH are much less active than alkali metal alkoxides.

Table 3.2: Effect of bases on reaction activity

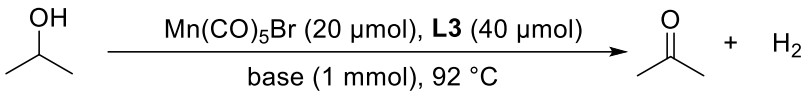

Entry	Base	V_{5h}(mL)	TON_{5h}
1	NaO^{i}Pr	35	78
2	NaO^{t}Bu	26	58
3	KO^{t}Bu	24	54
4	NaOEt	29	64
5	KOMe	22	49
6	NaOH	14	32
7	KOH	10	22

Furthermore, we also investigated the influence of different base concentrations in the system (Figure 3.2). At very low base loading (40 μmol), the system was almost inactive. The activity increased gradually with the increase of base concentration up to 1 mmol, when the amount of Na^{i}OPr was further increased to 2 mmol, activity dropped again.

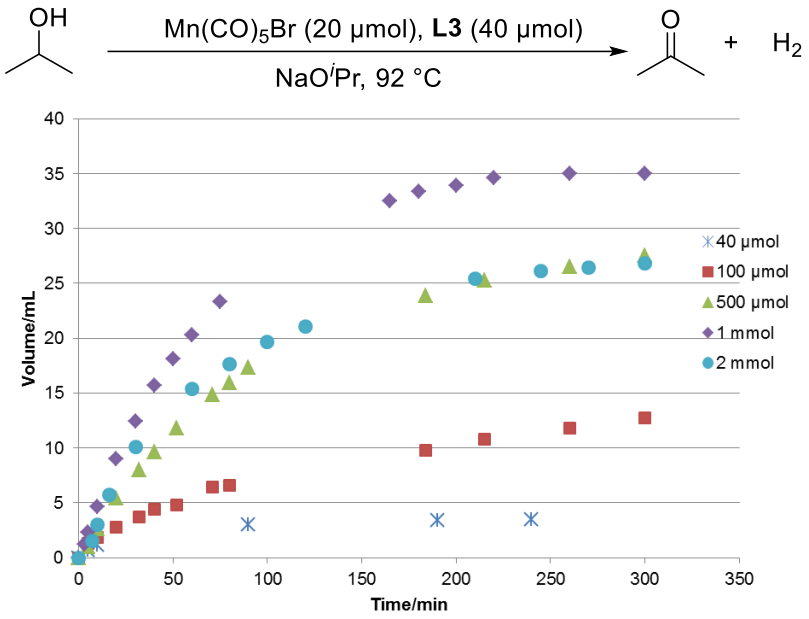

Figure 3.2: Effect of the base concentration on the hydrogenation of ^{i}PrOH

Besides, toluene and triglyme were investigated to check the solvent effect. With toluene as solvent, the system showed lower reactivity and in triglyme the reactivity (TON_{5h} = 79) was close to the one obtained under neat conditions (Figure 3.3).

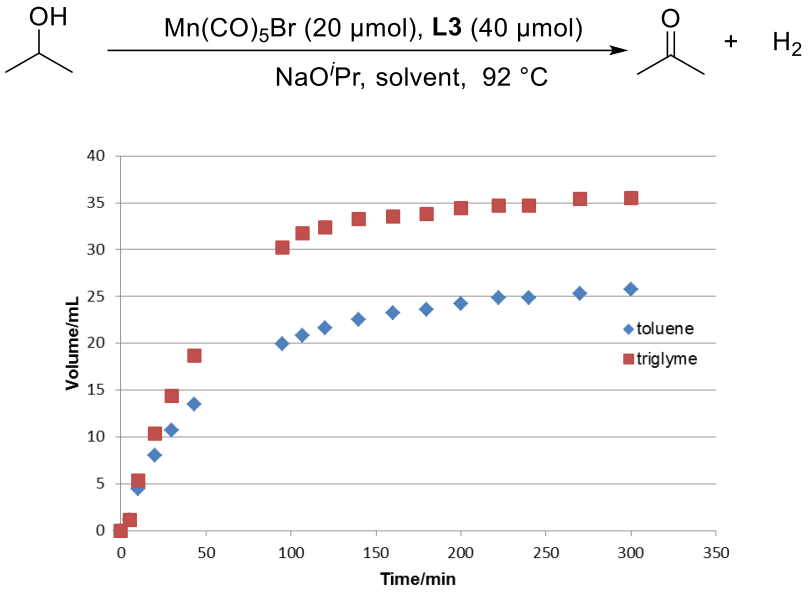

Figure 3.3: Influence of different solvents on the dehydrogenation activity

Apart from isopropanol, other alcohols were also tested in our system. Methanol was found inactive under similar conditions, while in ethanol the catalyst showed higher stability than in

isopropanol, no obvious sign of deactivation was observed after 9 hours and ethyl acetate was detected in the liquid residue by ^{1}H NMR spectroscopy.

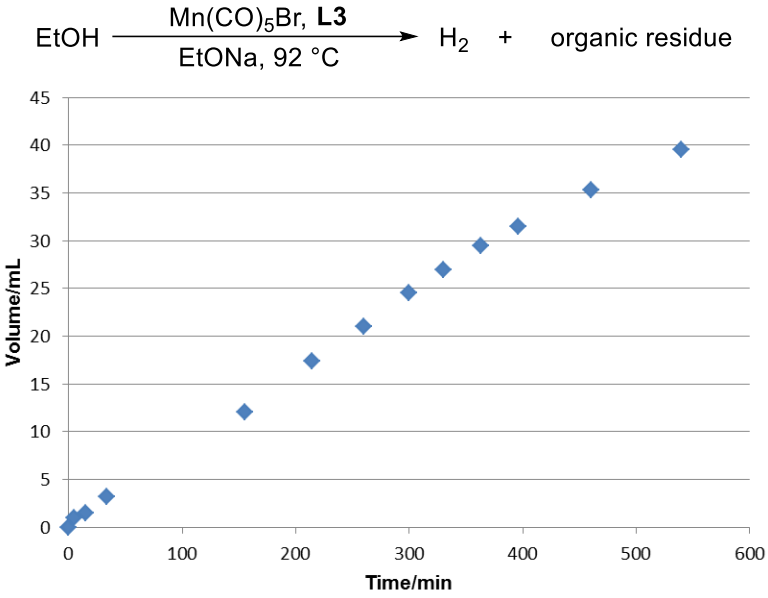

Figure 3.4: Mn catalyzed dehydrogenation of ethanol. Conditions: EtOH (8 mL), $Mn(CO)_5Br$ (20 μmol), **L3** (20 μmol), EtONa (1 mmol)

Finally, the dehydrogenation of higher alcohols was tested in an open system under gentle argon flow. Primary alcohols such as benzyl alcohol and *n*-hexanol gave the corresponding esters in 14% and 75% yields respectively. Secondary alcohol 1-phenylethanol only gave acetophenone in very low yield. In contrast, if the same reactions were performed in sealed tubes, much lower conversion and yield were observed even with higher catalyst loading, which indicates that the dehydrogenative reactions is suppressed by H_2.

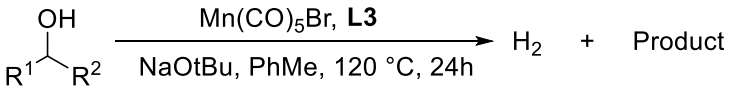

Entry	Substrate	Product	Yield (NMR)
1	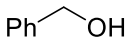	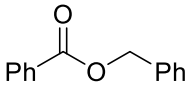	14%
2	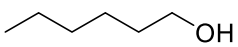	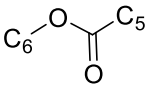	75%
3	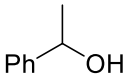	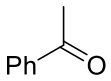	13%

Scheme 3.10: Dehydrogenation of other alcohols. Conditions:alcohol (5 mmol), Mn (0.05 mmol), L3 (0.1 mmol), Na^{i}OPr (0.25 mmol)

3.2.2 The synthesis of well-defined Mn complexes

In parallel with the condition optimization, we tried a lot endeavour to prepare the well-defined Mn complexes in order to get more insight into the system and thus improve the activity and stability of the catalyst.

When the Mn precursor $Mn(CO)_5Br$ and ligand **L3** were stirred in THF or isopropanol solution at room temperature, no observable changes occurred, while refluxing of the system led to an intractable mixture which was diffcult to analyze. Interestingly, when one equivalent of base was added to this system, CO release from the solution was observed, which indicates the complexation between Mn precursor and oxamide had taken place. However, efforts to isolate the resulting complex failed mainly due to its low solubility.

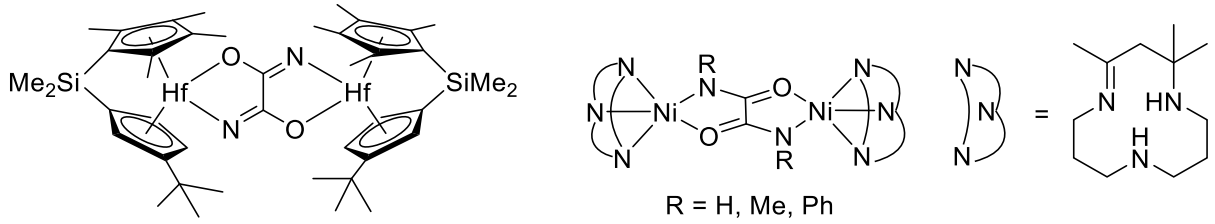

Scheme 3.11: Literature-known examples of oxamidide bridged dinuclear complexes

It was showed by García and Julve in 2004 that oxamidate can coordinate to two nickel centers forming oxamidate-bridged dinuclear Ni(II) complexes.[119a] Similar dinuclear species with bridging ligands were also observed by Cotton and Chirik for molybdenum[119b] and hafnium[119c]. Inspired by these observations, we also tried the dehydrogenation with different ligand/metal ratios, similar reactivity was observed regardless of such ratio, either ligand/metal = 1:2 or ligand/metal = 1:1 (Figure 3.5), these preliminary results indicate the oxamidite-bridged structure also possible for Mn. However, additional experiments are still needed to fully confirm this assumption.

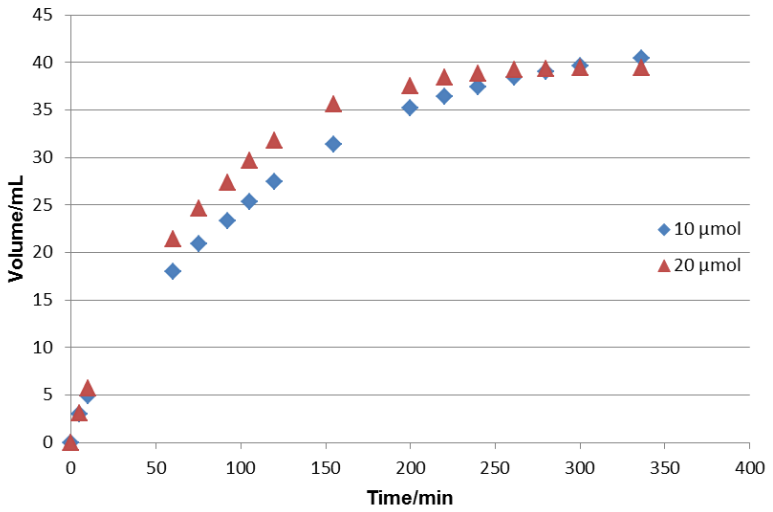

Figure 3.5: Gas evolution with various ligand/Mn ratios. Conditions: ^{i}PrOH (8 mL), Na^{i}OPr (1 mmol) $Mn(CO)_5Br$ (20 µmol), **L3** (as showed in the figure), 92 °C

Since the synthesis of well-defined Mn complexes using $Mn(CO)_5Br$ as precursor and the optimal ligand **L3** failed, we also tried to prepare other Mn complexes with other tested ligands. Adding ligand **L11** to $Mn(CO)_5Br$ in toluene, we observed CO evolution from the solution, after stirring overnight at room temperature a yellow precipitate was formed. We were able to characterize its structure through X-ray diffraction, the result showed bidentate coordination of the ligand to Mn through the amide oxygen and the amine nitrogen (Figure 3.6).

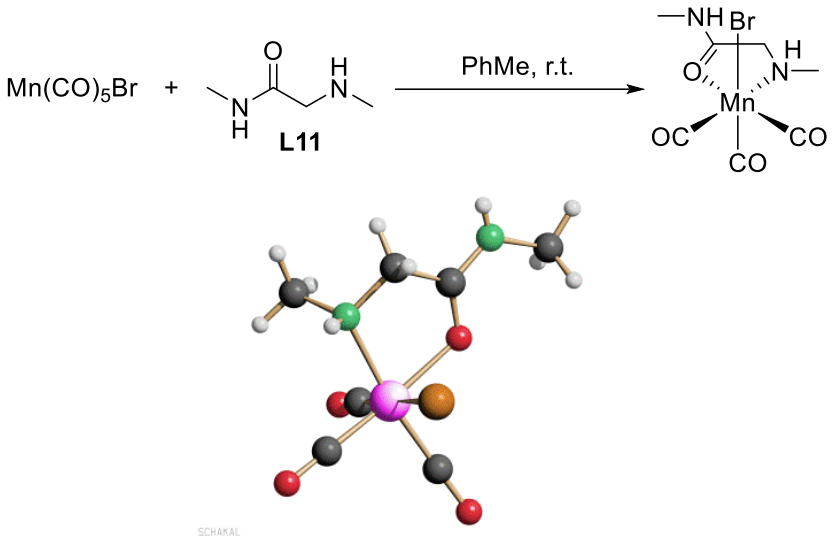

Figure 3.6: Synthesis of a Mn complex and its structure confirmed by X-ray structure

During the preparation of this thesis, we realized that under the optimal reaction conditions, both hydrogenation atoms on the amide group of ligand **L3** might be deprotonated and lead to the formation of an anionic Mn complex, since the loading of base is largely excess compared to the

loading of ligand (base:ligand = 25:1). Thus, we tried our last attempt to synthesize the well-defined Mn complex using **L3** in the presence of two equivalent of KO^{t}Bu, after reaction with $Mn(CO)_5Br$ in THF under refluxing condition for 3 hours, we were able to get crystal samples which are suitable for X-ray diffraction analysis. The structure obtained from X-ray analysis showed that the complex exists as an infinite chain in which the ligand **L3** coordinates to Mn via the two nitrogen atoms of oxamide, both of which are deprotonated as we expected, with four additional carbonyls coordinate to this Mn (Figure 3.7, Mn in blue color) centre, thus forming a mononuclear unit bearing octahedron configuration. Three of this mononuclear unit are further bonded to another Mn (Figure 3.7, Mn in red color) centre via the oxygen atoms of oxamide forming tetranuclear unite. The second Mn centre is best described as Mn(II) oxidation state resulting from the oxidation of Mn(I) precursor by oxygen, which might occurred during the crystallization of the sample since this process was not strictly exclusive of air. The tetranuclear units are bridged by potassium cations, each potassium cation is ligated by seven oxygen atoms six of which come from two sets of the tetranuclear unit and another one comes from THF molecular, thus forms a coordination polymer.

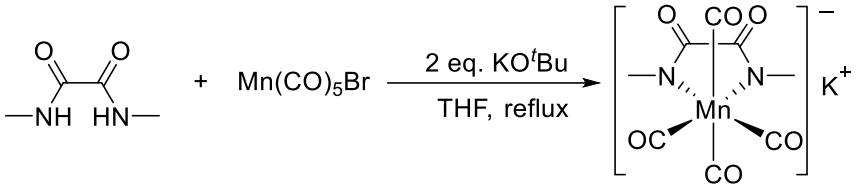

Scheme 3.12: Synthesis of an anionic Mn complex and its proposed structure

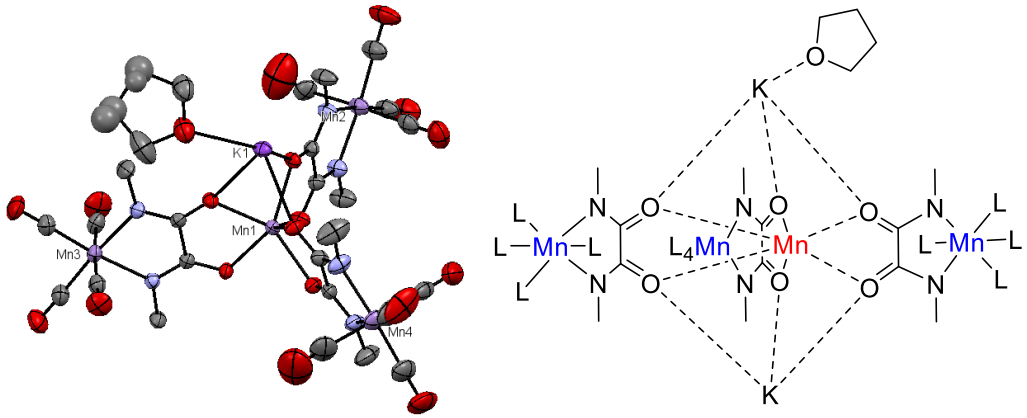

Figure 3.7: Structure of the Mn complex with deprotonated oxamide ligand: asymmetric unit is showed in the X-ray structure, thermal ellipsoids at 50% probability, hydrogen atoms were eliminated for clarity, the bigger ellipsoids of carbonyls were caused by disorder of THF; L = CO

3.2.3 Proposed mechanism

Based on our present observations and literature datas, a preliminary mechanism involving anionic Mn complexes was proposed (Scheme 3.13). According to the structure obtained from X-ray diffraction, an anionic Mn complex **I** is suggested to be the precatalyst. Under reaction conditions, one of the carbonyls of complex **I** is substituted by isopropanol forming a Mn isopropoxide intermediate **III**, which then gives ketone and Mn hydride species **IV** through β-H elimination. Release of H_2 from Mn hydride forms the pentacoordinated complex **V**, which is captured by isopropanol to restore the isopropoxide intermediate. This mechanism is quite similar to the one suggested by Madsen in the Mn(III) catalyzed dehydrogenation reactions[117] but anionic Mn complexes rather than neutral ones are involved. Indeed, several anionic Mn complexes have been studied, both in Mn(I) and Mn(III) state,[120] still, extra experimental dates are need to further confirm our proposed mechanism.

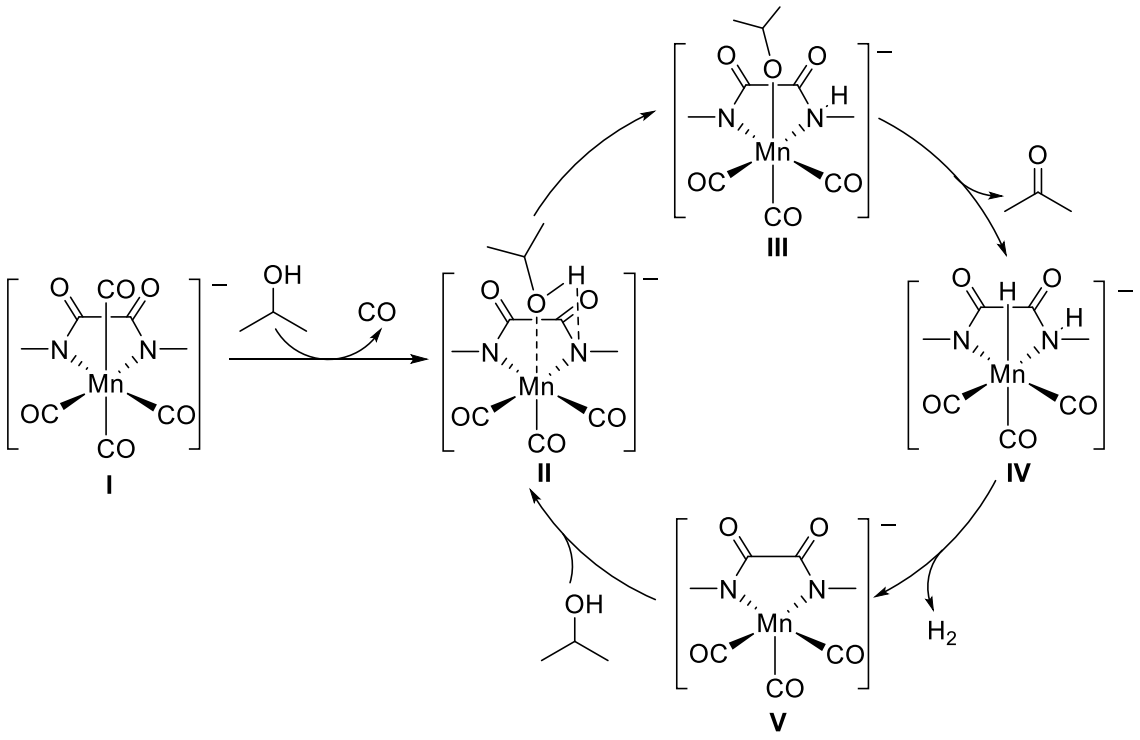

Scheme 3.13: Proposed mechanism for Mn catalyzed dehydrogenation of ^{i}PrOH

3.3 Summary

A catalytic system for Mn catalyzed dehydrogenation of alcohols was developed based on phosphine free oxamide ligands. Attempts to prepare the well-defined catalyst led to the isolate and characterize of a unique anionic Mn complex which was proposed as precatalyst, while further investigations are still needed to improve catalytic activity of this system and to get a better understanding of the mechanism.

4 Conclusion and outlook

During the course of this doctoral study, a highly active Co system bearing aliphatic PNP pincer ligands was developed for the selective formic acid dehydrogenation reaction, a TOF close to 1500 $h^{-1}$was obtained at 80 °C. Besides, the system is compatible with water as satisfactory activity was observed in aqueous media. Detailed mechanistic studies combining poisoning experiments, KIE experiments and DFT calculations showed that both the metal center and the ancillary ligand play an important role on the observed activity, while CO coordination to the Co centre will lead to catalyst deactivation. Two different mechanistic pathways are proposed based on the type of ligands (Scheme 4.1): the less electronic donating pincer ligand with phenyl group on phosphine leads to a highly active system involving an innocent non-classical bifunctional outer-sphere mechanism; while with more electronic donating pincer ligand with isopropyl group on phosphine, oxidative addition of FA to Co(I) was proposed. The resulting Co(III) species then comproportionated with the starting Co(I) complex to give inactive Co(II) species which accounts for the low activity observed in this case. The understanding of the Co system will be helpful for the development of more efficient and stable dehydrogenation catalysts and will also contribute to the understanding of Co catalyzed hydrogenation reactions.

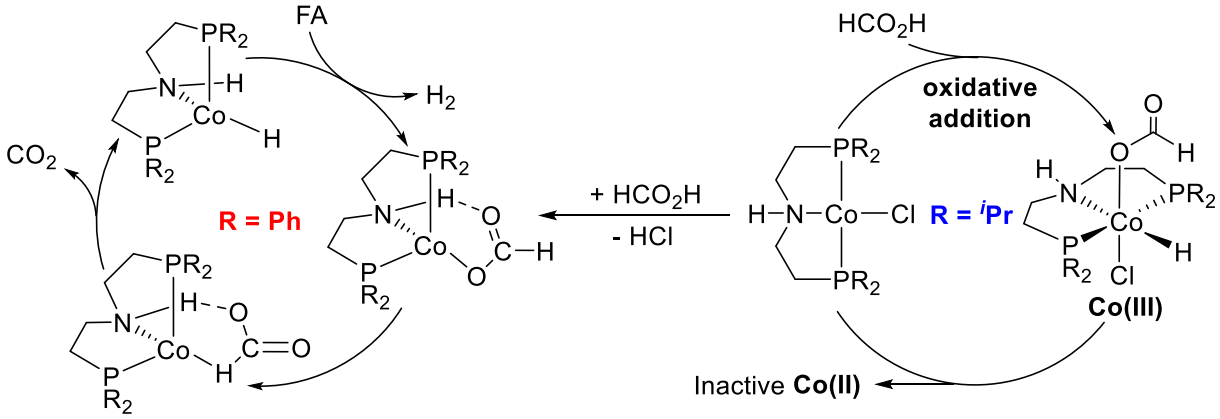

Scheme 4.1: Proposed mechanism for the Co catalyzed dehydrogenation of FA

In the second part, Mn catalyzed dehydrogenation of alcohols was investigated by employing phosphine free oxamide ligands. Endeavors towards the preparation of well-defined Mn complexes allow us to isolate and characterize an unique anionic Mn complex ligated by deprotonated *N,N'*-dimethyloxamide which is proposed as an active intermediate during the dehydrogenation process (Scheme 4.2). Our preliminary results demonstrated dehydrogenation is possible without using hazardous phosphine, further investigation will focus on the improvement of the activity and stability of the present system and also getting better understanding of the mechanism.

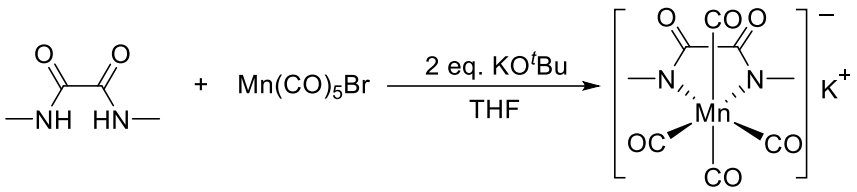

Scheme 4.2: Synthesis of an anionic Mn complex with oxamide ligand

The results disclosed in this dissertation will definitely be helpful for the development of H_2 storage based on greener and more economical methods, besides, they can also promote our understanding of the chemistry of first row transition metals.

5 Experiments and data analysis

5.1 General information

All reactions were performed under argon atmosphere with exclusion of air using standard Schlenk techniques. Chemicals were purchased from Strem, Alfa Aesar or Sigma Aldrich and used as received unless otherwise specified. Formic acid (FA), N,N-dimethyl-n-octylamine (DMOA), propylene carbonate (PC) and triglyme were refluxed and distilled following standard procedures and stored under argon atmosphere. Heptane, toluene, tetrahydrofuran (THF), diethylether, EtOH and MeOH were dried by passing through a column of anhydrous alumina using a solvent purification system equipment from Innovative Technology and stored under argon atmosphere. Water was degassed by bubbling argon overnight. Deuterated organic solvents were distilled over Na/benzophenone ketyl (THF-*d8*, C_6D_6 and toluene-*d8*) or CaH_2 (CD_2Cl_2). Other reagents were used and stored as received. Complexes **1**, **3**, **4**, **5**, **6**, **10** were prepared according to reported procedures.[92, 110]

^{1}H, ^{13}C and ^{31}P NMR spectra were obtained at Bruker AV-300 or Bruker AV-400. Chemical shifts are reported in referenced to the residual proton resonance and the natural abundance ^{13}C resonance of the solvents unless otherwise noted. Abbreviations used in the reported NMR experiments: br, broad; s, singlet; d, doublet; t, triplet; q, quartet; m, multiplet. Solution magnetic moments were determined by the method of Evans at 25 ºC using a ferrocene standard.

Diffraction data were collected on a Bruker Kappa APEX II Duo diffractometer. The structures were solved by direct methods (SHELXS-97: Sheldrick, G. M. *Acta Cryst.* **2008**, *A64*, 112.) and refined by full-matrix least-squares procedures on F^2 (SHELXL-2014: Sheldrick, G. M. *Acta Cryst.* **2015**, *C71*, 3.). XP (Bruker AXS) was used for graphical representations.

Manual burette setup for measuring gas evolution

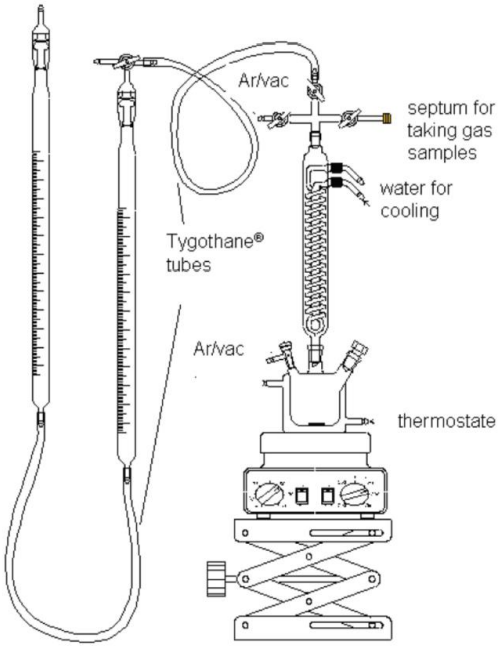

Figure 5.1: Manual burette setup

The reactor is a double-walled three-necked reaction vessel connected to two scaled gas burettes filled with water via a Dimroth condenser. The temperature of the vessel is controlled by a thermostat.

Calculation of TON

The measured gas volumes were corrected by a blank value (volume increase measured in a reaction performed under same conditions but without catalyst). The turnover number (TON) was calculated by equation **1**:

$$TON = \frac{V_{obs} - V_{blank}}{\frac{(V_{m,H_2,25°C} + V_{m,CO_2,25°C})}{n_{cat}}} \quad (\mathbf{1})$$

where V_{obs} and V_{blank} are the gas volume measured in the catalytic reaction and blank reaction, respectively.

The calculation of $V_{m,H_2,25°C}$ was carried out using Van der Waals equation (equation **2**):

$$V_{m,H_2,25°C} = \frac{RT}{p} + b - \frac{a}{RT} = 24.48 \frac{L}{mol} \quad (\mathbf{2})$$

Where:

R: 8.3145 $m^3 \cdot Pa \cdot mol^{-1}K^{-1}$;

T: 298.15 K;

P: 101325 Pa;

a: $24.7 \cdot 10^{-3} \cdot Pa \cdot m^6 \cdot mol^{-2}$;
b: $26.6 \cdot 10^{-6}\ m^3 \cdot mol^{-1}$

The calculation of $V_{m,CO_2,25°C}$ was carried out using Van der Waals equation (equation **3**):

$$V_{m,CO_2,25°C} = \frac{RT}{p} + b - \frac{a}{RT} = 24.36\ \frac{L}{mol} \qquad (\mathbf{3})$$

Where:

R: $8.3145\ m^3 \cdot Pa \cdot mol^{-1}K^{-1}$;
T: 298.15 K;
P: 101325 Pa;
a: $36.5 \cdot 10^{-2} \cdot Pa \cdot m^6 \cdot mol^{-2}$;
b: $42.7 \cdot 10^{-6}\ m^3 \cdot mol^{-1}$

GC calibrations

The gas constitution was determined by gas-phase GC. A GC sample was taken from the reaction system and was analyzed by one of the two available systems:

GC a): HP Plot Q / FID – hydrocarbons, Carboxen / TCD - permanent gases, He carrier gas.
GC b): Carboxen / TCD / Methanizer / FID - permanent gases, He carrier gas.

The gas integration was calibrated using certified gas mixtures from commercial suppliers (Linde and Air Liquide) with the following gas vol%:

GC a):

H_2: 1%, 10%, 25%, 50%, 100%
CO: 10 ppm, 100 ppm, 250 ppm, 1000 ppm, 1%, 10%
CO_2: 1%, 5%, 10%, 25%, 50%, 100%
CH_4: 1%, 5%, 10%

GC b):

H_2: 1%, 10%, 25%, 50%, 100%
CO: 1 ppm, 10 ppm, 75 ppm, 100 ppm, 250 ppm, 1000 ppm, 1%, 10%
CO_2: 1%, 5%, 10%, 25%, 50%, 100%
CH_4: 1%, 5%, 10%

The systems allow for the determination of H_2, Ar, CH_4, CO and CO_2 within the ranges:

$H_2 \geq 0.5$ vol% - 100 vol%
CO ≥ 10 ppm [GC a)], CO down to 1 ppm [GC b)]
$CO_2 \geq 100$ ppm - 100 vol% [GC a)], down to 1 ppm [GC b)]
$CH_4 \geq 1$ ppm [GC b)]

GC analysis provides volume percentage of the different components of the collected gas: H_2, CO_2, CO, and CH_4.

5.2 Cobalt catalyzed dehydrogenation of formic acid

5.2.1 Preparation of coblat complexes

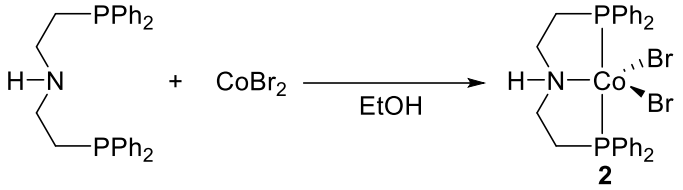

Complex **2**: $CoBr_2$ (109.4 mg, 0.5 mmol) dissolved in 10 mL EtOH, to this solution added the pincer ligand (220.7 mg, 0.5 mmol in 3 mL THF) at 60 °C, the color turned from blue to dark purple with precipitate. The system stirred at r.t. overnight and the resultant bluish green solvent removed via syringe, product washed with EtOH (10 mL × 3) and heptane (10 mL × 3), dried under vacuum to give a purple solid. Yield: 284.9 mg, 86%. Crystals suitable for X-ray analysis were grown by layering a DCM solution with EtOH. Anal. Calc: C, 50.94; H, 4.43; N, 2.12. Observed: C, 51.02; H, 5.59; N, 1.79.

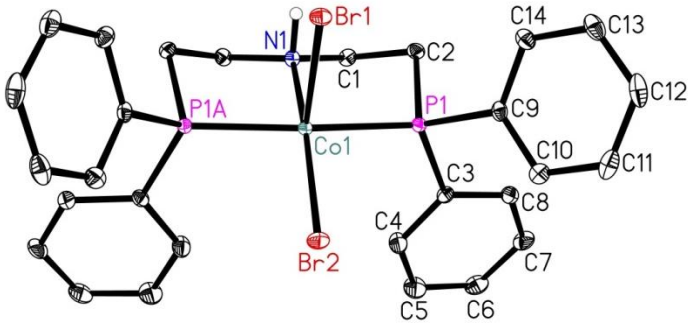

Figure 5.2: Molecular structure of complex **2** with thermal ellipsoids at 30% probability. All hydrogens except that attached to nitrogen were eliminated for clarity. Operator for generating equivalent atoms: x, -y+1/2, z

Table 5.1: Selected bond lengths and angles of complex **2**

Bond distances [Å]		Bond Angles [°]	
Br1-Co1	2.5463(6)	N1-Co1-P1	84.44(2)
Br2-Co1	2.3754(6)	P1-Co1-P1	167.28(4)
Co1-N1	2.014(3)	N1-Co1-Br2	165.45(10)
Co1-P1	2.2082(6)	P1-Co1-Br2	94.60(2)
		N1-Co1-Br1	89.37(9)
		P1-Co1-Br1	93.02(2)
		Br2-Co1-Br1	105.18(2)

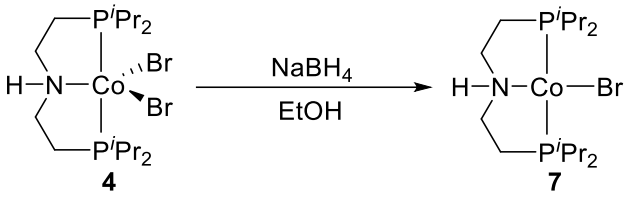

Complex **7**: complex **4** (182.1 mg, 0.347 mmol) and $NaBH_4$ (13.2 mg, 0.347 mmol) were placed in a 20 mL Schlenk tube and 10 mL of EtOH was added. The purple suspension turned to brown immediately and formed a green solution within few minutes, the system stirred under room temperature for 2h during which time the solution turned to dark blue. Solvent removed under vacuum and solid residue extracted with toluene (5 mL × 3), the toluene solution was concentrated to 4 mL, and 10 mL of heptane was added while vigorous stirring to yield the blue product. Solvent removed via syringe and product washed by heptane (5 mL × 3), dried under vacuum. Yield: 100.1 mg, 65%. Crystals suitable for X-ray analysis were grown from a concentrated solution of toluene cooled to -32 ºC. ^{1}H NMR (300 MHz, Benzene-d_6) δ 63.48 (br), 28.29 (br), 20.86 (br), 19.30 (br), 10.93 (br), -0.42 (br), -1.06 (br), -15.97 (br). Anal. Calc: C, 43.26; H, 8.40; N, 3.15. Observed: C, 43.22; H, 8.58; N, 3.03; μ_{eff} = 3.09 μ_B

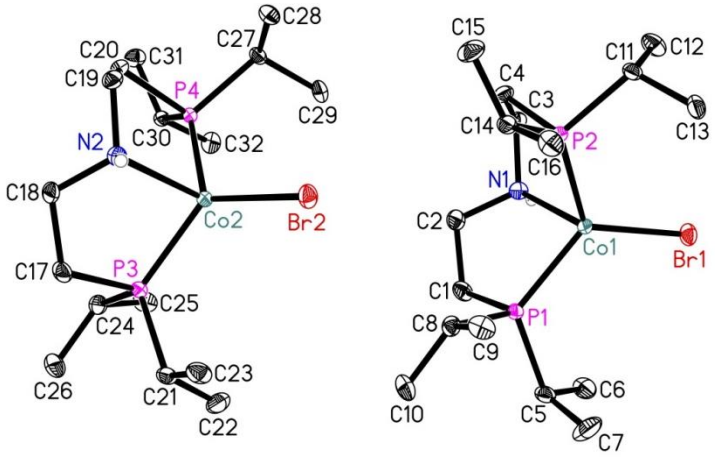

Figure 5.3: Molecular structure of complex **7** with thermal ellipsoids at 30% probability. All hydrogens except that attached to nitrogen were eliminated for clarity

Table 5.2: Selected bond lengths and angles of complex **7**

Bond distances [Å]				**Bond Angles [°]**			
Br1-Co1	2.3789(3)	Br2-Co2	2.3866(3)	N1-Co1-P2	86.39(5)	N2-Co2-P3	86.16(4)
Co1-N1	2.1479(16)	Co2-N2	2.1473(15)	N1-Co1-P1	86.44(4)	N2-Co2-P4	86.29(5)
Co1-P1	2.2408(5)	Co2-P3	2.2424(5)	P2-Co1-P1	114.747(19)	P3-Co2-P4	116.16(2)
Co1-P2	2.2395(5)	Co2-P4	2.2496(5)	N1-Co1-Br1	108.48(5)	N2-Co2-Br2	109.34(5)
				P1-Co1-Br1	123.752(16)	P3-Co2-Br2	125.178(17)
				P2-Co1-Br1	119.947(16)	P4-Co2-Br2	17.050(15)

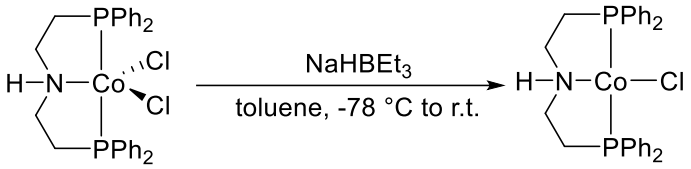

1 8

Complex **8**: to a suspension of complex **1** (571.3 mg, 1 mmol) in 25 mL toluene added $NaBEt_3H$ (1 mL, 1.0 M in toluene) at -78 ºC, the system was allowed warm up to r.t. gradually and stirred overnight. Solution filtered through Celite and concentrated to 5 mL, pentane (15 mL) was added to the solution while stirring to give a green precipitate, the solid product filtered, washed with pentane and dried under vacuum. Yield: 439.6 mg, 82%. Crystals suitable for X-ray analysis were grown by layering a benzene solution with pentane. ^{1}H NMR (300 MHz, Benzene-d_6) δ 15.95 (br), 13.36 (br), 7.99 (br), 7.15 – 6.25 (m), 5.05 (br), 4.37 (br), 4.08 (br), 2.86 – 0.62 (m), -1.05 (br). Anal. Calc: C, 62.76; H, 5.45; N, 2.61. Observed: C, 62.65; H, 5.74; N, 2.20; μ_{eff} = 2.57 μ_B

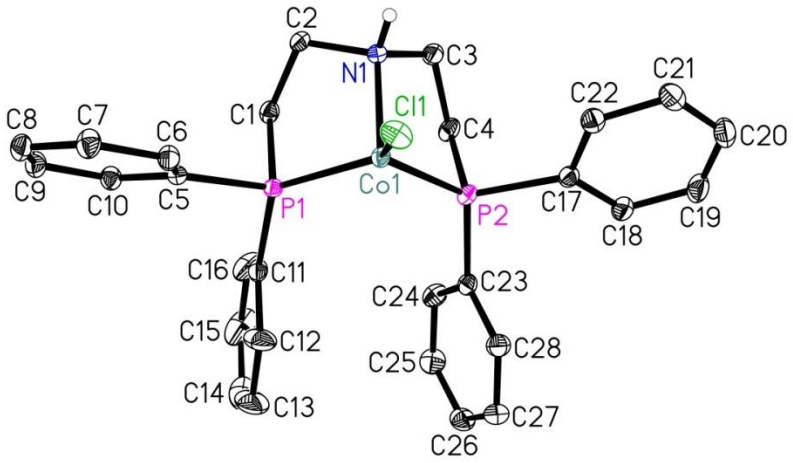

Figure 5.4: Molecular structure of complex **8** with thermal ellipsoids at 30% probability. All hydrogens except that attached to nitrogen and co-crystallized solvent (benzene) were eliminated for clarity

Table 5.3: Selected bond lengths and angles of complex **8**

Bond distances [Å]		**Bond Angles [°]**	
Cl1-Co1	2.2240(4)	N1-Co1-P2	86.17(4)
Co1-N1	2.1528(13)	N1-Co1-Cl1	113.03(4)
Co1-P2	2.2094(4)	P2-Co1-Cl1	127.384(17)
Co1-P1	2.2313(4)	N1-Co1-P1	86.04(4)
		P2-Co1-P1	102.380(15)
		Cl1-Co1-P1	126.349(17)

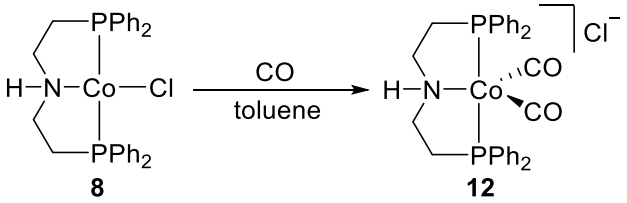

8 12

Complex **12**: complex **8** (200 mg, 0.37 mmol) dissolved in 10 mL toluene, the solution stirred under CO atmosphere overnight to give a precipitate, solvent removed through filtered cannula, solid washed with toluene (8 mL × 4) and ether (4 mL × 2) dried under vacuum to give the pale pink product. Yield: 144.6 mg, 66%. ^{1}H NMR (300 MHz, Methylene Chloride-d_2) δ 8.51 (s, 1H), 7.84 – 7.65 (m, 8H), 7.65 – 7.55 (m, 6H), 7.54 – 7.43 (m, 6H), 3.55 (br, s, 2H), 2.99 (br, s, 4H) , 2.52 (br, s, 2H). {^{1}H}^{13}C NMR (101 MHz, Methylene Chloride-d_2) δ 133.58 (t, J = 25.9 Hz), 132.19 (t, J = 5.4 Hz), 131.17 (d, J = 31.5 Hz), 129.02 (dt, J = 32.1, 5.3 Hz), 52.15 , 33.76 (t, J = 12.2 Hz). {^{1}H}^{31}P NMR δ 72.82 (s). Anal. Calc: C, 60.88; H, 4.94; N, 2.37. Observed: C, 61.49; H, 4.98; N, 3.21. IR (ATR): 2004 cm^{-1}(CO), 1926 cm^{-1}(CO)

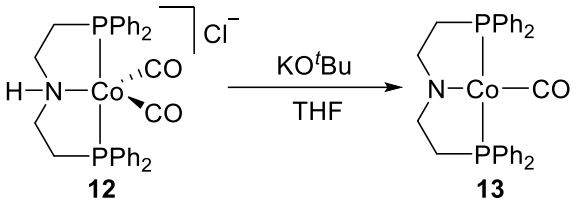

12 13

Complex **13**: complex 12 (118.4 mg, 0.20 mmol) dissolved in 5 mL THF (not completely dissolved), KO^{t}Bu (22.4 mg, 0.20 mmol) in 2 mL THF was added to the suspension at -40 °C, solid dissolved gradually and the solution turned to dark red, after one hour cooling bath was removed and the system stirred for another hour under r.t. before solvent was removed under vacuum. Solid extracted with toluene (4 mL × 4), filtered through Celite, solvent removed under vacuum to give a red solid product. Yield: 75.6 mg, 72%. Crystals suitable for X-ray analysis were obtained by vaper diffusion of hexane into a concentrated benzene solution. ^{1}H NMR (400 MHz, Benzene-d_6) (400 MHz, Benzene-d_6) δ 8.03 – 7.77 (m, 8H), 7.11 – 6.95 (m, 12H), 3.42 – 3.03 (m, 4H), 2.67 – 2.52 (m, 4H). {^{1}H}^{13}C NMR (101 MHz, Benzene-d_6) δ 135.05 (t, J = 20.2 Hz), 132.66 (t, J = 6.1 Hz), 129.43 , 128.25 (t, J = 4.7 Hz), 57.71 (t, J = 8.6 Hz), 33.54 (t, J = 11.7 Hz). carbonyl carbon resonance not observed. {^{1}H}^{31}P NMR δ 76.17 (s, br). Anal. Calc: C, 66.04; H, 5.35; N, 2.66. Observed: C, 65.78; H, 5.31; N, 2.31. IR (ATR): 1873 cm^{-1}(CO)

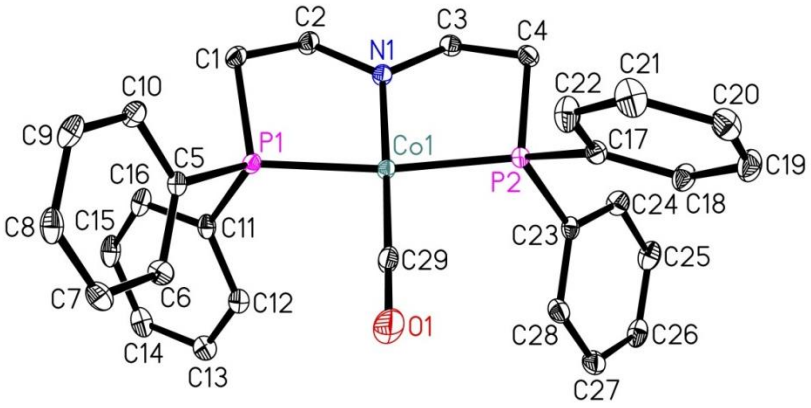

Figure 5.5: Molecular structure of complex **13** with thermal ellipsoids at 30% probability. All hydrogens were eliminated for clarity

Table 5.4: Selected bond lengths and angles of complex **13**

Bond distances [Å]		**Bond Angles [°]**	
C29-Co1	1.7032(18)	O1-C29-Co1	178.3(3)
Co1-N1	1.8615(14)	C29-Co1-N1	178.03(10)
Co1-P1	2.1589(5)	C29-Co1-P1	94.43(6)
Co1-P2	2.1742(5)	N1-Co1-P1	84.59(5)
C29-O1	1.165(2)	C29-Co1-P2	95.56(6)
		N1-Co1-P2	85.47(5)
		P1-Co1-P2	169.934(19)

5.2.2 General procedure for cobalt catalyzed dehydrogenation of formic acid

Substrates (FA, base, solvent) were given into a double walled reaction vessel. The system was heated to the desired reaction temperature and let equilibrate for 25 minutes. Then, the cobalt complex 3 (5.4 mg, 10µmol), dissolved in 0.4 mL toluene, was added to the reaction mixture and immediately the gas evolution was started to be recorded in dependence of time.

In the case of the *in-situ* formed Co(I) catalyst, the corresponding Co(II) complex (10µmol) was suspended in 0.2 mL of toluene, and $NaBEt_3H$ (0.2 mL, 1.0 M in toluene) was added under room temperature, system stirred for 15 minutes before adding to the FA solvent for dehydrogenation reaction.

5.3 Manganese catalyzed dehydrogenation of alcohols

5.3.1 Synthesis of ligands

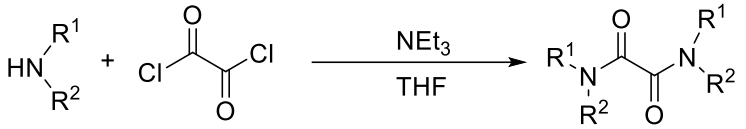

General procedure for the synthesis of oxamides: A 50 mL THF solution containing amine (20 mmol) and NEt_3 (30 mmol, 4.18 mL), oxalyl chloride (10 mmol, 0.86 mL) was added to this mixture under water/ice bath. The system was then allowed warm up to r.t. and stirred overnight. Solvent removed under vacuum, residue treated with 20 mL of water and filtered, solid washed with diethyl ether and dried under vacuum to give the oxamide product.

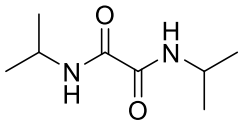

L5[121], white solid (1.55g, 90%). ^{1}H NMR (300 MHz, DMSO-d_6) δ 8.46 (d, J = 8.5 Hz, 2H), 3.91 (dp, J = 8.5, 6.6 Hz, 2H), 1.12 (d, J = 6.6 Hz, 12H); ^{13}C NMR (101 MHz, DMSO-d_6) δ 159.15, 40.91, 21.82.

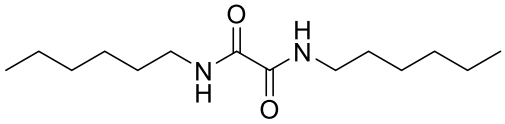

L6[122], white solid (2.05g, 80%). ^{1}H NMR (300 MHz, Chloroform-*d*) δ 7.49 (s, 2H), 3.33 (td, J = 7.2, 6.2 Hz, 4H), 1.66 – 1.50 (m, 4H), 1.44 – 1.22 (m, 12H), 0.99 – 0.83 (m, 6H); ^{13}C NMR (75 MHz, Chloroform-*d*) δ 160.01, 39.85, 31.53, 29.32, 26.64, 22.65, 14.12.

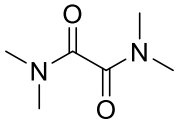

L8[123], white solid (1.20g, 83%). ^{1}H NMR (300 MHz, Chloroform-*d*) δ 2.97 (s, 6H), 2.97 (s, 6H); ^{13}C NMR (75 MHz, Chloroform-*d*) δ 165.18, 37.13, 33.76.

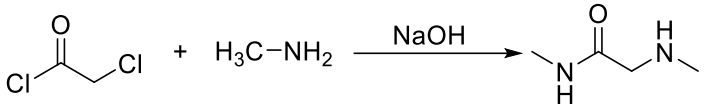

Synthesis of **L11**[124]: To an aqueous solution of methylamine (40%, 30 mL) added NaOH (10 M, 8 mL), chloroacetyl chloride (50 mmol, 3.8 mL) was added to the mixture at 0 °C slowly. The system stirred under r.t. overnight. The solution saturated with NaCl, extracted by DCM, separated, organic phase dried with Na_2SO_4, concentrated and distilled (0.28 mbar, 66 °C) to give

the title product as colorless liquid (3.5238g, 69%). ^{1}H NMR (300 MHz, Chloroform-*d*) δ 7.18 (s, 1H), 3.29 – 3.04 (m, 2H), 2.78 (dq, *J* = 5.0, 0.6 Hz, 3H), 2.36 (d, *J* = 0.9 Hz, 3H); ^{13}C NMR (75 MHz, Chloroform-*d*) δ 172.22, 54.63, 36.84, 25.67.

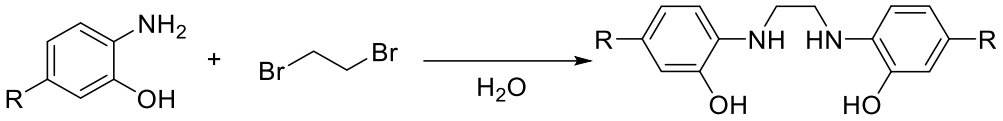

Synthesis of **L14** and **L15**: To a suspension of corresponding phenol (20 mmol) in water (15 mL) was added 1,2-dibromoethane (10 mmol, 0.86 mL). The mixture was refluxed for 5 h, and the resulting solid was filtered and recrystallized from ethanol to give the title product.

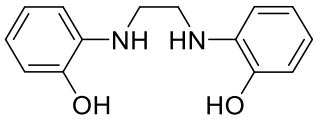

L14[125], grey solid (1.0g, 41%). ^{1}H NMR (300 MHz, DMSO-d_6) δ 9.19 (s, 2H), 6.68 – 6.59 (m, 4H), 6.57 – 6.50 (m, 2H), 6.40 (td, *J* = 7.5, 1.6 Hz, 2H), 3.29 – 3.24 (m, 4H); ^{13}C NMR (75 MHz, DMSO-d_6) δ 144.55, 137.86, 120.17, 116.18, 113.85, 110.07, 42.61.

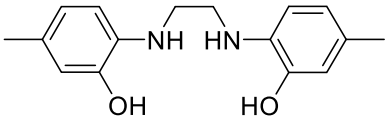

L15[126], pale grey solid (1.0g, 37%). ^{1}H NMR (300 MHz, DMSO-d_6) δ 9.07 (s, 2H), 6.49 (dt, *J* = 1.4, 0.7 Hz, 2H), 6.46 – 6.41 (m, 4H), 4.53 (s, 2H), 3.27 – 3.16 (m, 4H), 2.10 (s, 6H); ^{13}C NMR (75 MHz, DMSO-d_6) δ 144.13, 135.05, 124.40, 119.79, 114.48, 109.82, 42.57, 20.37.

5.3.2 General procedure for manganese catalyzed dehydrogenation of isopropanol

A solution (8mL) of ^{i}PrOH containing intended amount of basse was heated to 92°C and the system was equilibrated for 25 min. Afterwards, Mn precursor Mn(CO)5Br (20 μmol, 5.5 mg) and ligand (40 μmol)was added in a Teflon cap, setting this point as the starting point for measuring the evolved gas volume.

Reference

[1] a) BP's Statistical Review of World Energy, **2017,** https://www.bp.com/en/global/corporate/energy-economics/statistical-review-of-world-energy.html; b) International Energy Agency, Key world energy statistics, **2017,** https://www.iea.org/

[2] Deffeyes K. S. Beyond Oil: The View from Hubbert's Peak, Hill and Wang, New York, **2005,** *pp. 1–224*.

[3] Fifth Assessment Report, Intergovernmental panel on climate change **2015,** http://www.ipcc.ch/report/ar5/index.shtml

[4] Armaroli, N.; Balzani, V. *Angew. Chem. Int. Ed.* **2007,** *46*, 52-66.

[5] a) Balzani, V.; Credi, A.; Venturi, M. *ChemSusChem* **2008,** *1*, 26-58; b) Gust, D.; Moore, T. A.; Moore, A. L. *Acc. Chem. Res.* **2009,** *42*, 1890-1898.

[6] Armaroli, N.; Balzani, V. *ChemSusChem* **2011,** *4*, 21-36.

[7] Hydrogen as a Future Energy Carrier (Eds.: A. Züttel, A. Borgschulte, L. Schlapbach), Wiley-VCH, Weinheim, **2008**; b). Schlapbach, L.; Züttel, A. *Nature* **2001,** *414*, 353.

[8] a) Mekhilef, S.; Saidur, R.; Safari, A. *Renewable and Sustainable Energy Reviews* **2012,** *16*, 981-989; b) Yuan, X.-Z., Wang, H. Handbook of Combustion, Vol. 1, Wiley-VCH, Weinheim, **2010,** *pp*. 333–355.

[9] Zhang, H.; Shen, P. K. *Chem. Rev.* **2012,** *112*, 2780-2832

[10] a) Hamilton, C. W.; Baker, R. T.; Staubitz, A.; Manners, I. *Chem. Soc. Rev.* **2009,** *38*, 279-293; b) Makowski, P.; Thomas, A.; Kuhn, P.; Goettmann, F. *Energy Environ. Sci.* **2009,** *2*, 480-490; c) Eberle, U.; Felderhoff, M.; Schüth, F. *Angew. Chem. Int. Ed.* **2009,** *48*, 6608-6630; d) Dalebrook, A. F.; Gan, W.; Grasemann, M.; Moret, S.; Laurenczy, G. *Chem. Commun.* **2013,** *49*, 8735-8751.

[11] a) Murray, L. J.; Dincă, M.; Long, J. R. *Chem. Soc. Rev.* **2009,** *38*, 1294-1314; b) Sculley, J.; Yuan, D.; Zhou, H.-C. *Energy Environ. Sci.* **2011,** *4*, 2721-2735; c) Li, S.-L.; Xu, Q. *Energy Environ. Sci.* **2013,** *6*, 1656-1683.

[12] a) Sakintuna, B.; Lamari-Darkrim, F.; Hirscher, M. *Int. J. Hydrogen Energy* **2007,** *32*, 1121-1140; b) Bogdanović, B.; Brand, R. A.; Marjanović, A.; Schwickardi, M.; Tölle, J. *J. Alloys Compd.* **2000,** *302*, 36-58; c) Ley, M. B.; Jepsen, L. H.; Lee, Y.-S.; Cho, Y. W.; Bellosta von Colbe, J. M.; Dornheim, M.; Rokni, M.; Jensen, J. O.; Sloth, M.; Filinchuk, Y.; Jørgensen, J. E.; Besenbacher, F.; Jensen, T. R. *Materials Today* **2014,** *17*, 122-128; d) Rusman, N. A. A.; Dahari, M. *Int. J. Hydrogen Energy* **2016,** *41*, 12108-12126.

[13] a) Marder, T. B. *Angew. Chem. Int. Ed.* **2007,** *46*, 8116-8118; b) Stephens, F. H.; Pons, V.; Tom Baker, R. *Dalton Trans.* **2007,** 2613-2626; c) Zhan, W.-W.; Zhu, Q.-L.; Xu, Q. *ACS Catalysis* **2016,** *6*, 6892-6905; d) Demirci, U. B. *Int. J. Hydrogen Energy* **2017,** *42*, 9978-10013.

[14] a) Moores, A.; Poyatos, M.; Luo, Y.; Crabtree, R. H. *New J. Chem.* **2006,** *30*, 1675-1678; b) Okada, Y.; Sasaki, E.; Watanabe, E.; Hyodo, S. *Int. J. Hydrogen Energy* **2006,** *31*, 1348-1356; c) Crabtree, R. H., *Energy Environ. Sci.* **2008,** *1*, 134-138; d) Brückner, N.; Obesser, K.; Bösmann, A.; Teichmann, D.; Arlt, W.; Dungs, J.; Wasserscheid, P. *ChemSusChem* **2014,** *7*, 229-235.

[15] Satyapal, S.; Petrovic, J.; Read, C.; Thomas, G.; Ordaz, G., *Catal. Today* **2007,** *120*, 246-256.

[16] Crable, B. R.; Plugge, C. M.; McInerney, M. J.; Stams, A. J. M., *Enzyme Research* **2011,** *2011*, 8.

[17] Loges, B.; Boddien, A.; Gärtner, F.; Junge, H.; Beller, M. *Top. Catal.* **2010,** *53*, 902−914.

[18] Tingelöf, T.; Hedström, L.; Holmström, N.; Alvfors, P.; Lindbergh, G., *Int. J. Hydrogen Energy* **2008,** *33*, 2064-2072.

[19] Gunanathan, C.; Milstein, D., *Science* **2013,** *341*, 1229712.

[20] Sabatier, P., Mailhe, A., *Compt. Rend.* **1912**, *152*, 1212–1215.

[21] Adkins, H.; Nissen, B. H., *J. Am. Chem. Soc.* **1923,** *45*, 809-815.

[22] a) Rienäcker, G.; Hildebrandt, H., *Z. Anorg. Allg. Chem.* **1941,** *248*, 52-64; b) Rienäcker, G.; Bade, H., *Z. Anorg. Allg. Chem.* **1941,** *248*, 45–51.

[23] Williams, R.; Crandall, R. S.; Bloom, A., *Appl. Phys. Lett.* **1978,** *33*, 381-383.

[24] a). Li, J.; Zhu, Q.-L.; Xu, Q., *CHIMIA* **2015,** *69*, 348-352; b) Li, Z.; Xu, Q., *Acc. Chem. Res.* **2017,** *50*, 1449-1458; c) Wang, X.; Meng, Q.; Gao, L.; Jin, Z.; Ge, J.; Liu, C.; Xing, W., *Int. J. Hydrogen Energy* **2018,** *43*, 7055-7071; d) Zhong, H.; Iguchi, M.; Chatterjee, M.; Himeda, Y.; Xu, Q.; Kawanami, H., *Adv. Sustainable Syst.* **2018,** *2*, 1700161.

[25] Zhou, X.; Huang, Y.; Xing, W.; Liu, C.; Liao, J.; Lu, T., *Chem. Commun.* **2008**, 3540-3542.

[26] Ojeda, M.; Iglesia, E., *Angew. Chem. Int. Ed.* **2009,** *48*, 4800-4803.

[27] a) Tedsree, K.; Li, T.; Jones, S.; Chan, C. W. A.; Yu, K. M. K.; Bagot, P. A. J.; Marquis, E. A.; Smith, G. D. W.; Tsang, S. C. E., *Nat. Nanotechnol.* **2011,** *6*, 302-307; b) Boddien, A.; Junge, H., *Nat. Nanotechnol.* **2011,** *6*, 265-266.

[28] Zhang, S.; Metin, Ö.; Su, D.; Sun, S., *Angew. Chem. Int. Ed.* **2013,** *52*, 3681-3684.

[29] a) Gu, X.; Lu, Z.-H.; Jiang, H.-L.; Akita, T.; Xu, Q., *J. Am. Chem. Soc.* **2011,** *133*, 11822-11825; b) Zhu, Q.-L.; Tsumori, N.; Xu, Q., *Chem. Sci.* **2014,** *5*, 195-199.

[30] a) Bi, Q.-Y.; Du, X.-L.; Liu, Y.-M.; Cao, Y.; He, H.-Y.; Fan, K.-N., *J. Am. Chem. Soc.* **2012,** *134*, 8926-8933; b) Bi, Q.-Y.; Lin, J.-D.; Liu, Y.-M.; He, H.-Y.; Huang, F.-Q.; Cao, Y., *Angew. Chem. Int. Ed.* **2016,** *55*, 11849-11853.

[31] a) Cai, Y.-Y.; Li, X.-H.; Zhang, Y.-N.; Wei, X.; Wang, K.-X.; Chen, J.-S., *Angew. Chem. Int. Ed.* **2013,** *52*, 11822-11825; b) Zheng, Z.; Tachikawa, T.; Majima, T., *J. Am. Chem. Soc.* **2015,** *137*, 948-957.

[32] Mellmann, D.; Sponholz, P.; Junge, H.; Beller, M., *Chem. Soc. Rev.* **2016,** *45*, 3954-3988.

[33] Coffey, R. S., *Chem. Commun.* **1967**, 923-924.

[34] Forster, D.; Beck, G. R., *Chem. Commun***. 1971**, 1072-1072.

[35] Strauss, S. H.; Whitmire, K. H.; Shriver, D. F., *J. Organomet. Chem.* **1979,** *174*, C59-C62.

[36] Paonessa, R. S.; Trogler, W. C., *J. Am. Chem. Soc.* **1982,** *104*, 3529-3530.

[37] a) Gao, Y.; Kuncheria, J.; J. Puddephatt, R.; P. A. Yap, G., *Chem. Commun.* **1998**, 2365-2366; b) Gao, Y.; Kuncheria, J. K.; Jenkins, H. A.; Puddephatt, R. J.; Yap, G. P. A., *Dalton Trans.* **2000**, 3212-3217.

[38] Ogo, S.; Nishida, H.; Hayashi, H.; Murata, Y.; Fukuzumi, S., *Organometallics* **2005,** *24*, 4816-4823.

[39] Fukuzumi, S.; Kobayashi, T.; Suenobu, T., *ChemSusChem* **2008,** *1*, 827-834.

[40] Morris, D. J.; Clarkson, G. J.; Wills, M., *Organometallics* **2009,** *28*, 4133-4140.

[41] a) Loges, B.; Boddien, A.; Junge, H.; Beller, M., *Angew. Chem. Int. Ed.* **2008,** *47*, 3962-3965; b) Boddien, A.; Loges, B.; Junge, H.; Beller, M., *ChemSusChem* **2008,** *1*, 751-758; c) Boddien, A.; Loges, B.; Junge, H.; Gärtner, F.; Noyes, J. R.; Beller, M., *Adv. Synth. Catal.* **2009,** *351*, 2517-2520.

[42] Loges, B.; Boddien, A.; Junge, H.; Noyes, J. R.; Baumann, W.; Beller, M., *Chem. Commun.* **2009**, 4185-4187.

[43] Boddien, A.; Gärtner, F.; Federsel, C.; Sponholz, P.; Mellmann, D.; Jackstell, R.; Junge, H.; Beller, M., *Angew. Chem. Int. Ed.* **2011,** *50*, 6411-6414.

[44] a) Fellay, C.; Dyson, P. J.; Laurenczy, G., *Angew. Chem. Int. Ed.* **2008,** *47*, 3966-3968; b) Fellay, C.; Yan, N.; Dyson, P. J.; Laurenczy, G., *Chem. Eur. J.* **2009,** *15*, 3752-3760; c) Gan, W.; Fellay, C.; Dyson, P. J.; Laurenczy, G., *J. Coord. Chem.* **2010,** *63*, 2685-2694.

[45] a) Czaun, M.; Goeppert, A.; May, R.; Haiges, R.; Prakash, G. K. S.; Olah, G. A., *ChemSusChem* **2011,** *4*, 1241-1248; b) Czaun, M.; Goeppert, A.; Kothandaraman, J.; May, R. B.; Haiges, R.; Prakash, G. K. S.; Olah, G. A., *ACS Catalysis* **2014,** *4*, 311-320.

[46] Guan, C.; Zhang, D.-D.; Pan, Y.; Iguchi, M.; Ajitha, M. J.; Hu, J.; Li, H.; Yao, C.; Huang, M.-H.; Min, S.; Zheng, J.; Himeda, Y.; Kawanami, H.; Huang, K.-W., *Inorg. Chem.* **2017,** *56*, 438-445.

[47] a) Mellone, I.; Peruzzini, M.; Rosi, L.; Mellmann, D.; Junge, H.; Beller, M.; Gonsalvi, L., *Dalton Trans.* **2013,** *42*, 2495-2501; b) Filonenko, G. A.; van Putten, R.; Schulpen, E. N.; Hensen, E. J. M.; Pidko, E. A., *ChemCatChem* **2014,** *6*, 1526-1530.

[48] a) Himeda, Y.; Onozawa-Komatsuzaki, N.; Sugihara, H.; Kasuga, K., *J. Am. Chem. Soc.* **2005,** *127*, 13118-13119; b) Himeda, Y., *Green Chem.* **2009,** *11*, 2018-2022; c) Hull, J. F.; Himeda, Y.; Wang, W.-H.;

Hashiguchi, B.; Periana, R.; Szalda, D. J.; Muckerman, J. T.; Fujita, E., *Nature Chem.* **2012,** *4*, 383-388; d) Onishi, N.; Ertem, M. Z.; Xu, S.; Tsurusaki, A.; Manaka, Y.; Muckerman, J. T.; Fujita, E.; Himeda, Y., *Catal. Sci. Technol.* **2016,** *6*, 988-992.

[49] Zhang, P.; Guo, Y.-J.; Chen, J.; Zhao, Y.-R.; Chang, J.; Junge, H.; Beller, M.; Li, Y., *Nat. Catal.* **2018,** *1*, 332-338.

[50] a) Fukuzumi, S.; Kobayashi, T.; Suenobu, T., *J. Am. Chem. Soc.* **2010,** *132*, 1496-1497; b) Maenaka, Y.; Suenobu, T.; Fukuzumi, S., *Energy Environ. Sci.* **2012,** *5*, 7360-7367.

[51] Tanaka, R.; Yamashita, M.; Chung, L. W.; Morokuma, K.; Nozaki, K., *Organometallics* **2011,** *30*, 6742-6750.

[52] a) Oldenhof, S.; de Bruin, B.; Lutz, M.; Siegler, M. A.; Patureau, F. W.; van der Vlugt, J. I.; Reek, J. N. H., *Chem. Eur. J.* **2013,** *19*, 11507-11511; b) Oldenhof, S.; Lutz, M.; de Bruin, B.; Ivar van der Vlugt, J.; Reek, J. N. H., *Chem. Sci.* **2015,** *6*, 1027-1034.

[53] Celaje, J. J. A.; Lu, Z.; Kedzie, E. A.; Terrile, N. J.; Lo, J. N.; Williams, T. J., *Nat. Commun.* **2016,** *7*, 11308.

[54] a) Meerwein, H.; Schmidt, R., *Liebigs Ann.***1925,** *444*, 221-238; b). Verley, A., *Bull. Soc. Chim. Fr.* **1925,** 37, 537–542; c) Ponndorf, W., *Angew. Chem.* **1926,** *39*, 138-143.

[55] Oppenauer, R. V., *Recl. Trav. Chim. Pays-Bas* **1937,** *56*, 137-144.

[56] a) Charman, H. B., *Nature* **1966,** *212*, 278-279; b) Charman, H. B., *J. Chem. Soc. B* **1970**, 584-587.

[57] a) Dobscn, A.; Robinson, S. D., *J. Organomet. Chem.* **1975,** *87*, C52-C53; b) Dobson, A.; Robinson, S. D., *Inorg. Chem.* **1977,** *16*, 137-142.

[58] a) Morton, D.; Cole-Hamilton, D. J., *J. Chem. Soc., Chem. Commun.* **1987**, 248-249; b) Morton, D.; Cole-Hamilton, D. J.; Utuk, I. D.; Paneque-Sosa, M.; Lopez-Poveda, M., *J. Chem. Soc., Dalton Trans.* **1989**, 489-495.

[59] a) Junge, H.; Beller, M., *Tetrahedron Lett.* **2005,** *46*, 1031-1034; b) Junge, H.; Loges, B.; Beller, M., *Chem. Commun.* **2007**, 522-524.

[60] a) Nielsen, M.; Kammer, A.; Cozzula, D.; Junge, H.; Gladiali, S.; Beller, M., *Angew. Chem. Int. Ed.* **2011,** *50*, 9593-9597; b) Nielsen, M.; Junge, H.; Kammer, A.; Beller, M., *Angew. Chem. Int. Ed.* **2012,** *51*, 5711-5713.

[61] a) Blum, O.; Milstein, D., *J. Organomet. Chem.* **2000,** *593-594*, 479-484; b) Ritter, J. C. M.; Bergman, R. G., *J. Am. Chem. Soc.* **1998,** *120*, 6826-6827; c) Handgraaf, J.-W.; Meijer, E. J., *J. Am. Chem. Soc.* **2007,** *129*, 3099-3103.

[62] a) Nielsen, M.; Alberico, E.; Baumann, W.; Drexler, H.-J.; Junge, H.; Gladiali, S.; Beller, M., *Nature* **2013,** *495*, 85-89; b) Alberico, E.; Lennox, A. J. J.; Vogt, L. K.; Jiao, H.; Baumann, W.; Drexler, H.-J.; Nielsen, M.; Spannenberg, A.; Checinski, M. P.; Junge, H.; Beller, M., *J. Am. Chem. Soc.* **2016,** *138*, 14890-14904.

[63] Rodríguez-Lugo, R. E.; Trincado, M.; Vogt, M.; Tewes, F.; Santiso-Quinones, G.; Grützmacher, H., *Nature Chem.* **2013,** *5*, 342.

[64] a) Milstein, D., *Top. Catal.* **2010,** *53*, 915-923; b) Gunanathan, C.; Milstein, D., *Acc. Chem. Res.* **2011,** *44*, 588-602; c) Gunanathan, C.; Milstein, D., *Top. Organomet. Chem.* **2011** *37*, 55–84.

[65] Zhang, J.; Gandelman, M.; Shimon, L. J. W.; Rozenberg, H.; Milstein, D., *Organometallics* **2004,** *23*, 4026-4033.

[66] a) Zhang, J.; Leitus, G.; Ben-David, Y.; Milstein, D., *J. Am. Chem. Soc.* **2005,** *127*, 10840-10841; b) Gunanathan, C.; Ben-David, Y.; Milstein, D., *Science* **2007,** *317*, 790-792.

[67] a) Gunanathan, C.; Shimon, L. J. W.; Milstein, D., *J. Am. Chem. Soc.* **2009,** *131*, 3146-3147; b) Zhang, J.; Balaraman, E.; Leitus, G.; Milstein, D., *Organometallics* **2011,** *30*, 5716-5724; c) Balaraman, E.; Khaskin, E.; Leitus, G.; Milstein, D., *Nature Chem.* **2013,** *5*, 122.

[68] Hu, P.; Diskin-Posner, Y.; Ben-David, Y.; Milstein, D., *ACS Catalysis* **2014,** *4*, 2649-2652.

[69] a) Fujita, K.-i.; Tanino, N.; Yamaguchi, R., *Org. Lett.* **2007,** *9*, 109-111; b) Fujita, K.-i.; Yoshida, T.; Imori, Y.; Yamaguchi, R., *Org. Lett.* **2011,** *13*, 2278-2281; c) Kawahara, R.; Fujita, K.-i.; Yamaguchi, R., *J. Am. Chem. Soc.* **2012,** *134*, 3643-3646; d) Fujita, K. i.; Kawahara, R.; Aikawa, T.; Yamaguchi, R., *Angew. Chem.*

Int. Ed. **2015,** *54*, 9057-9060; e) Maenaka, Y.; Suenobu, T.; Fukuzumi, S., *J. Am. Chem. Soc.* **2012,** *134*, 9417-9427.

[70] a) Campos, J.; Sharninghausen, L. S.; Manas, M. G.; Crabtree, R. H., *Inorg. Chem.* **2015,** *54*, 5079-5084; b) Manas, M. G.; Campos, J.; Sharninghausen, L. S.; Lin, E.; Crabtree, R. H., *Green Chem.* **2015,** *17*, 594-600.

[71] Musa, S.; Shaposhnikov, I.; Cohen, S.; Gelman, D., *Angew. Chem. Int. Ed.* **2011,** *50*, 3533-3537.

[72] For recent reviews, see: a) Filonenko, G. A.; van Putten, R.; Hensen, E. J. M.; Pidko, E. A., *Chem. Soc. Rev.* **2018,** *47*, 1459-1483; b) Sordakis, K.; Tang, C.; Vogt, L. K.; Junge, H.; Dyson, P. J.; Beller, M.; Laurenczy, G., *Chem. Rev.* **2018,** *118*, 372-433; c) Alig, L.; Fritz, M.; Schneider, S. *Chem. Rev.* ***2019****, 119, 2681-2751.*

[73] a) Boddien, A.; Loges, B.; Gärtner, F.; Torborg, C.; Fumino, K.; Junge, H.; Ludwig, R.; Beller, M., *J. Am. Chem. Soc.* **2010,** *132*, 8924-8934; b) Boddien, A.; Gärtner, F.; Jackstell, R.; Junge, H.; Spannenberg, A.; Baumann, W.; Ludwig, R.; Beller, M., *Angew. Chem. Int. Ed.* **2010,** *49*, 8993-8996.

[74] a) Boddien, A.; Mellmann, D.; Gärtner, F.; Jackstell, R.; Junge, H.; Dyson, P. J.; Laurenczy, G.; Ludwig, R.; Beller, M., *Science* **2011,** *333*, 1733-1736; b) Montandon-Clerc, M.; Dalebrook, A. F.; Laurenczy, G., *J. Catal.* **2016,** *343*, 62-67.

[75] Bertini, F.; Mellone, I.; Ienco, A.; Peruzzini, M.; Gonsalvi, L., *ACS Catalysis* **2015,** *5*, 1254-1265.

[76] a) Zell, T.; Butschke, B.; Ben-David, Y.; Milstein, D., *Chem. Eur. J.* **2013,** *19*, 8068-8072; b) Mellone, I.; Gorgas, N.; Bertini, F.; Peruzzini, M.; Kirchner, K.; Gonsalvi, L., *Organometallics* **2016,** *35*, 3344-3349.

[77] Bielinski, E. A.; Lagaditis, P. O.; Zhang, Y.; Mercado, B. Q.; Würtele, C.; Bernskoetter, W. H.; Hazari, N.; Schneider, S., *J. Am. Chem. Soc.* **2014,** *136*, 10234-10237.

[78] a) Enthaler, S.; Brück, A.; Kammer, A.; Junge, H.; Irran, E.; Gülak, S. *ChemCatChem* **2015**, *7*, 65-69; b) Scotti, N.; Psaro, R.; Ravasio, N.; Zaccheria, F. *RSC Advances* **2014**, *4*, 61514-61517.

[79] a) Alberico, E.; Sponholz, P.; Cordes, C.; Nielsen, M.; Drexler, H. J.; Baumann, W.; Junge, H.; Beller, M., *Angew. Chem. Int. Ed.* **2013,** *52*, 14162-14166; b) Peña-López, M.; Neumann, H.; Beller, M., *ChemCatChem* **2015,** *7*, 865-871.

[80] Chakraborty, S.; Lagaditis, P. O.; Förster, M.; Bielinski, E. A.; Hazari, N.; Holthausen, M. C.; Jones, W. D.; Schneider, S., *ACS Catalysis* **2014,** *4*, 3994-4003.

[81] Bielinski, E. A.; Förster, M.; Zhang, Y.; Bernskoetter, W. H.; Hazari, N.; Holthausen, M. C., *ACS Catalysis* **2015,** *5*, 2404-2415.

[82] Wakizaka, M.; Matsumoto, T.; Tanaka, R.; Chang, H.-C., *Nat. Commun.* **2016,** *7*, 12333.

[83] a) Chakraborty, S.; Piszel, P. E.; Brennessel, W. W.; Jones, W. D., *Organometallics* **2015,** *34*, 5203-5206; b) Sengupta, D.; Bhattacharjee, R.; Pramanick, R.; Rath, S. P.; Saha Chowdhury, N.; Datta, A.; Goswami, S., *Inorg. Chem.* **2016,** *55*, 9602-9610; c) Dai, Z.; Luo, Q.; Jiang, H.; Luo, Q.; Li, H.; Zhang, J.; Peng, T., *Catal. Sci. Technol.* **2017,** *7*, 2506-2511.

[84] a) Adkins, H.; Krsek, G., *J. Am. Chem. Soc.* **1949,** *71*, 3051-3055; b) Heck, R. F.; Breslow, D. S., *J. Am. Chem. Soc.* **1961,** *83*, 4023-4027.

[85] For selected reviews, see: a) Cahiez, G.; Moyeux, A., *Chem. Rev.* **2010,** *110*, 1435-1462; b) Chirik, P. J., *Acc. Chem. Res.* **2015,** *48*, 1687-1695; c) Liu, W.; Sahoo, B.; Junge, K.; Beller, M., *Acc. Chem. Res.* **2018,** *51*, 1858-1869; d) Ai, W.; Zhong, R.; Liu, X.; Liu, Q., *Chem. Rev.* **2018**. DOI: 10.1021/acs.chemrev.8b00404.

[86] a) Zhang, G.; Scott, B. L.; Hanson, S. K., *Angew. Chem. Int. Ed.* **2012,** *51*, 12102-12106; b) Zhang, G.; Hanson, S. K., *Org. Lett.* **2013,** *15*, 650-653; c) Zhang, G.; Hanson, S. K., *Chem. Commun.* **2013,** *49*, 10151-10153.

[87] Zhang, G.; Vasudevan, K. V.; Scott, B. L.; Hanson, S. K., *J. Am. Chem. Soc.* **2013,** *135*, 8668-8681.

[88] Monfette, S.; Turner, Z. R.; Semproni, S. P.; Chirik, P. J., *J. Am. Chem. Soc.* **2012,** *134*, 4561-4564.

[89] a) Ibrahim, A. D.; Tokmic, K.; Brennan, M. R.; Kim, D.; Matson, E. M.; Nilges, M. J.; Bertke, J. A.; Fout, A. R., *Dalton Trans.* **2016,** *45*, 9805-9811; b) Tokmic, K.; Markus, C. R.; Zhu, L.; Fout, A. R., *J. Am. Chem. Soc.* **2016,** *138*, 11907-11913.

[90] a) Srimani, D.; Mukherjee, A.; Goldberg, A. F. G.; Leitus, G.; Diskin-Posner, Y.; Shimon, L. J. W.; Ben David, Y.; Milstein, D., *Angew. Chem. Int. Ed.* **2015,** *54*, 12357-12360; b) Mukherjee, A.; Srimani, D.; Chakraborty, S.; Ben-David, Y.; Milstein, D., *J. Am. Chem. Soc.* **2015,** *137*, 8888-8891.

[91] a) Daw, P.; Chakraborty, S.; Garg, J. A.; Ben-David, Y.; Milstein, D., *Angew. Chem. Int. Ed.* **2016,** *55*, 14373-14377; b) Daw, P.; Ben-David, Y.; Milstein, D., *ACS Catalysis* **2017,** *7*, 7456-7460.

[92] Junge, K.; Wendt, B.; Cingolani, A.; Spannenberg, A.; Wei, Z.; Jiao, H.; Beller, M., *Chem. Eur. J* **2018,** *24*, 1046-1052.

[93] a) Federsel, C.; Ziebart, C.; Jackstell, R.; Baumann, W.; Beller, M., *Chem. Eur. J.* **2012,** *18*, 72-75; b) Jeletic, M. S.; Mock, M. T.; Appel, A. M.; Linehan, J. C., *J. Am. Chem. Soc.* **2013,** *135*, 11533-11536; c) Badiei, Y. M.; Wang, W.-H.; Hull, J. F.; Szalda, D. J.; Muckerman, J. T.; Himeda, Y.; Fujita, E., *Inorg. Chem.* **2013,** *52*, 12576-12586; d) Spentzos, A. Z.; Barnes, C. L.; Bernskoetter, W. H., *Inorg. Chem.* **2016,** *55*, 8225-8233; e) Daw, P.; Chakraborty, S.; Leitus, G.; Diskin-Posner, Y.; Ben-David, Y.; Milstein, D., *ACS Catalysis* **2017,** *7*, 2500-2504.

[94] One early example of Co catalyzed decomposition of FA, see: Onishi, M., *J. Mol. Catal.* **1993,** *80*, 145-149.

[95] Tang, C.; Surkus, A.-E.; Chen, F.; Pohl, M.-M.; Agostini, G.; Schneider, M.; Junge, H.; Beller, M., *Angew. Chem. Int. Ed.* **2017,** *56*, 16616-16620.

[96] Zhou, W.; Wei, Z.; Spannenberg, A.; Jiao, H.; Junge, K.; Junge, H.; Beller, M., *Chem. Eur. J*. Accepted Author Manuscript. doi:10.1002/chem.201805612

[97] Rozenel, S. S.; Padilla, R.; Arnold, J., *Inorg. Chem.* **2013,** *52*, 11544-11550.

[98] Andérez-Fernández, M.; Vogt, L. K.; Fischer, S.; Zhou, W.; Jiao, H.; Garbe, M.; Elangovan, S.; Junge, K.; Junge, H.; Ludwig, R.; Beller, M., *Angew. Chem. Int. Ed.* **2017,** *56*, 559-562.

[99] Semproni, S. P.; Milsmann, C.; Chirik, P. J., *J. Am. Chem. Soc.* **2014,** *136*, 9211-9224.

[100] a) Schaefer, B. A.; Margulieux, G. W.; Small, B. L.; Chirik, P. J., *Organometallics* **2015,** *34*, 1307-1320; b) Spentzos, A. Z.; Barnes, C. L.; Bernskoetter, W. H., *Inorg. Chem.* **2016,** *55*, 8225-8233.

[101] Scheuermann, M. L.; Johnson, E. J.; Chirik, P. J., *Org. Lett.* **2015,** *17*, 2716-2719.

[102] Tokmic, K.; Jackson, B. J.; Salazar, A.; Woods, T. J.; Fout, A. R., *J. Am. Chem. Soc.* **2017,** *139*, 13554-13561.

[103] Example of a related Co(I) benzoate complex, see: Neely, J. M.; Bezdek, M. J.; Chirik, P. J., *ACS Cent. Sci.* **2016,** *2*, 935-942.

[104] a) Pearson, R. G., *J. Am. Chem. Soc.* **1963,** *85*, 3533-3539; b) Hancock, R. D.; Martell, A. E., *Chem. Rev.* **1989,** *89*, 1875-1914.

[105] Values from Wikipedia. https://en.wikipedia.org/wiki/Standard_electrode_potential_(data_page)

[106] a) Perrée-Fauvet, M.; Gaudemer, A., *J. Chem. Soc., Chem. Commun.* **1981**, 874-875; b) Katsuki, T., *Coord. Chem. Rev.* **1995,** *140*, 189-214; c) Katsuki, T., *J. Mol. Catal. A: Chem.* **1996,** *113*, 87-107; d) McGarrigle, E. M.; Gilheany, D. G., *Chem. Rev.* **2005,** *105*, 1563-1602; e) Saisaha, P.; de Boer, J. W.; Browne, W. R., *Chem. Soc. Rev.* **2013,** *42*, 2059-2074; f) Paradine, S. M.; Griffin, J. R.; Zhao, J.; Petronico, A. L.; Miller, S. M.; White, M. C., *Nature Chem.* **2015,** *7*, 987-994; g) Huang, X.; Bergsten, T. M.; Groves, J. T., *J. Am. Chem. Soc.* **2015,** *137*, 5300-5303; h) Ren, R.; Zhao, H.; Huan, L.; Zhu, C., *Angew. Chem. Int. Ed.* **2015,** *54*, 12692-12696; i) Clark, J. R.; Feng, K.; Sookezian, A.; White, M. C., *Nature Chem.* **2018,** *10*, 583-591.

[107] Mukherjee, A.; Nerush, A.; Leitus, G.; Shimon, L. J. W.; Ben David, Y.; Espinosa Jalapa, N. A.; Milstein, D., *J. Am. Chem. Soc.* **2016,** *138*, 4298-4301.

[108] a) Chakraborty, S.; Gellrich, U.; Diskin-Posner, Y.; Leitus, G.; Avram, L.; Milstein, D., *Angew. Chem. Int. Ed.* **2017,** *56*, 4229-4233; b) Chakraborty, S.; Das, U. K.; Ben-David, Y.; Milstein, D., *J. Am. Chem. Soc.* **2017,** *139*, 11710-11713; c) Espinosa-Jalapa, N. A.; Kumar, A.; Leitus, G.; Diskin-Posner, Y.; Milstein, D., *J. Am. Chem. Soc.* **2017,** *139*, 11722-11725; d) Kumar, A.; Espinosa-Jalapa, N. A.; Leitus, G.; Diskin-Posner, Y.; Avram, L.; Milstein, D., *Angew. Chem. Int. Ed.* **2017,** *56*, 14992-14996; e) Das, U. K.; Ben-David, Y.;

Diskin-Posner, Y.; Milstein, D., *Angew. Chem. Int. Ed.* **2018,** *57*, 2179-2182; f) Das, U. K.; Ben-David, Y.; Leitus, G.; Diskin-Posner, Y.; Milstein, D., *ACS Catalysis* **2019,** *9*, 479-484.

[109] a) Espinosa-Jalapa, N. A.; Nerush, A.; Shimon, L. J. W.; Leitus, G.; Avram, L.; Ben-David, Y.; Milstein, D., *Chem. Eur. J* **2017,** *23*, 5934-5938; b) Kumar, A.; Janes, T.; Espinosa-Jalapa, N. A.; Milstein, D., *Angew. Chem. Int. Ed.* **2018,** *57*, 12076-12080.

[110] a) Elangovan, S.; Topf, C.; Fischer, S.; Jiao, H.; Spannenberg, A.; Baumann, W.; Ludwig, R.; Junge, K.; Beller, M., *J. Am. Chem. Soc.* **2016,** *138*, 8809-8814; b) Elangovan, S.; Garbe, M.; Jiao, H.; Spannenberg, A.; Junge, K.; Beller, M., *Angew. Chem. Int. Ed.* **2016,** *55*, 15364-15368; c) Papa, V.; Cabrero-Antonino, J. R.; Alberico, E.; Spanneberg, A.; Junge, K.; Junge, H.; Beller, M., *Chem. Sci.* **2017,** *8*, 3576-3585.

[111] a) Peña-López, M.; Piehl, P.; Elangovan, S.; Neumann, H.; Beller, M., *Angew. Chem. Int. Ed.* **2016,** *55*, 14967-14971; b) Elangovan, S.; Neumann, J.; Sortais, J.-B.; Junge, K.; Darcel, C.; Beller, M., *Nat. Commun.* **2016,** *7*, 12641.

[112] Perez, M.; Elangovan, S.; Spannenberg, A.; Junge, K.; Beller, M., *ChemSusChem* **2017,** *10*, 83-86.

[113] a) Kallmeier, F.; Irrgang, T.; Dietel, T.; Kempe, R., *Angew. Chem. Int. Ed.* **2016,** *55*, 11806-11809; b) Mastalir, M.; Glatz, M.; Pittenauer, E.; Allmaier, G.; Kirchner, K., *J. Am. Chem. Soc.* **2016,** *138*, 15543-15546; c) Mastalir, M.; Pittenauer, E.; Allmaier, G.; Kirchner, K., *J. Am. Chem. Soc.* **2017,** *139*, 8812-8815.

[114] Tondreau, A. M.; Boncella, J. M., *Organometallics* **2016,** *35*, 2049-2052.

[115] a) Bertini, F.; Glatz, M.; Gorgas, N.; Stöger, B.; Peruzzini, M.; Veiros, L. F.; Kirchner, K.; Gonsalvi, L., *Chem. Sci.* **2017,** *8*, 5024-5029; b) Kar, S.; Goeppert, A.; Kothandaraman, J.; Prakash, G. K. S., *ACS Catalysis* **2017,** *7*, 6347-6351.

[116] a) Dubey, A.; Nencini, L.; Fayzullin, R. R.; Nervi, C.; Khusnutdinova, J. R., *ACS Catalysis* **2017,** *7*, 3864-3868; b) Bruneau-Voisine, A.; Wang, D.; Dorcet, V.; Roisnel, T.; Darcel, C.; Sortais, J.-B., *Org. Lett.* **2017,** *19*, 3656-3659.

[117] Samuelsen, Simone V.; Santilli, C.; Ahlquist, M. S. G.; Madsen, R., *Chem. Sci.* **2019,** *10*, 1150-1157.

[118] Schneekönig, J.; Junge, K.; Beller, M., *Synlett* **2019,** *30*, 503-507.

[119] a) Santana, M. D.; García, G.; Julve, M.; Lloret, F.; Pérez, J.; Liu, M.; Sanz, F.; Cano, J.; López, G., *Inorg. Chem.* **2004,** *43*, 2132-2140; b) Cotton, F. A.; Liu, C. Y.; Murillo, C. A.; Villagrán, D.; Wang, X., *J. Am. Chem. Soc.* **2004,** *126*, 14822-14831; c) Knobloch, D. J.; Lobkovsky, E.; Chirik, P. J., *J. Am. Chem. Soc.* **2010,** *132*, 15340-15350.

[120] a) Larsen, S. K.; Pierpont, C. G.; DeMunno, G.; Dolcetti, G., *Inorg. Chem.* **1986,** *25*, 4828-4831; b) Brookhart, M.; Noh, S. K.; Timmers, F. J., *Organometallics* **1987,** *6*, 1829-1831; c) Brookhart, M.; Noh, S. K.; Timmers, F. J.; Hong, Y. H., *Organometallics* **1988,** *7*, 2458-2465.

[121] Du, Z.; Li, W.; Zhu, X.; Xu, F.; Shen, Q., *J. Org. Chem.* **2008,** *73*, 8966-8972.

[122] Lu, S.; Drees, M.; Yao, Y.; Boudinet, D.; Yan, H.; Pan, H.; Wang, J.; Li, Y.; Usta, H.; Facchetti, A., *Macromolecules* **2013,** *46*, 3895-3906.

[123] Campaigne, E.; Skowronski, G.; Rogers, R. B., *Synth. Commun.* **1973,** *3*, 325-332.

[124] Saavedra, J.; Keefer, L.; Roller, P.; Akamatsu, M., U.S. Patent **1997**, 5632981.

[125] Whiteoak, C. J.; Torres Martin de Rosales, R.; White, A. J. P.; Britovsek, G. J. P., *Inorg. Chem.* **2010,** *49*, 11106-11117.

[126] Ochoa, M. E.; Rojas-Lima, S.; Höpfl, H.; Rodríguez, P.; Castillo, D.; Farfán, N.; Santillan, R., *Tetrahedron* **2001,** *57*, 55-64.

Appendix

I.Spectra of synthesized compounds

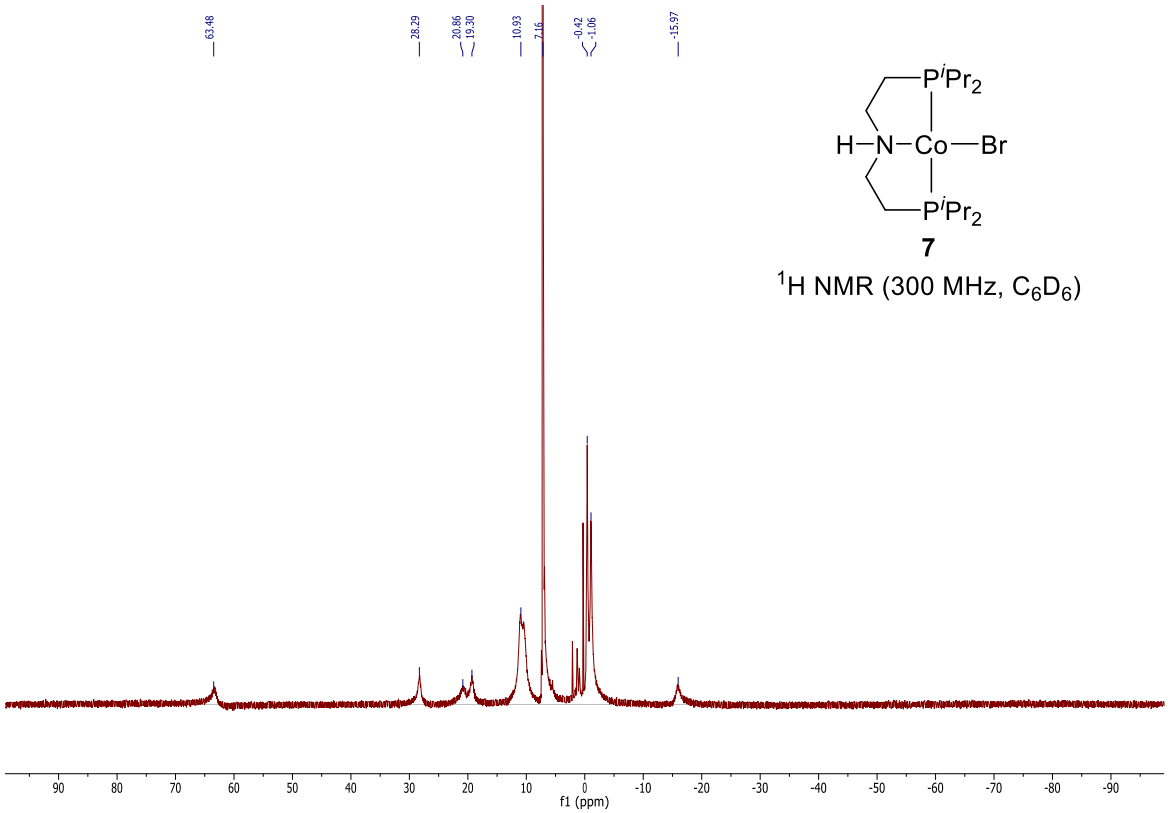

7

^{1}H NMR (300 MHz, C_6D_6)

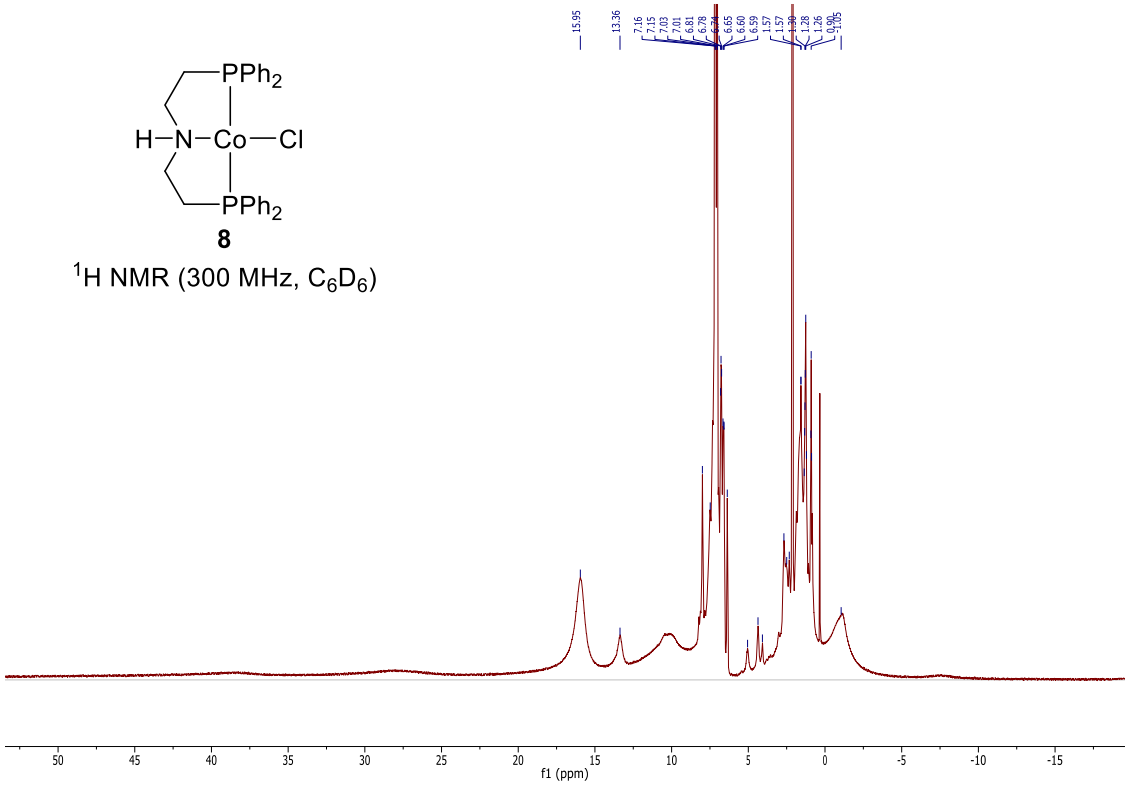

8

^{1}H NMR (300 MHz, C_6D_6)

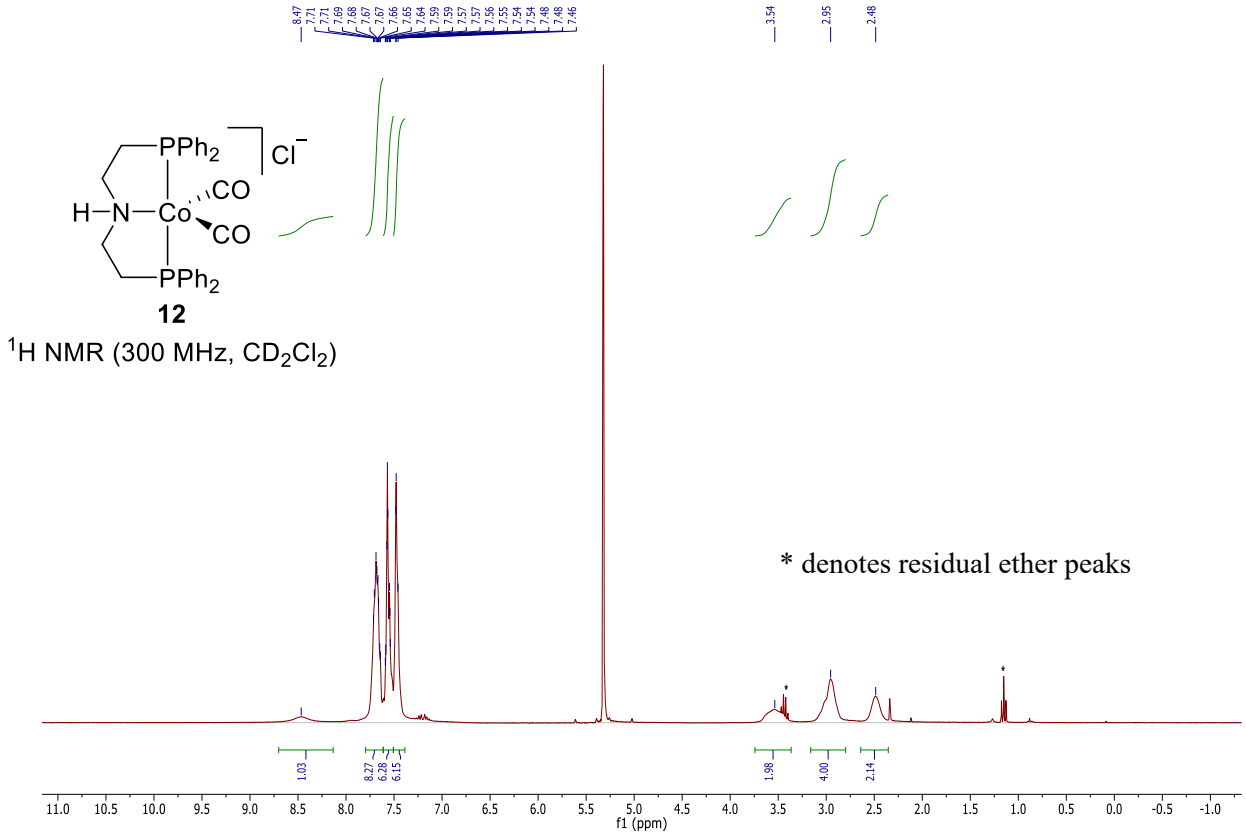
PPh2
Cl−
CO
H−N−Co
CO
PPh2
12
1H NMR (300 MHz, CD2Cl2)
* denotes residual ether peaks
f1 (ppm)

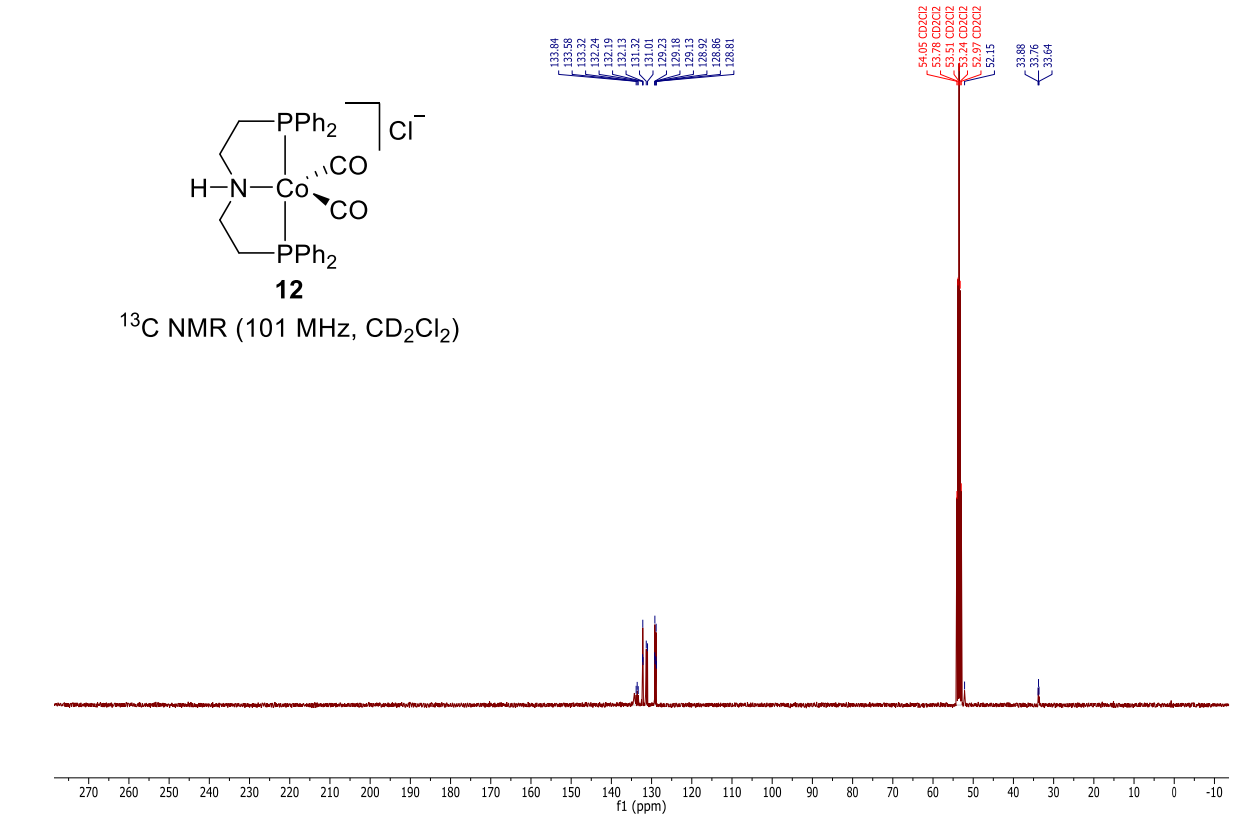
PPh2
Cl−
CO
H−N−Co
CO
PPh2
12
13C NMR (101 MHz, CD2Cl2)
f1 (ppm)

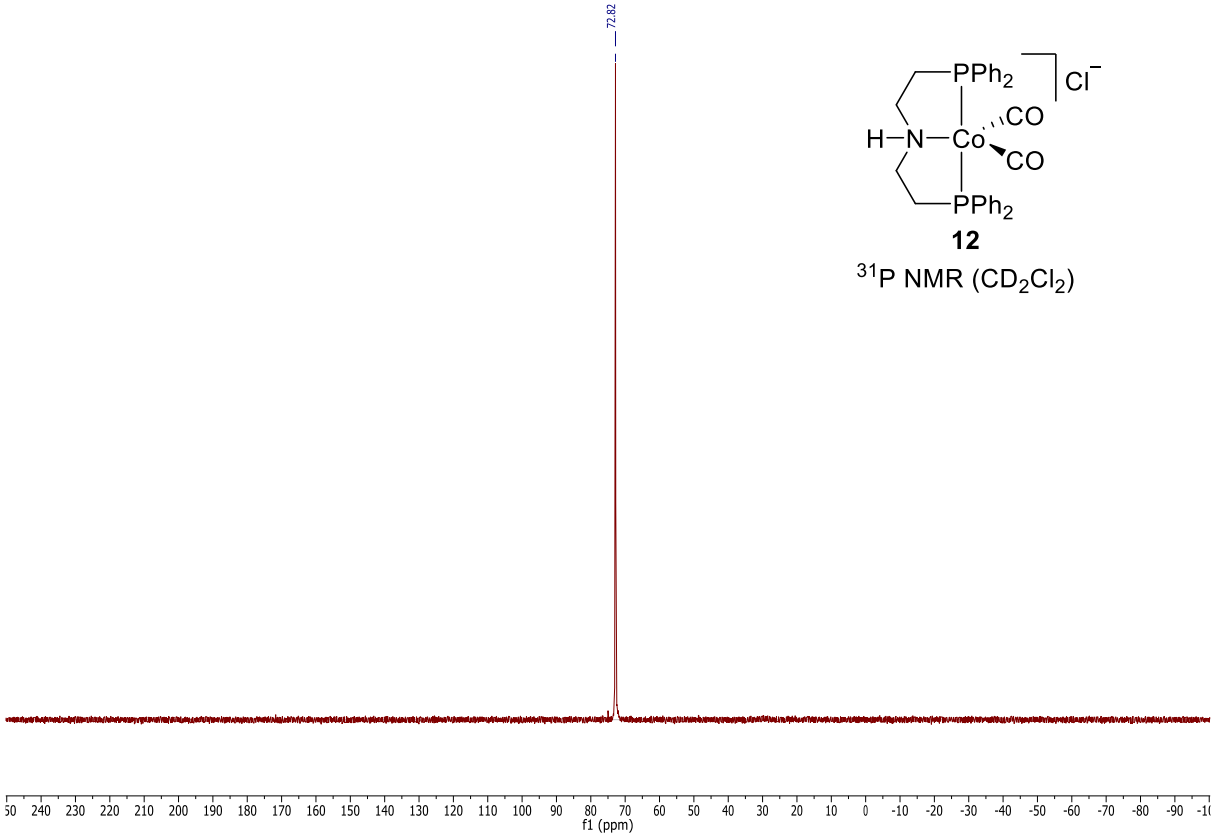

12

^{31}P NMR (CD_2Cl_2)

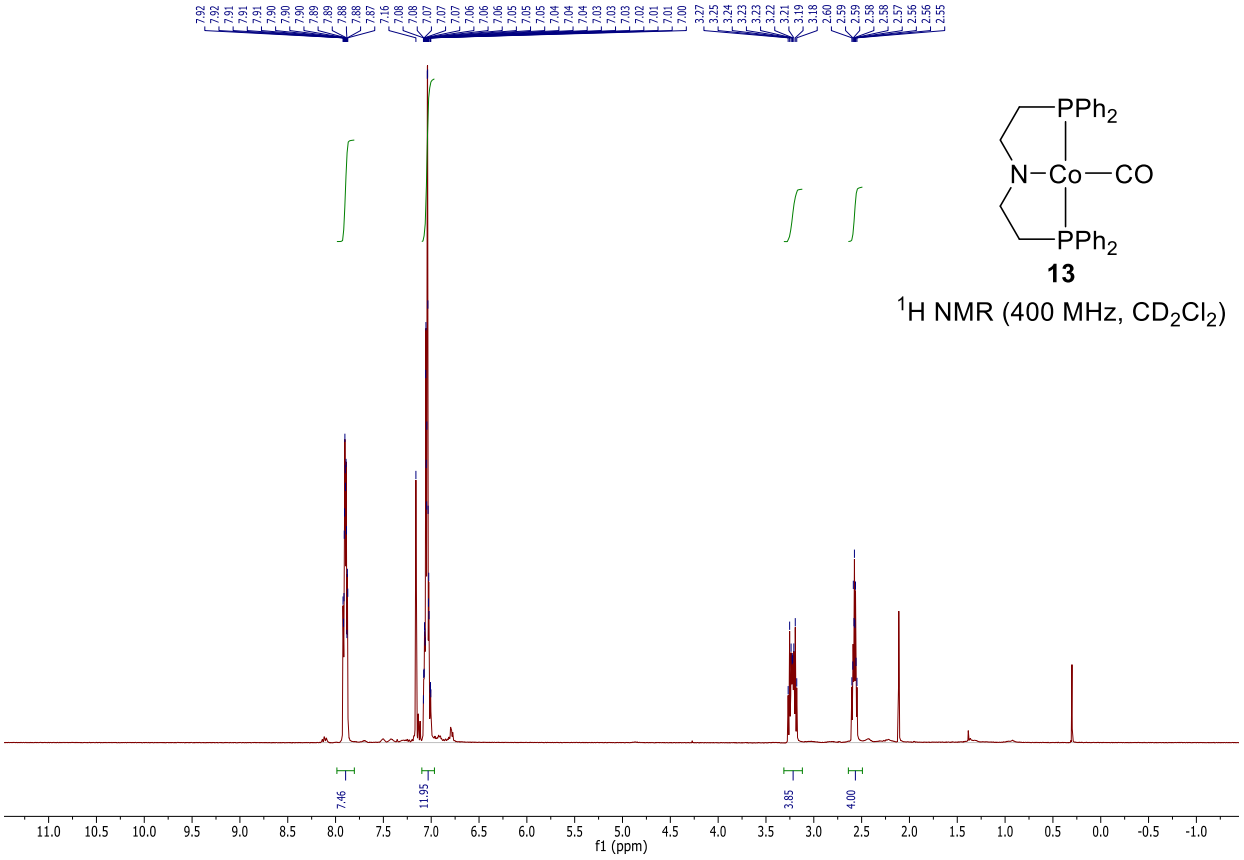

13

^{1}H NMR (400 MHz, CD_2Cl_2)

C

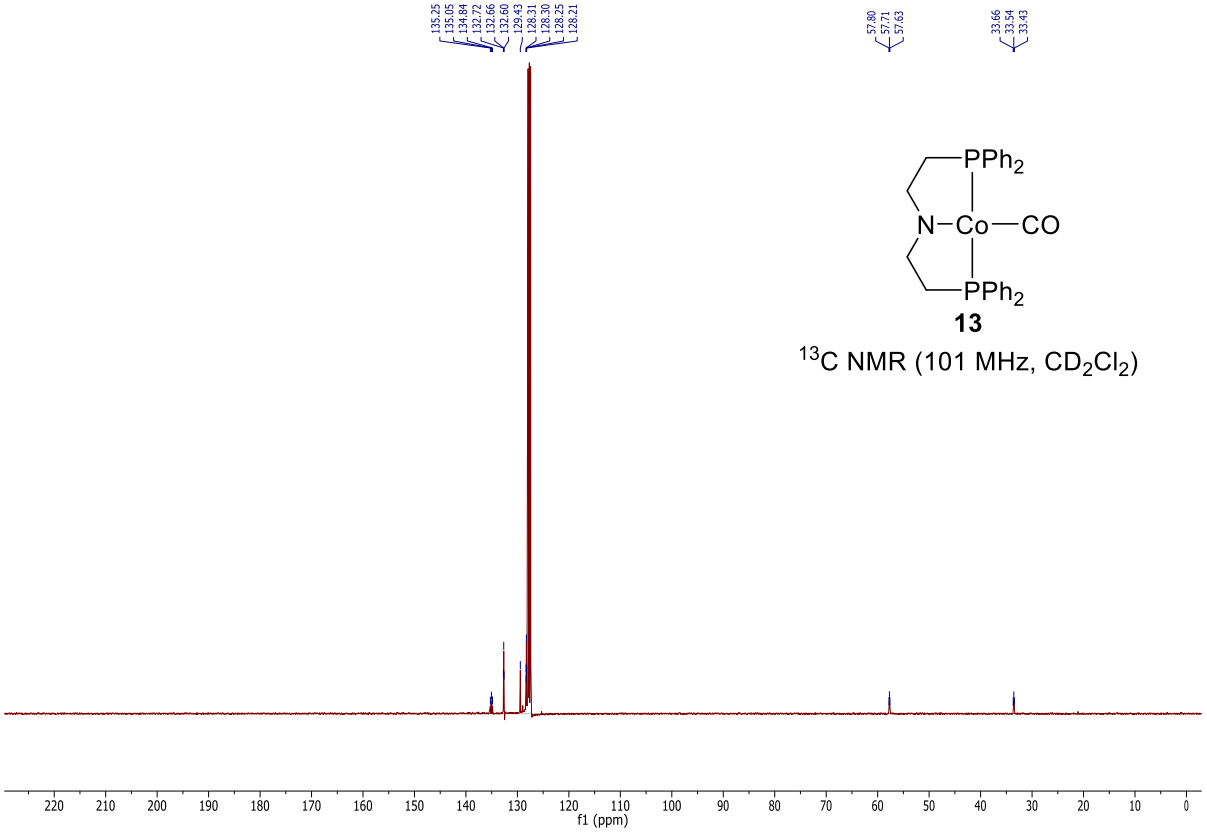
135.25
135.05
134.84
132.72
132.66
132.60
129.43
128.31
128.30
128.25
128.21
57.80
57.71
57.63
33.66
33.54
33.43
PPh2
N–Co–CO
PPh2
13
13C NMR (101 MHz, CD2Cl2)
f1 (ppm)

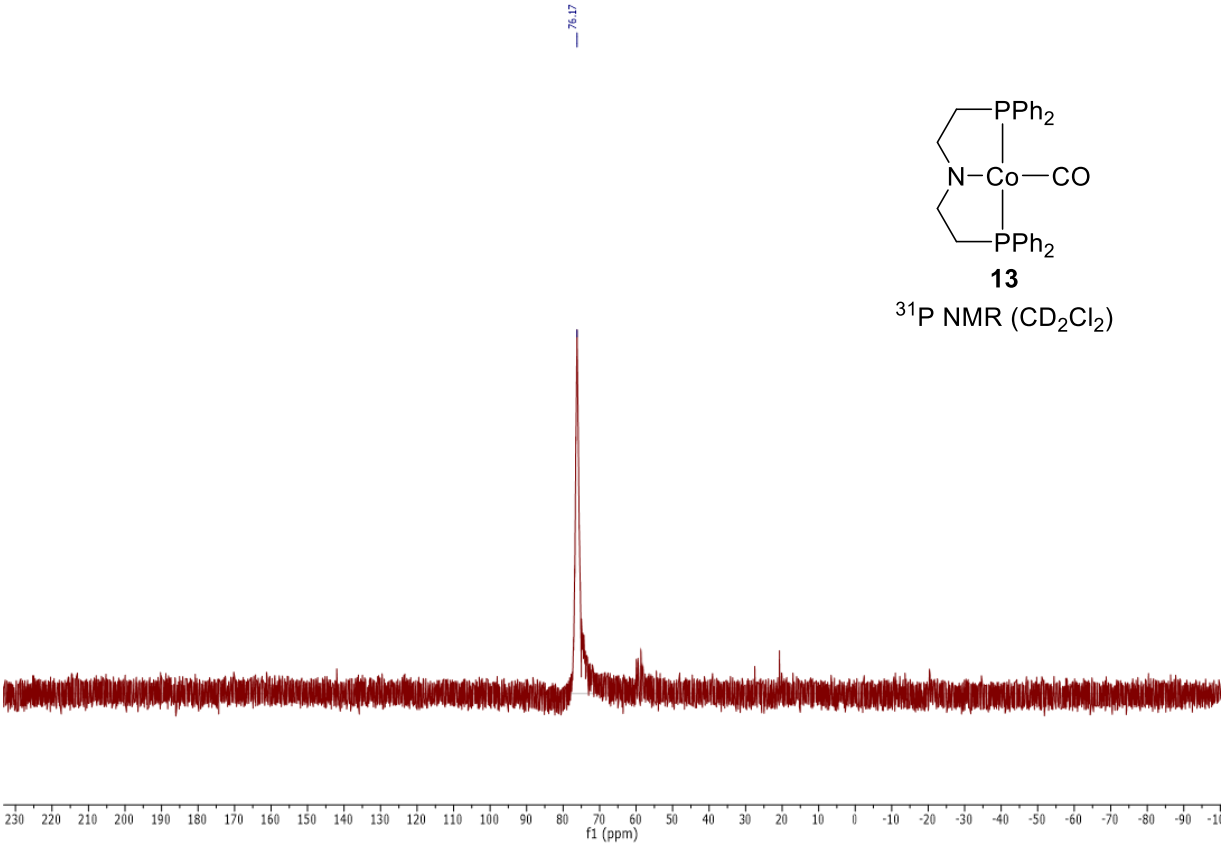
76.17
PPh2
N–Co–CO
PPh2
13
31P NMR (CD2Cl2)
f1 (ppm)

D

L5

^{1}H NMR (300 MHz, DMSO-*d6*)

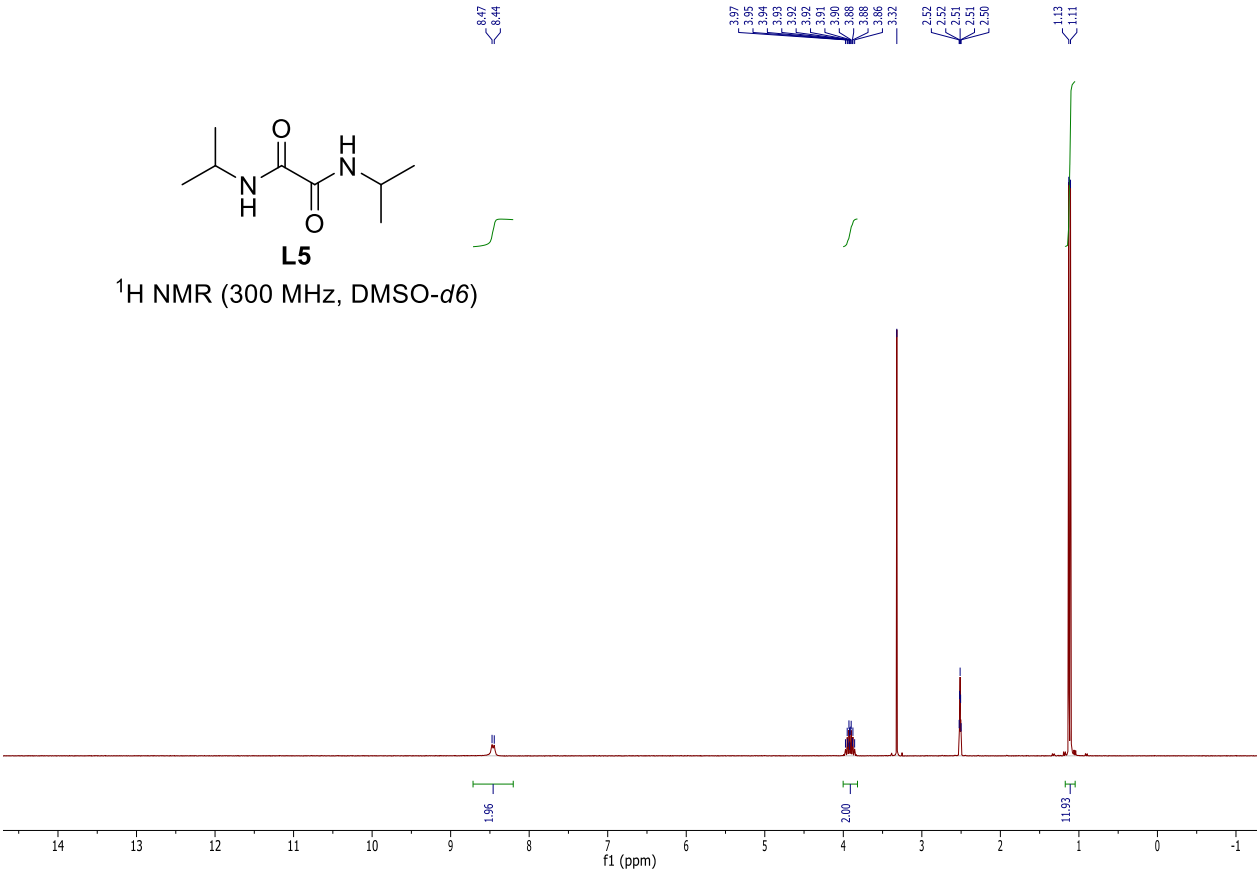

L5

^{13}C NMR (101 MHz, DMSO-*d6*)

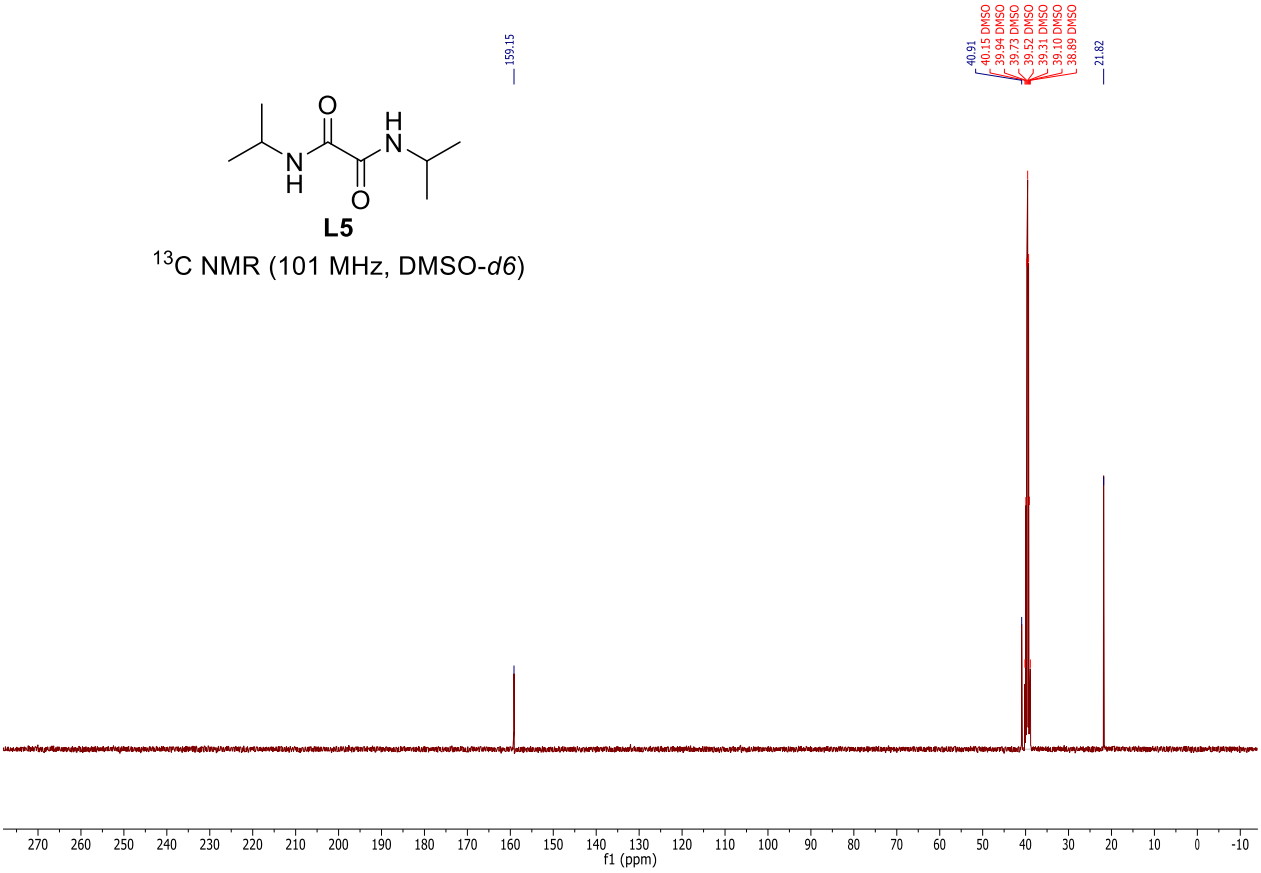

L6

^{1}H NMR (300 MHz, $CDCl_3$)

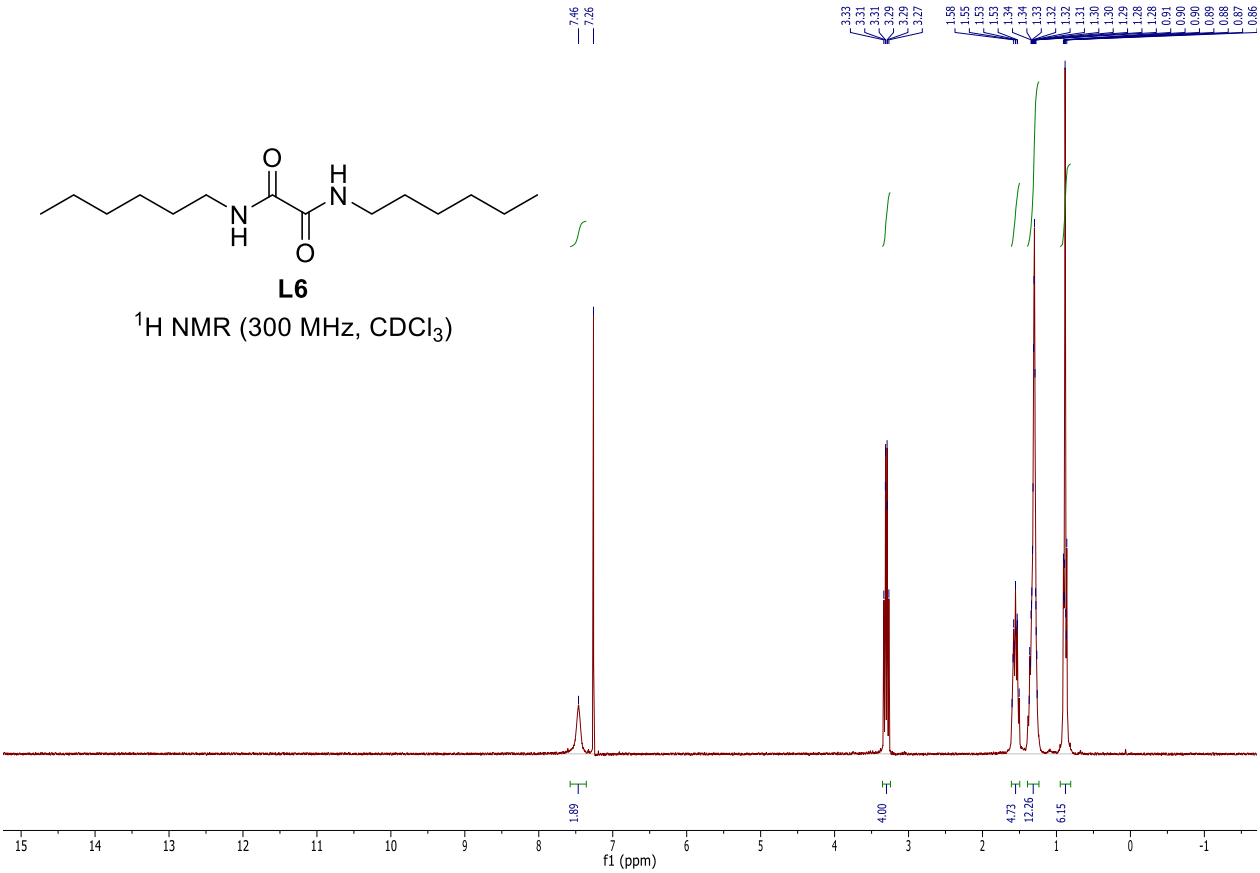

L6

^{13}C NMR (75 MHz, $CDCl_3$)

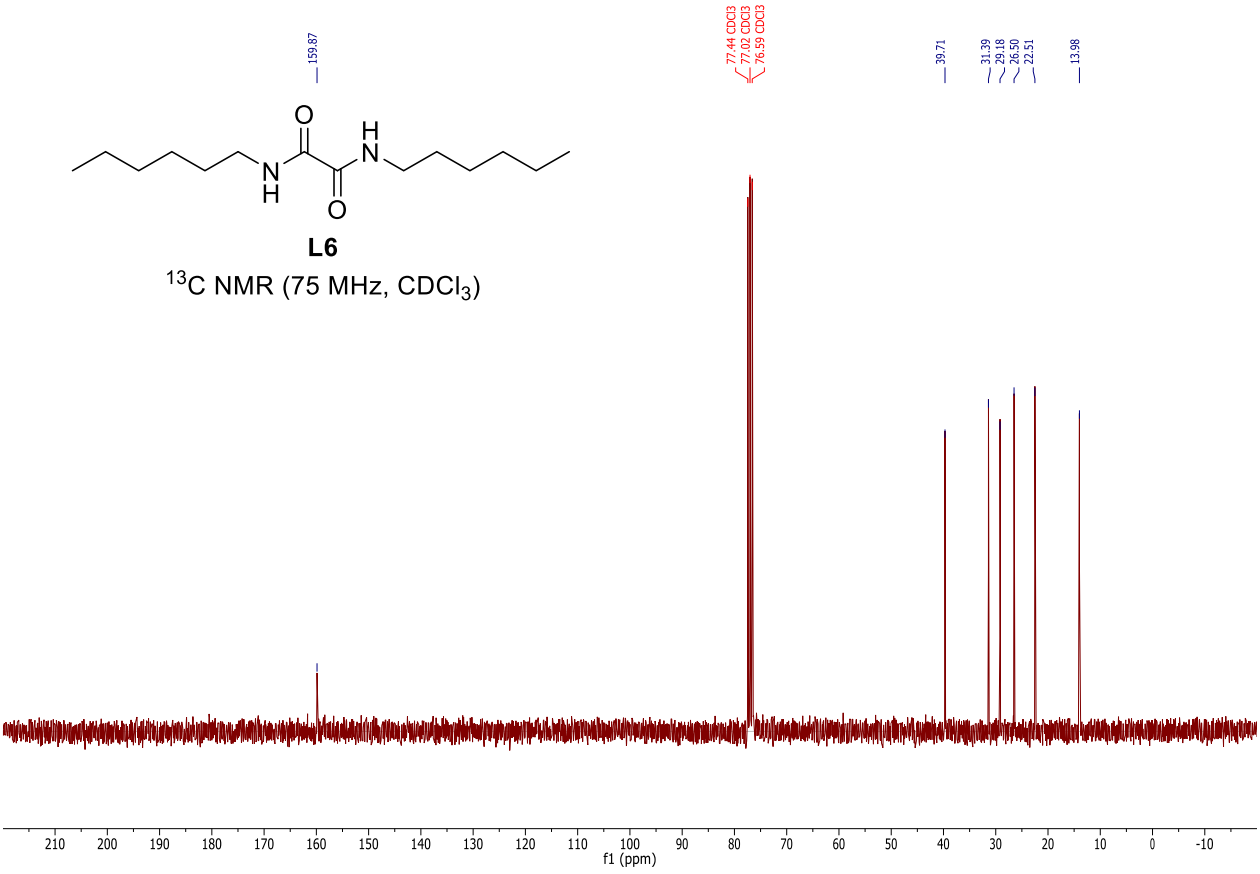

L8

^{1}H NMR (300 MHz, $CDCl_3$)

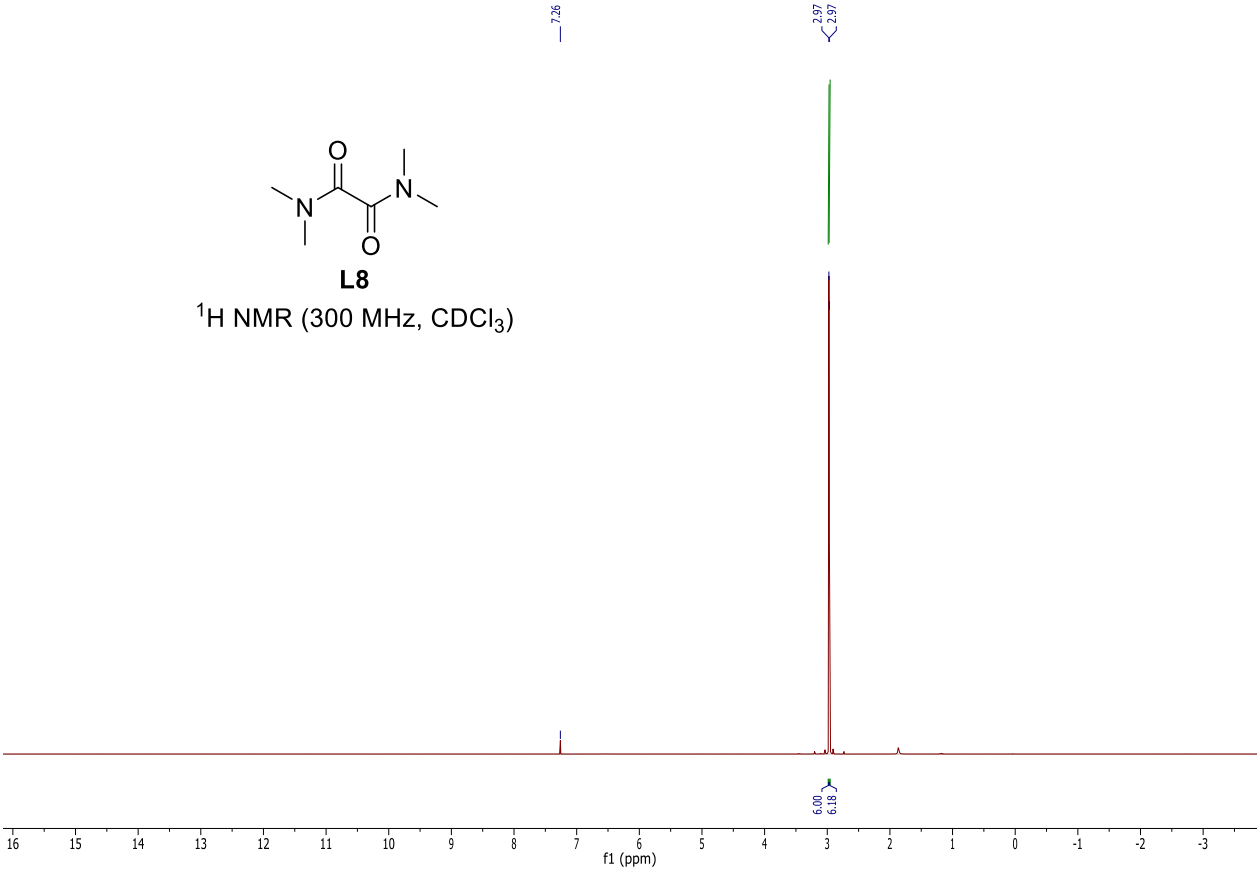

L8

^{13}C NMR (75 MHz, $CDCl_3$)

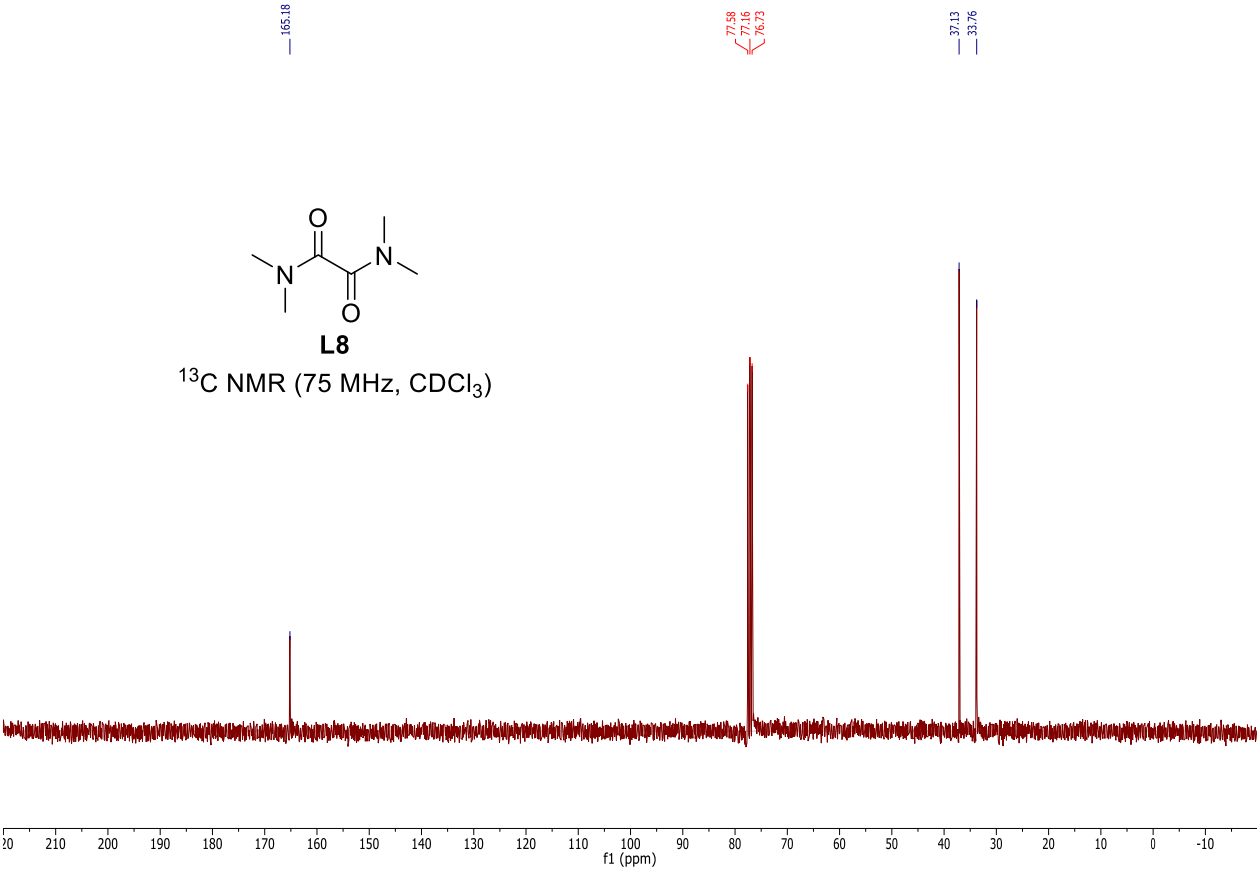

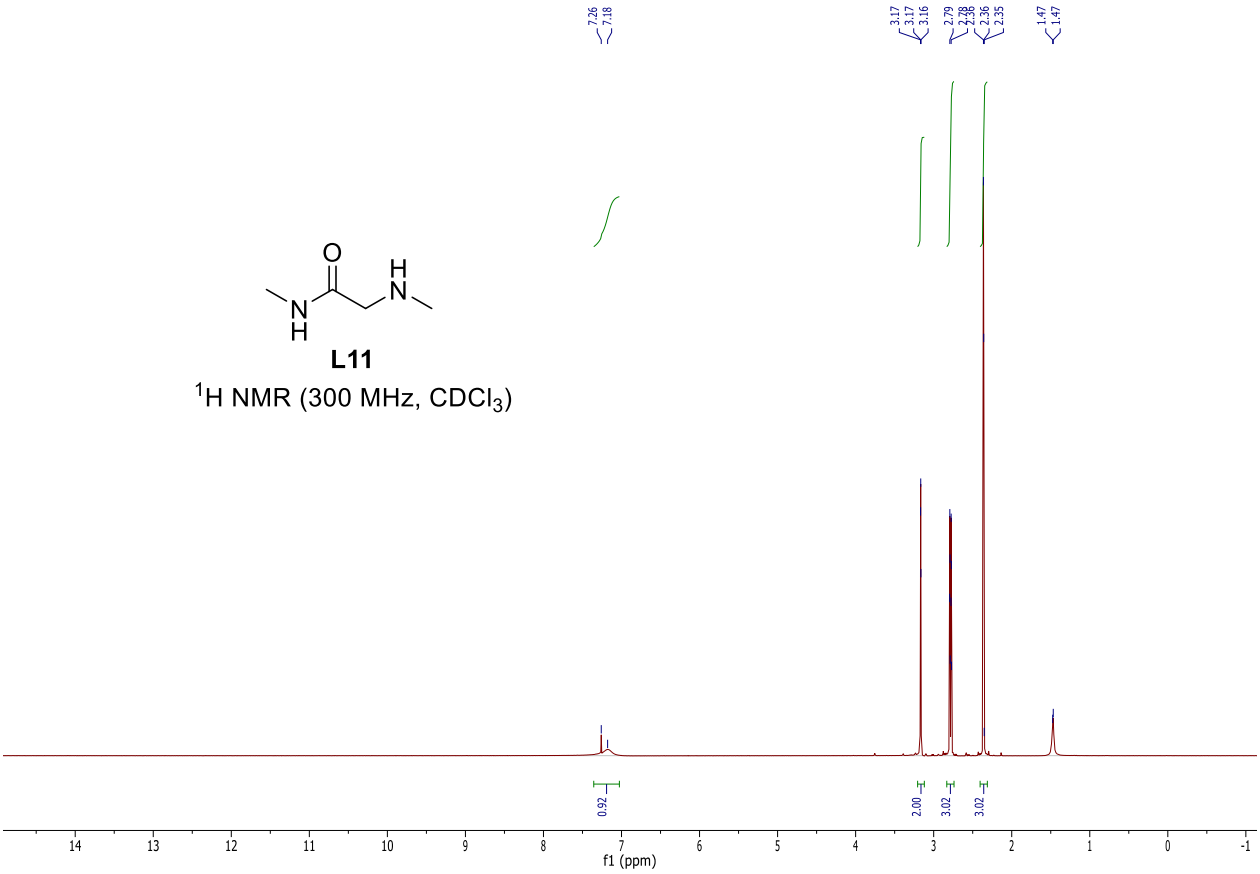

L11

^{1}H NMR (300 MHz, $CDCl_3$)

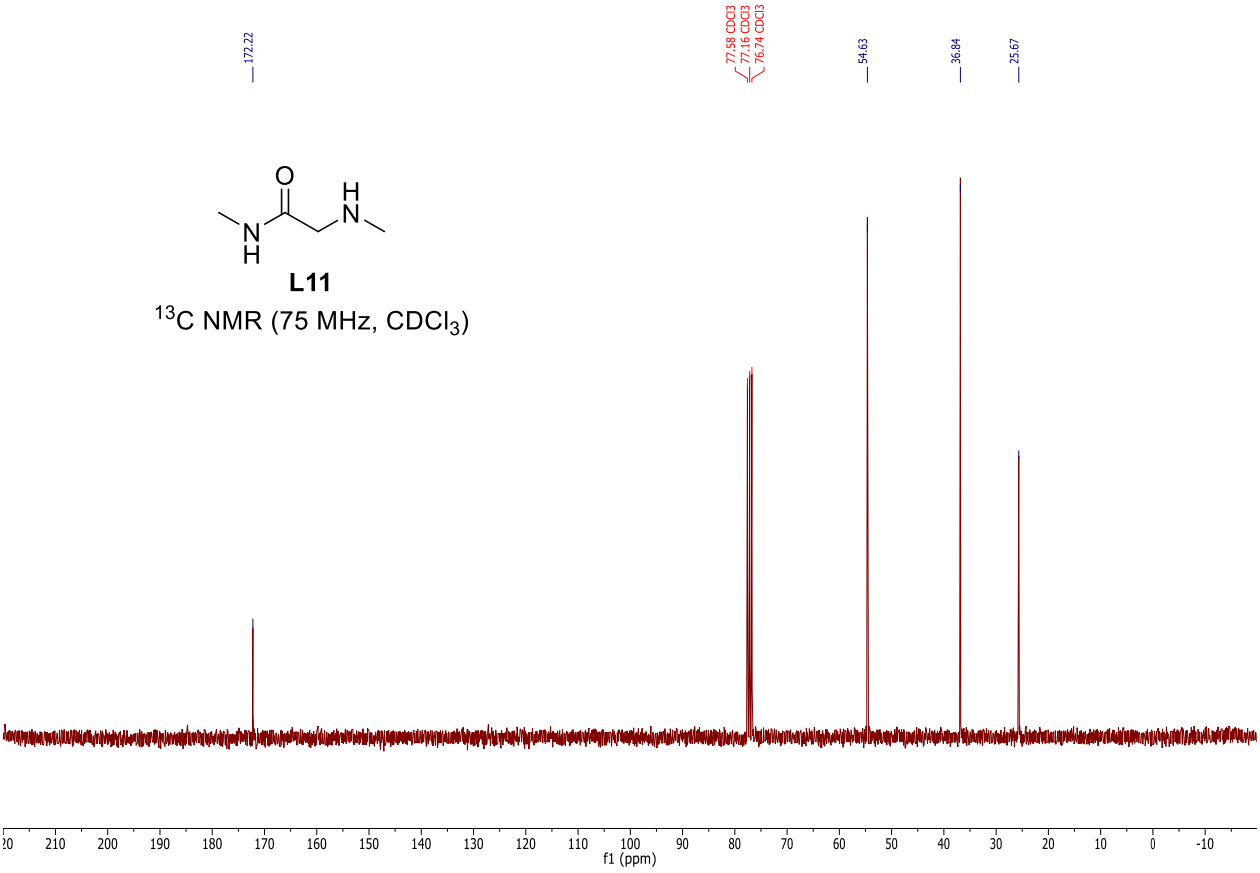

L11

^{13}C NMR (75 MHz, $CDCl_3$)

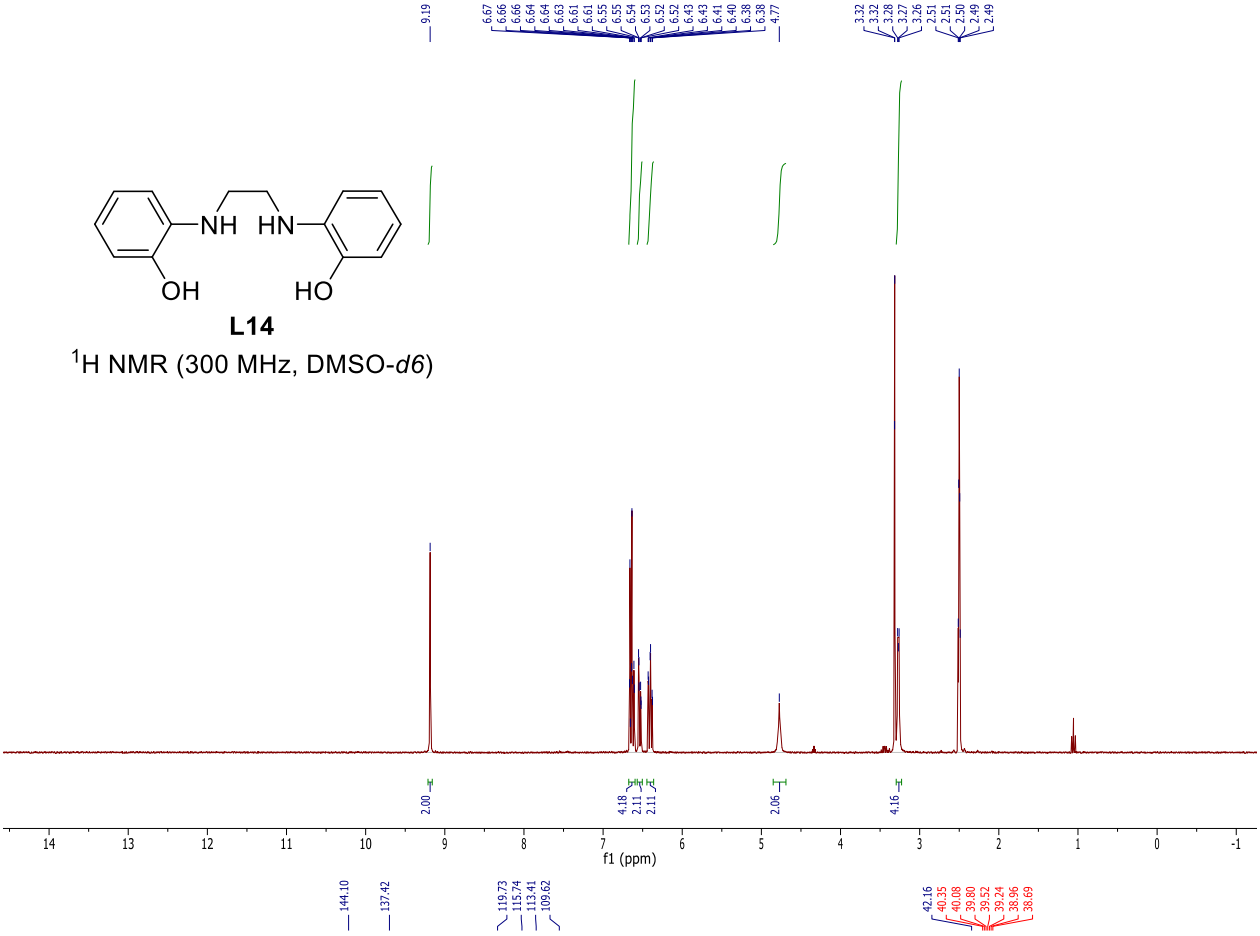

L14

^{1}H NMR (300 MHz, DMSO-*d6*)

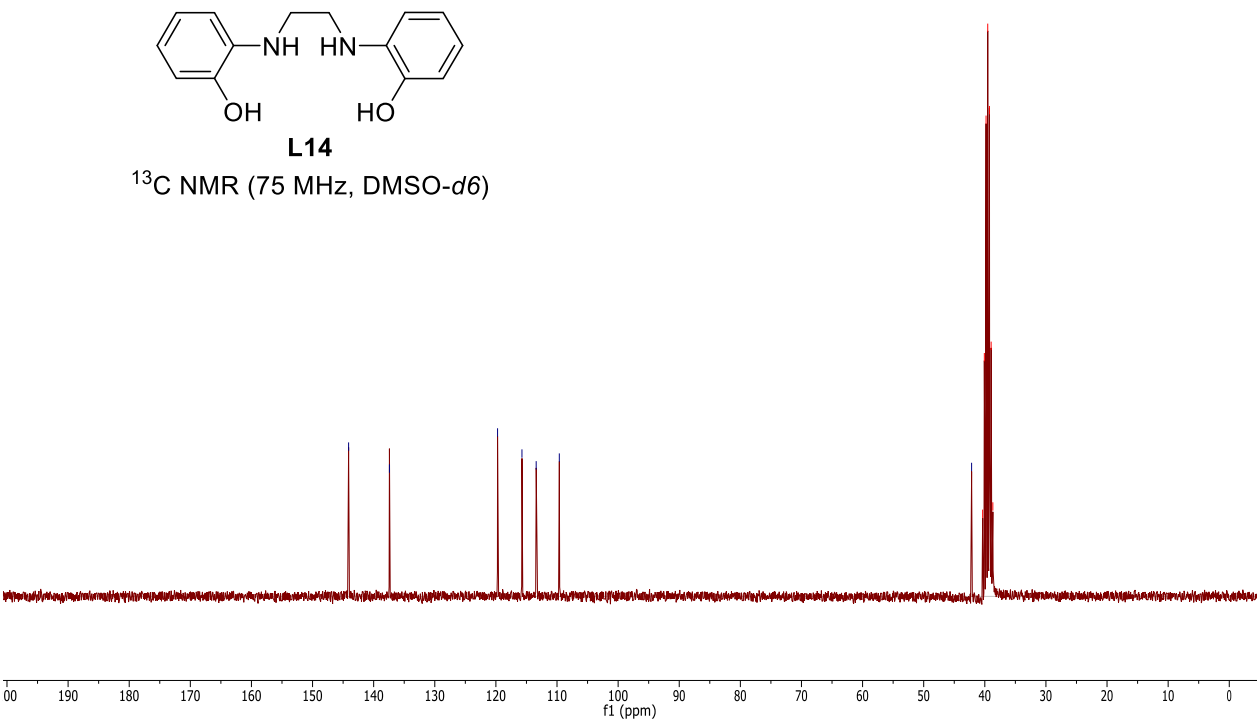

L14

^{13}C NMR (75 MHz, DMSO-*d6*)

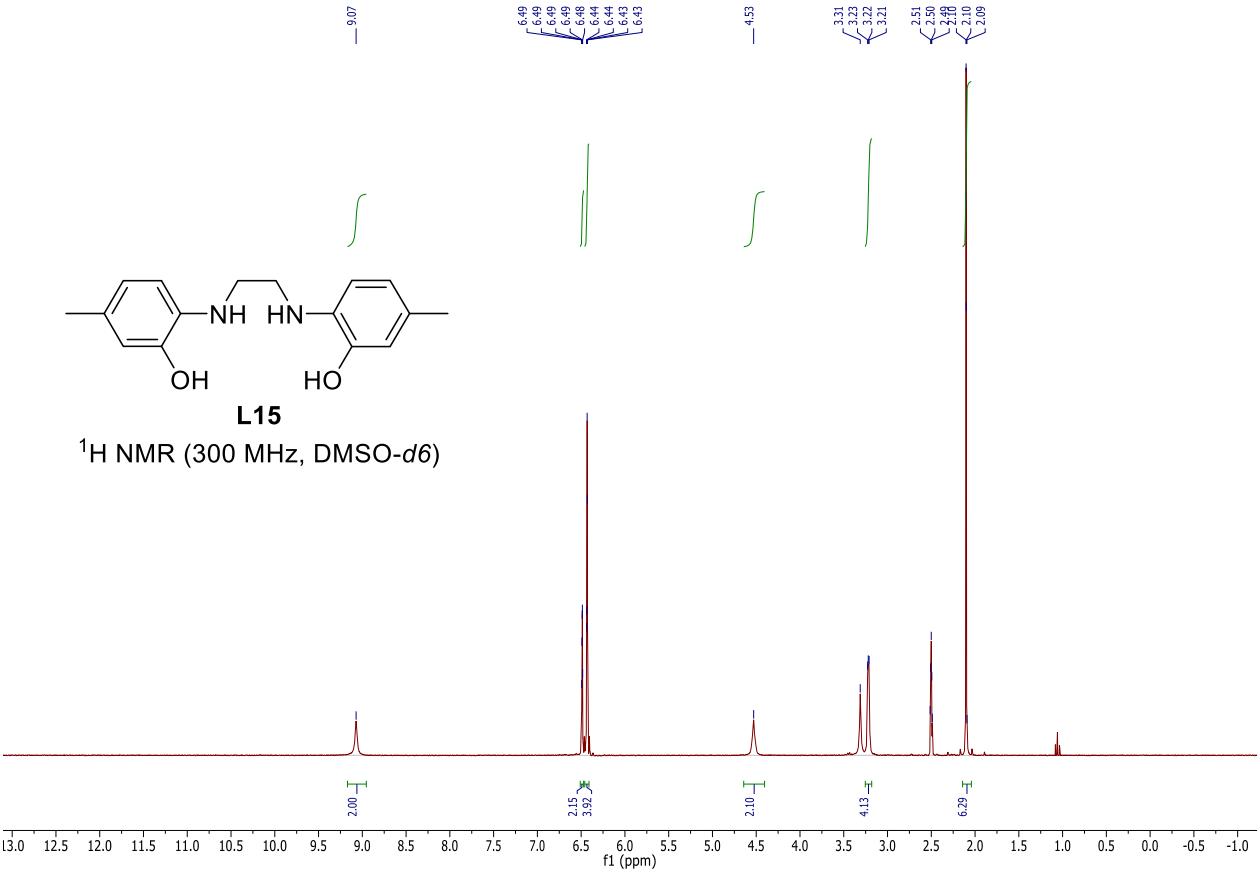

L15

^{1}H NMR (300 MHz, DMSO-*d6*)

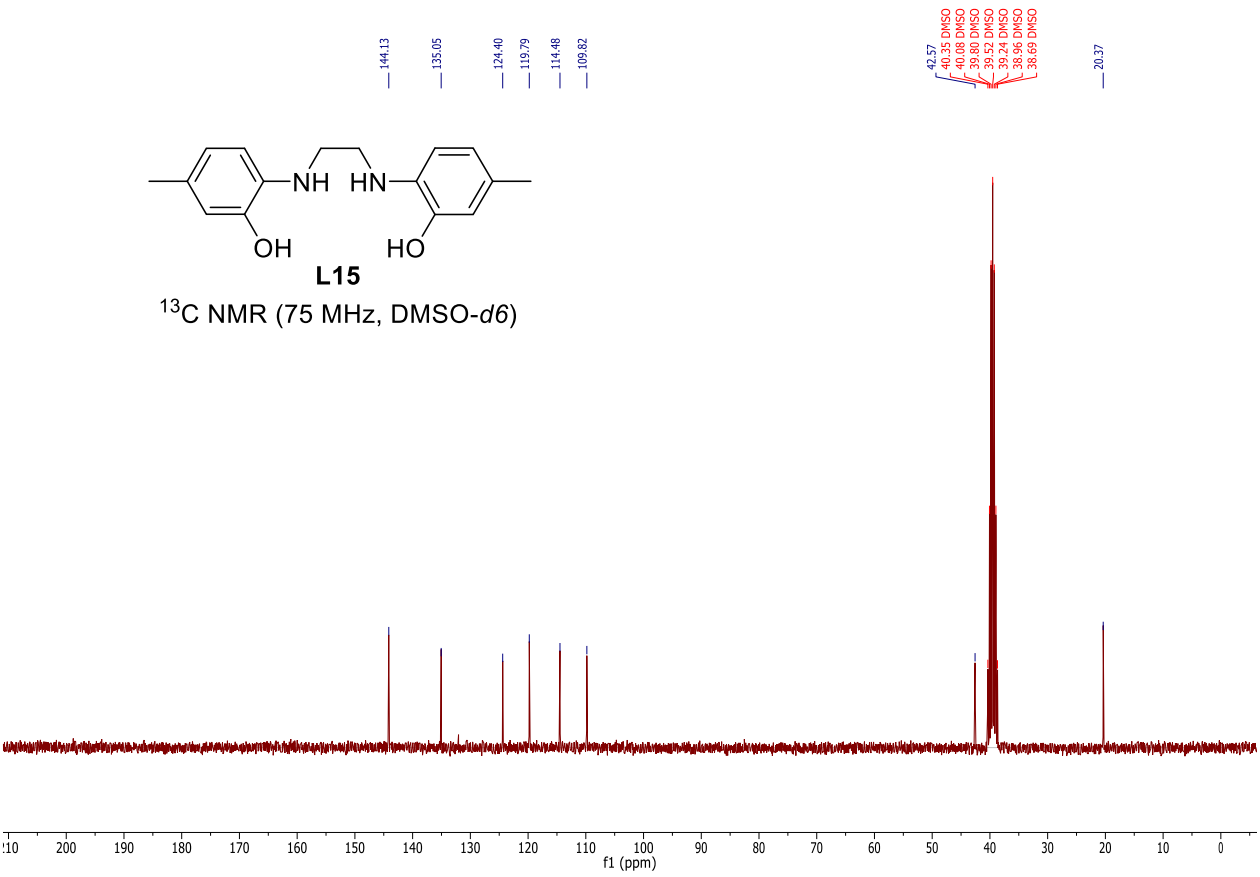

L15

^{13}C NMR (75 MHz, DMSO-*d6*)

II.Representative GC spectra of gas samples

```
========================================================================
Acq. Operator   : zw
Acq. Instrument : GC Lab 1.132                    Location :   -
Injection Date  : 2/10/2019 1:26:50 PM
                                                  Inj Volume : Manually
Acq. Method     : C:\CHEM32\1\METHODS\SAUERSTOFFMESSUNG.M
Last changed    : 2/10/2019 12:31:12 PM by zw
Analysis Method : C:\CHEM32\1\METHODS\H2COLOWCON.M
Last changed    : 4/24/2019 4:13:44 PM by AA
                  (modified after loading)
Additional Info : Peak(s) manually integrated
```

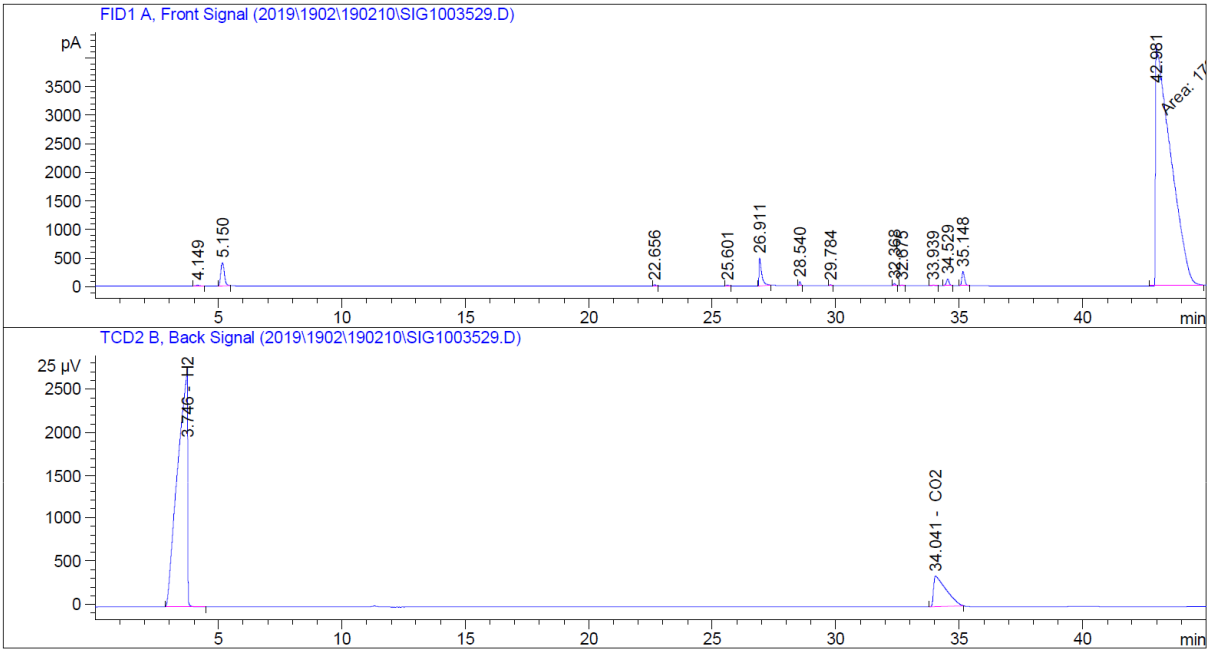


```
========================================================================
                      External Standard Report
========================================================================

Sorted By             :      Signal
Calib. Data Modified  :      4/24/2019 4:13:44 PM
Multiplier            :      1.0000
Dilution              :      1.0000
Use Multiplier & Dilution Factor with ISTDs

Signal 1: FID1 A, Front Signal


Signal 2: TCD2 B, Back Signal

RetTime  Type     Area      Amt/Area    Amount   Grp   Name
 [min]          [25 µV*s]              [% Vol.]
-------|------|----------|----------|----------|--|------------------
  3.746 BB     7.72546e4  2.63053e-4   20.32205    H2
 14.700            -          -          -        CO
 26.900            -          -          -        CH4
 34.041 BB     1.24447e4  1.84201e-3   22.92324    CO2
```

```
RetTime  Type     Area     Amt/Area    Amount   Grp   Name
 [min]         [25 µV*s]              [% Vol.]
-------|------|----------|----------|----------|--|------------------
Totals :                               43.24529


1 Warnings or Errors :

Warning : Calibrated compound(s) not found

================================================================================
                          *** End of Report ***
```

Figure I: GC report for the cobalt catalyzed dehydrogenation of FA

```
================================================================================
Acq. Operator   : zw
Acq. Instrument : Lab 1.126                        Location : Vial 1
Injection Date  : 23/08/2017 17:05:00 PM                Inj :   1
                                                  Inj Volume : Manually
Acq. Method     : C:\HPCHEM\1\METHODS\WASSERST.M
Last changed    : 21/08/2017 20:19:03 by AK
                  (modified after loading)
Analysis Method : C:\CHEM32\1\METHODS\CAL1602.M
Last changed    : 24/04/2019 15:55:56 by AK
                  (modified after loading)
Additional Info : Peak(s) manually integrated
```

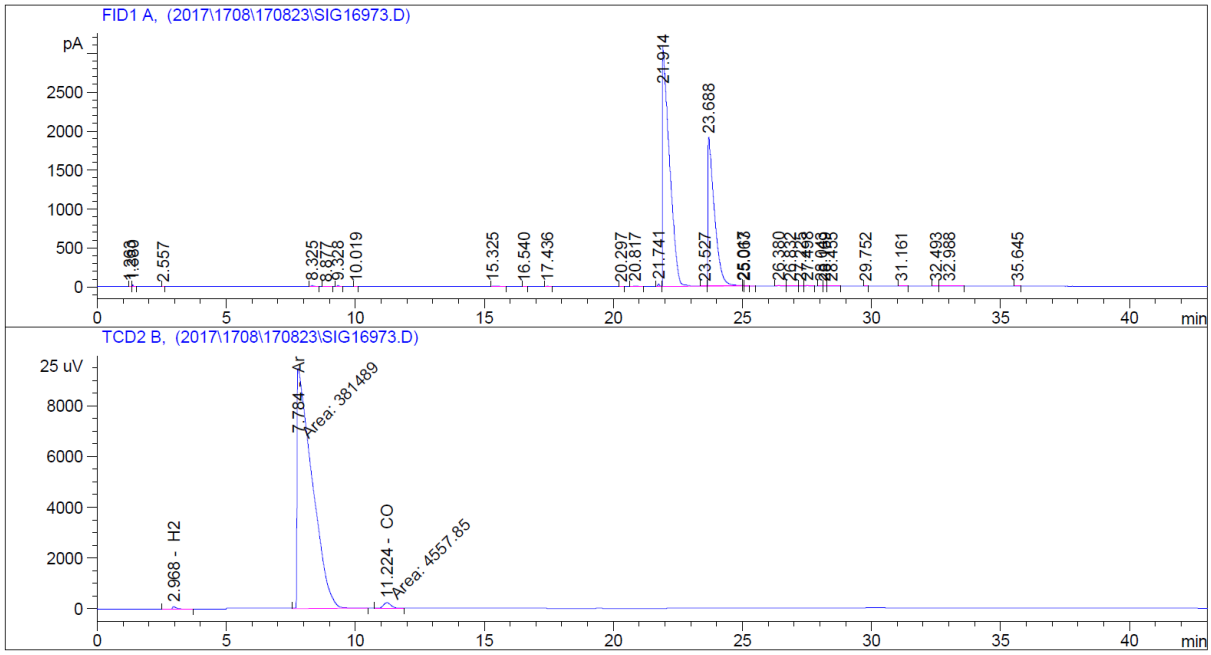


```
================================================================================
                        External Standard Report
================================================================================

Sorted By             :      Retention Time
Calib. Data Modified  :      24/04/2019 15:59:48
Multiplier            :      1.0000
Dilution              :      1.0000
Sample Amount:                :      1.00000  [vol%]    (not used in calc.)
Use Multiplier & Dilution Factor with ISTDs

Signal 1: FID1 A,
Signal 2: TCD2 B,

RetTime Sig Type     Area      Amt/Area    Amount    Grp   Name
 [min]                                    [vol%]
-------|--|------|----------|----------|----------|--|---------------
  2.968  2 BB      859.26147 1.39302e-2   11.96965     H2
  7.784  2 MM     3.81489e5  2.23925e-4   85.42509     Ar
 11.224  2 MM     4557.84668 2.15646e-4 9.82882e-1     CO
 21.000  2            -          -          -         CH4
```

RetTime [min]	Sig	Type	Area	Amt/Area	Amount [vol%]	Grp	Name
25.000	2		-	-	-		CO2

Totals : 98.37762

1 Warnings or Errors :

Warning : Calibrated compound(s) not found

*** End of Report ***

Figure II: GC report for the manganese catalyzed dehydrogenation of isopropanol

Universität Rostock
Dezernat 1
Referat 1.2

Doktorandinnen/Doktoranden-Erklärung gemäß § 4 Absatz 1 Buchstaben g und h der Promotionsordnung der Mathematisch-Naturwissenschaftlichen Fakultät der Universität Rostock

Name Zhou, Wei
(Name, Vorname)

Anschrift Nobelstr. 2, 18059, Rostock
(Straße, PLZ, Wohnort)

Ich habe eine Dissertation zum Thema

Base Metal Catalyzed Dehydrogenation of Formic Acid and Alcohols

an der Mathematisch-Naturwissenschaftlichen Fakultät der Universität Rostock angefertigt. Dabei wurde ich von Frau/Herrn

Prof. Dr. Matthias Beller

betreut.

Ich gebe folgende Erklärung ab:

1. Die Gelegenheit zum vorliegenden Promotionsvorhaben ist mir nicht kommerziell vermittelt worden. Insbesondere habe ich keine Organisation eingeschaltet, die gegen Entgelt Betreuerinnen/Betreuer für die Anfertigung von Dissertationen sucht oder die mir obliegenden Pflichten hinsichtlich der Prüfungsleistungen für mich ganz oder teilweise erledigt.

2. Ich versichere hiermit an Eides statt, dass ich die vorliegende Arbeit selbstständig angefertigt und ohne fremde Hilfe verfasst habe. Dazu habe ich keine außer den von mir angegebenen Hilfsmitteln und Quellen verwendet und die den benutzten Werken inhaltlich und wörtlich entnommenen Stellen habe ich als solche kenntlich gemacht.

Rostock, den 25.04.2019

Wei Zhou
(Unterschrift)

Wei Zhou

Albert-Einstein-Straße 29a
18059, Rostock, Germany
0381-1281345
wei.zhou@catalysis.de

Education

2016.7 — Present Ph.D. Student, Chemistry, Leibniz Institute for Catalysis at the University of Rostock, Rostock, Germany

2012.9 — 2015.6 M.Sc., Organic Chemistry, Shanghai Institute of Organic Chemistry, CAS, Shanghai, China

2007.9 — 2011.6 B.Sc., Chemistry, Nankai University, Tianjin, China

Research Experience

2016.7 — Present Early Stage Researcher, Leibniz Institute for Catalysis
Advisor: **Prof. Matthias Beller**
Base metal-catalyzed dehydrogenation of liquid hydrogen carriers

2015.7 — 2016.5 Research Assistant, Shanghai Institute of Organic Chemistry, CAS, Shanghai, China
Advisor: **Prof. Dawei Ma**
Copper catalyzed cross coupling reactions of aryl chlorides

Publications

[1]. **Zhou, W.**; Wei, Z.; Spannenberg, A.; Jiao, H.; Junge, K.; Junge, H.; Beller, M.: Cobalt Catalyzed Aqueous Dehydrogenation of Formic Acid. *Chem. Eur. J.* Accepted Author Manuscript. doi:10.1002/chem.201805612

[2]. Andérez-Fernández, M.; Vogt Lydia, K.; Fischer, S.; **Zhou, W.**; Jiao, H.; Garbe, M.; Elangovan, S.; Junge, K.; Junge, H.; Ludwig, R.; Beller, M.: A Stable Manganese Pincer Catalyst for the Selective Dehydrogenation of Methanol. *Angew. Chem., Int. Ed.* **2016**, *56*, 559.

[3]. Fan, M.; **Zhou, W.**; Jiang, Y.; Ma, D.: CuI/Oxalamide Catalyzed Couplings of (Hetero)aryl Chlorides and Phenols for Diaryl Ether Formation. *Angew. Chem. Int. Ed.* **2016**, *55*, 6211.

[4]. Fan, M.; **Zhou, W.**; Jiang, Y.; Ma, D.: Assembly of Primary (Hetero)Arylamines via CuI/Oxalic Diamide-Catalyzed Coupling of Aryl Chlorides and Ammonia. *Org. Lett.* **2015**, *17*, 5934.

[5]. **Zhou, W.**; Fan, M.; Yin, J.; Jiang, Y.; Ma, D.: CuI/Oxalic Diamide Catalyzed Coupling Reaction of (Hetero)Aryl Chlorides and Amines. *J. Am. Chem. Soc.* **2015**, *137*, 11942.

CONFERENCE PRESENTATION

[1]. Andérez-Fernández, M.; Vogt Lydia, K.; Fischer, S.; **Zhou, W.**; Jiao, H.; Garbe, M.; Elangovan, S.; Junge, K.; Junge, H.; Ludwig, R.; Beller, M., Highly stable manganese pincer catalyst for the selective dehydrogenation of methanol. Poster, ICOMC-2018, Florence, Italy, 15-20 July, 2018.

Award

Marie Curie Intra-European Fellowship
2016